IFAC

INTERNATIONAL FEDERATION OF AUTOMATIC CONTROL

WARSZAWA 1969

Adaptive Instruments and Controllers

Fourth Congress of the International Federation of Automatic Control
Warszawa 16–21 June 1969

TECHNICAL SESSION 50

NOT

Organized by
Naczelna Organizacja Techniczna w Polsce

INTERNATIONAL FEDERATION OF AUTOMATIC CONTROL

Adaptive Instruments and Controllers

TECHNICAL SESSION No 50

FOURTH CONGRESS OF THE INTERNATIONAL
FEDERATION OF AUTOMATIC CONTROL
WARSZAWA 16 – 21 JUNE 1969

Organized by
Naczelna Organizacja Techniczna w Polsce

Contents

Paper No			Page
30.1	JA	- I.Morishita - Dynamic Behavior of a Linear Threshold Element with Self-Adjusting Weights	3
30.2	CDN	- J.S.Riordon - An Adaptive Automaton Controller for Discrete Time Markov Processes.....	22
30.3	GB	- A.L.Jones, D.P.McLeod - A Digital Controller for Process Industries with Adaptive-Type Behaviour.....	38
30.4	D /DFR/	- W.Speth - Simple Method for the Rapid Self-Adaptation of Automatic Controllers in Drive Applications.....	52
30.5	SU	- D.Ya.Svet - Self-Adaptive Systems for True Temperature Measurement in Optical Range....	68
30.6	PL	- Z.Barski - Adaptable Regulation System of Temperature and Humidity in Air - Conditioned Objects.....	78
30.7	SU	- L.I.Gutenmakher - New Analogue Models for Control Purposes.....	103

Wydawnictwa Czasopism Technicznych NOT - Polska

Zakład Poligraficzny WCT NOT. Zam. 80/69.

DYNAMIC BEHAVIOR OF A LINEAR THRESHOLD ELEMENT WITH SELF-ADJUSTING WEIGHTS

Iwao Morishita
Department of Mathematical Engineering and Instrumentation Physics
University of Tokyo
Tokyo, Japan

Introduction

During the last decade the problem of self-organization has received considerable attention. F.Rosenblatt[1] reported on the cross-coupled Perceptron. H.D.Block et al.[2] investigated the four-layer series-coupled Perceptron. E.R.Caianiello[3] proposed a model for brain functioning. In these papers, a special class of linear threshold elements were introduced. The elements have a set of variable weights, the values of which change automatically following a certain rule of growth. Networks of such elements have the function of self-organization. Similar elements were also presented, in the studies of the problem of "learning without a teacher", by C.V. Jakowatz et al.[4], E.M.Glaser[5], D.B.Cooper and P.W.Cooper[6], H.J.Scudder[7], E.M. Braverman[8], B.Widrow[9] and others including the author[10].

In the previous work, however, the behavior of such elements was investigated only from the standpoint of nonsupervised learning for pattern recognition or signal detection, and little attempt was made to understand their general properties.

In this paper, a new structure of element is presented, and its dynamic behavior is investigated in detail apart from the standpoint of a particular application. As a necessary result of this investigation, its general properties become evident and we can discuss what the element can do.

The element is basically a summing device. It gives a weighted sum of its inputs as the output. At the same time, each weight changes by an amount proportional to the corresponding input, where the direction of the change is determined by the polarity of the output. In spite of this simple structure, the element has a remarkable property, that is, it has a tendency to separate its inputs into a "spectrum" or a family of orthogonal components, and to pick out the component of largest power for its output. This property enables it to perform a variety of types of information processing such as majority decision logic, data storage, pattern dichotomy and signal filtering. It should be noted that threshold function is used just for the

weight adjustment and the output is the weighted sum itself.

The Element

A block diagram of the element is shown in Fig.1. The element consists of a set of variable weights, a summing device, a comparator and a set of weight adjusters. The inputs $x_i(t)$, i=1,2,...,N, are assumed to be zero-mean signals, i.e.,

$$\overline{x_i(t)}=0, \qquad i=1,2,\ldots,N. \tag{1}$$

The output of the element is a weighted sum of the inputs, i.e.,

$$y(t)=\sum_{i=1}^{N} w_i(t)x_i(t). \tag{2}$$

The weights are adjusted automatically according to the equations

$$T\frac{dw_i(t)}{dt}+w_i(t)=ax_i(t)\operatorname{sgn}\left[y(t)\right], \qquad i=1,2,\ldots,N. \tag{3}$$

Using the vector notations

$$\underline{x}(t)=\begin{bmatrix} x_1(t) \\ x_2(t) \\ \vdots \\ x_N(t) \end{bmatrix}, \qquad \underline{w}(t)=\begin{bmatrix} w_1(t) \\ w_2(t) \\ \vdots \\ w_N(t) \end{bmatrix}, \tag{4}$$

we have the simpler aspect

$$y(t)=\underline{w}(t)'\underline{x}(t), \tag{5}$$

$$T\frac{d\underline{w}(t)}{dt}+\underline{w}(t)=a\underline{x}(t)\operatorname{sgn}\left[y(t)\right], \tag{6}$$

where the prime ' denotes a transpose operation.

Analysis

Since it is difficult to solve the system of nonlinear differential equations (2),(3) exactly, an approximate analysis will be attempted.

First, the input signals $x_i(t)$ are assumed to be stationary gaussian signals. The correlation coefficient between $x_i(t)$ and $x_j(t)$ can be obtained approximately by averaging $x_i(t)x_j(t)$ for a time interval h, i.e.,

$$r_{ij}\triangleq\overline{x_i(t)x_j(t)}=\frac{1}{h}\int_{t-h}^{t} x_i(t)x_j(t)dt, \qquad \text{for all } i, j. \tag{7}$$

Assume that the time constant T is much larger than h. Then, $w_i(t)$ do not change appreciably for the interval h. Thus, averaging the right side of (3) from t-h to t, we obtain the approximate equations

$$T\frac{dw_i(t)}{dt}+w_i(t)=\frac{a}{h}\int_{t-h}^{t} x_i(t)\operatorname{sgn}\left[y(t)\right]dt, \qquad i=1,2,\ldots,N. \tag{8}$$

As is well known, if f(t),g(t) are zero-mean gaussian signals, then we have

$$\overline{f(t)\,\mathrm{sgn}[g(t)]}=\sqrt{\frac{2}{\pi}}\,\frac{1}{\sigma_g}\,\overline{f(t)g(t)}, \tag{9}$$

where

$$\sigma_g^2=\overline{g(t)^2} \tag{10}$$

In this case, y(t) is also a zero-mean gaussian signal, because a weighted sum of zero-mean gaussian signals is also a zero-mean gaussian signal. Hence,

$$\frac{1}{h}\int_{t-h}^{t} x_i(t)\,\mathrm{sgn}[y(t)]\,dt=\sqrt{\frac{2}{\pi}}\,\frac{1}{\sigma(t)}\,\frac{1}{h}\int_{t-h}^{t} x_i(t)y(t)\,dt, \tag{11}$$

where

$$\sigma(t)^2=\frac{1}{h}\int_{t-h}^{t} y(t)^2\,dt \tag{12}$$

Note that y(t) is not a stationary signal, because $w_i(t)$ change with time. Substituting (2) into (11) and carrying out the integration under the assumption that $w_i(t)$ are constants, we obtain

$$\frac{1}{h}\int_{t-h}^{t} x_i(t)\,\mathrm{sgn}[y(t)]\,dt=\sqrt{\frac{2}{\pi}}\,\frac{1}{\sigma(t)}\sum_{j=1}^{N} r_{ij}w_j(t). \tag{13}$$

Hence,

$$T\frac{dw_i(t)}{dt}+w_i(t)=\frac{\alpha}{\sigma(t)}\sum_{j=1}^{N} r_{ij}w_j(t),\qquad \alpha=\sqrt{\frac{2}{\pi}}\,a, \tag{14}$$

$$\sigma(t)^2=\sum_i\sum_j r_{ij}w_i(t)w_j(t), \tag{15}$$

or

$$T\frac{d\underline{w}(t)}{dt}+\underline{w}(t)=\frac{\alpha}{\sigma(t)}R\underline{w}(t), \tag{16}$$

$$\sigma(t)^2=\underline{w}(t)'R\underline{w}(t), \tag{17}$$

where R is a N×N matrix with elements r_{ij}.

Steady-state solutions of the above equations are given by

$$R\underline{w}^*=\left(\frac{\sigma^*}{\alpha}\right)\underline{w}^*,\qquad \sigma^{*2}=\underline{w}^{*\prime}R\underline{w}^*. \tag{18}$$

This means that the solution vector $\underline{w}^*$ has the same direction with one of the eigenvectors of R. Since a covariance matrix is symmetric and positive definite, R has N real and positive eigenvalues $\lambda_1, \lambda_2, \ldots, \lambda_N$, and there exist N eigenvectors corresponding to these eigenvalues. Let the eigenvectors be $\underline{u}_1, \underline{u}_2, \ldots, \underline{u}_N$. Then, the solutions are given by

$$\underline{w}_i^*=c_i\underline{u}_i,\qquad i=1,2,\ldots,N, \tag{19}$$

where c_i are determined by

$$\sigma_i^2=\alpha^2\lambda_i^2=c_i^2\underline{u}_i'R\underline{u}_i. \tag{20}$$

If $\underline{w}^*$ is a solution, then $-\underline{w}^*$ is also a solution. The origin $\underline{0}$ is clearly a solution. Thus, there exist in total 2N+1 solutions.

There exists an orthogonal matrix P such that

$$PRP^{-1}=\mathrm{diag}(\lambda_1,\lambda_2,\ldots,\lambda_N). \tag{21}$$

Therefore, from the transformations

$$\begin{aligned}\underline{v}(t)&=P\underline{w}(t),\\ \underline{z}(t)&=P\underline{x}(t),\end{aligned} \tag{22}$$

it follows that

$$y(t)=\underline{v}(t)'\underline{z}(t), \tag{23}$$

$$T\frac{d\underline{v}(t)}{dt}+\underline{v}(t)=\frac{a}{h}\int_{t-h}^{t}\underline{z}(t)\,\mathrm{sgn}[y(t)]\,dt, \tag{24}$$

Hence,

$$T\frac{d\underline{v}(t)}{dt}+\underline{v}(t)=\frac{\alpha}{\sigma(t)}\,\mathrm{diag}(\lambda_1,\lambda_2,\ldots,\lambda_N)\underline{v}(t), \tag{25}$$

$$\sigma(t)^2=\underline{v}(t)'\,\mathrm{diag}(\lambda_1,\lambda_2,\ldots,\lambda_N)\underline{v}(t)=\sum\lambda_i v_i(t)^2. \tag{26}$$

When the eigenvalues are all distinct, the equilibriums are given by

$$\underline{v}_i^*=\begin{bmatrix}0\\ \vdots\\ 0\\ v_i^*\\ 0\\ \vdots\\ 0\end{bmatrix},\qquad -\underline{v}_i^*=\begin{bmatrix}0\\ \vdots\\ 0\\ -v_i^*\\ 0\\ \vdots\\ 0\end{bmatrix},\qquad i=0,1,2,\ldots,N, \tag{27}$$

where

$$\begin{aligned}&v_0^*=0,\qquad \sigma_0^*=0,\\ &v_i^*=\alpha\sqrt{\lambda_i}\ ,\ \sigma_i^*=\alpha\lambda_i\qquad ,\qquad i=1,2,\ldots,N.\end{aligned} \tag{28}$$

When $\lambda_k=\lambda_{k+1}=\ldots=\lambda_{k+r-1}$ and the others are all distinct, the solutions are

$$\underline{v}_i^*=\begin{bmatrix}0\\ \vdots\\ 0\\ v_i^*\\ \vdots\\ 0\end{bmatrix},\qquad -\underline{v}_i^*=\begin{bmatrix}0\\ \vdots\\ 0\\ -v_i^*\\ \vdots\\ 0\end{bmatrix},\qquad i=0,1,2,\ldots,k-1,k+r,\ldots,N, \tag{29}$$

where

$$\begin{aligned}&v_0^*=0,\qquad \sigma_0^*=0,\\ &v_i^*=\alpha\sqrt{\lambda_i}\ ,\qquad \sigma_i^*=\alpha\lambda_i,\qquad i=1,2,\ldots,k-1,k+r,\ldots,N,\end{aligned} \tag{30}$$

and

$$\underline{v}_k^*=\begin{bmatrix}0\\ \vdots\\ 0\\ v_k^*\\ \vdots\\ v_{k+r-1}^*\\ 0\\ \vdots\\ 0\end{bmatrix}, \tag{31}$$

where

$$\sum_{i=k}^{k+r-1}v_i^{*2}=\alpha^2\lambda_k,\qquad \sigma_k^*=\alpha\lambda_k. \tag{32}$$

The stabilities of these points can be discussed using the second method of Liapunov. We can show that only a pair of equilibriums corresponding to the largest eigenvalue are stable and the others are all unstable. Moreover, we can show that all solutions tend to either of the two as $t\to\infty$. As an example, phase-plane trajectories have been calculated for a two-input element with values $\alpha=1$, $\lambda_1=1$, $\lambda_2=0.6$ and $\alpha=1$, $\lambda_1=\lambda_2=1$. Fig.2 shows the results.

The outputs in the equilibriums $\underline{v}_1^*$, $\underline{v}_2^*$,..., $\underline{v}_N^*$ are given by

$$y_i(t)^*=v_i^* z_i(t), \qquad i=1,2,\ldots,N. \tag{33}$$

Clearly $y_i(t)^*$ make a family of orthogonal functions. Then, let us define a family of normalized orthogonal components

$$e_i(t)=y_i(t)^*/\alpha\lambda_i, \qquad i=1,2,\ldots,N. \tag{34}$$

From (33),(34) it follows that

$$x_i(t)=\sum_{j=1}^{N} c_{ij}e_j(t), \qquad i=1,2,\ldots,N, \tag{35}$$

where

$$(c_{ij})=P^{-1}\mathrm{diag}(\sqrt{\lambda_1},\sqrt{\lambda_2},\ldots,\sqrt{\lambda_N}). \tag{36}$$

Also, we obtain

$$\sum_{i=1}^{N} c_{ij}^2=\lambda_j. \tag{37}$$

Thus, each input can be represented by a weighted sum of the components and the eigenvalue λ_i is equal to the total power of the i-th component $e_i(t)$. Since all solutions tend to either of the two points corresponding to the largest eigenvalue, it is clear that the element picks out, at the steady-state, the component of largest total power as the output. This is one of the most fundamental properties of the element.

Even in the general case where the inputs are not restricted to gaussian signals, the 2N+1 points given by (27) are also equilibriums, where we should define

$$v_i^*=a\overline{z_i(t)\mathrm{sgn}[z_i(t)]}, \qquad i=1,2,\ldots,N. \tag{38}$$

Also, the equations (35),(37) still hold, if we define

$$\lambda_i=\overline{z_i(t)^2}, \qquad i=1,2,\ldots,N. \tag{39}$$

However, the stabilities of the equilibriums are not necessarily same to the above results, because in general they are affected by the waveforms of the inputs. In a special case, it is possible that N pairs of equilibriums are all stable. Stability of one point, for example, of $\underline{v}_k^*$ can be discussed using the linearlized equations

$$T\frac{d\eta_k(t)}{dt}+\eta_k(t)=0, \tag{40}$$

$$T\frac{d\mu_i(t)}{dt}+\mu_i(t)=-\frac{a}{v_k^*h}\frac{2}{\sum_{j=1}^{N}}\left\{\sum_{r=1}^{m}s_{r,r+1}\frac{z_i(t_r)z_j(t_r)}{\dot{z}_k(t_r)}\right\}\mu_j(t), \tag{41}$$

where

$$\mu_k(t)=(v_k(t)-v_k^*)/v_k^*,$$
$$\mu_i(t)=v_i(t)/v_k^*, \quad \text{for all } i\neq k, \tag{42}$$

and

t_r, r=1,2,...,m, are the time instants between t-h and t such that $z_k(t_r)=0$,

$s_{r,r+1}$, r=1,2,...,m, are the polarity of $z_k(t)$ between t_r and t_{r+1},

$$\dot{z}_k(t_r)=\frac{d}{dt}z_k(t)\Big|_{t=t_r}.$$

If $z_k(t)$ is a binary signal, the point $\underline{v}_k^*$ is stable, because $\dot{z}_k(t_r)=\infty$ for all r and the right side of (41) vanishes. For sin wave inputs equilibriums of a two-input element have been investigated. Let $z_1(t)=c_1\cos\omega t$, $z_2(t)=c_2\cos 2\omega t$. Then, $\underline{v}_1^*$ is stable or unstable according as $c_1\geq c_2$ or $c_1<c_2$, and $\underline{v}_2^*$ is stable or unstable according as $c_1<\sqrt{2}c_2$ or $c_1>\sqrt{2}c_2$. Let $z_1(t)=c_1\sin\omega t$, $z_2(t)=c_2\sin 2\omega t$. Then, $\underline{v}_1^*$ is always stable, and $\underline{v}_2^*$ is stable or unstable according as $c_1<\sqrt{2}c_2$ or $c_1>\sqrt{2}c_2$.

Simulations on an Analog Computer

A number of simulations were carried out to verify the theoretical results obtained above. A part of them will be shown in the following.

On an computer Hitachi ALM-502T, a two-input element,

$$y(t)=w_1(t)x_1(t)+w_2(t)x_2(t),$$

$$T\frac{dw_1(t)}{dt}+w_1(t)=ax_1(t)\mathrm{sgn}[y(t)],\quad T\frac{dw_2(t)}{dt}+w_2(t)=ax_2(t)\mathrm{sgn}[y(t)],$$

was simulated with the experimental value T=10s. As input signals, pseudo-random signals, sin waves and binary signals were used.

Simulation 1

Two pseudo-random signals were given as the inputs. That is,

$$x_1(t)=c_1n_1(t),\ x_2(t)=c_2n_2(t),$$

where $n_1(t)$ and $n_2(t)$ were obtained by passing a binary signal of M-sequence and its delayed replica through low pass filters. Their waveforms are shown in Fig.3. The phase-plane trajectories obtained with experimental values $c_1=1, c_2=0.8$ and $c_1=c_2=0.8$ are shown in Fig.4(a) and (b), respectively. They show good agreements with the theoretical trajectories shown in Fig.2.

Simulation 2

Two sin waves were given as the inputs. That is,

$x_1(t)=c_1 \sin 2t$, $x_2(t)=c_2 \sin 3.6t$.

With values $c_1=1, c_2=0.5$ and $c_1=1, c_2=0.8$, the experimental trajectories shown in Fig.5(a) and (b) were obtained, respectively. The results verify the theoretical prediction described above. The experimental trajectories obtained with values $c_1=0.5, c_2=1$ and $c_1=0.8, c_2=1$ are shown in Fig.6(a) and (b). If $x_1(t)=c_1 \sin 2t$, $x_2(t)=c_2 \sin 4t$, then $\underline{w}_1^*$ should be stable, but in this case the frequency of $x_2(t)$ is not just twice of that of $x_1(t)$ and their relative phase slowly varies with time. Thus, with values $c_1=0.5$, $c_2=1$, $\underline{w}_1^*$ becomes unstable. Similar results were also obtained with the inputs $x_1(t)=c_1 \cos 2t$, $x_2(t)=c_2 \cos 3.6t$.

Simulation 3

Two binary signals were given as the inputs. That is,

$x_1(t)=c_1 \mathrm{sgn}[\sin 2t]$, $x_2(t)=c_2 \mathrm{sgn}[\sin 3.6t]$.

With values $c_1=1, c_2=0.5$ and $c_1=2, c_2=0.5$, the trajectories shown in Fig.7(a) and (b) were obtained. In the ideal condition, $\underline{w}_2^*$ should be stable always, but the results show that when c_1 is 4 times as large as c_2, the point is practically unstable. Large fluctuation of $w_1(t)$ due to the large amplitude of $x_1(t)$ enables (w_1, w_2) to go out from a stable region restricted to the neighborhood of $\underline{w}_2^*$.

Simulation 4

When values of c_1, c_2 are changed with time, the stabilities of $\underline{w}_1^*, \underline{w}_2^*$ also change. A simulation result with the inputs

$x_1(t)=c_1 \sin 2t$, $x_2(t)=c_2 \sin 3.6t$

is shown in Fig.8(a). Fig.8(b) shows another example where the inputs used were

$x_1(t)=e_1(t)+e_2(t)$, $x_2(t)=e_1(t)-e_2(t)$,

$e_1(t)=c_1 \sin 2t$, $e_2(t)=c_2 \sin 3.6t$.

The result shows clearly that the selection of the output is performed on the basis of the total power of each component.

After all, it has been shown that without regard to initial values of $w_1(t), w_2(t)$, the element picks out the component of largest total power as the output, if its power is much larger than that of the other.

Discussions on Some Possible Applications

In this section let us discuss how the behavior of the element may be interpreted for some types of information processing.

A. Majority Decision Logic and Data Storage

Select an arbitrary family of N normalized orthogonal components $e_i(t)$. Let each input of the element be one of the components. Then, in the equilibriums, one of the components is given as the output. Thus, interpreting the output of i-th component as the representation of the state "i", we can use the element as a logical element of N states.

When a component $e_k(t)$ is fed to input terminals of number n_k, the total power of this component is equal to n_k. Thus, if n_k is much larger than the others, the element goes to the state "k". Majority decision logic can be obtained. Changing values of $n_1, n_2, \ldots, n_N$, we can make the element go to a new state. On the other hand, the element can remain at the last state, if all n_i have nearly same values. This means a data storage operation.

For example, consider a three-input element with three components $e_1(t)$, $e_2(t), e_3(t)$. Let $e_1(t)$ and $e_2(t)$ be fed to the first and second input terminals, respectively. Then, according as $e_1(t)$ or $e_2(t)$ is fed to the third terminal, the element goes to the state "1" or "2". If the third component $e_3(t)$ or no signal is fed to it, the element remains at the last state.

B. Pattern Dichotomy

Consider a sensory retina consisting of N units. Each sensory unit is connected to an input terminal of the element as shown in Fig.9(a). The i-th unit gives a binary output $u_i(t)=1$ or -1 according to the intensity of light on it. A sequence of patterns is presented to the retina, where each pattern belongs to one of the two categories "+", "-". Consider a zero-mean binary signal p(t). Let subsequences of patterns belonging to "+" or "-" be presented according as $p(t)=1$ or -1. Then, the signals $u_i(t)$ may be classified into three sets, i.e.,

the first set Ω_1: $u_i(t)=p(t)$ or $-p(t)$,

the second set Ω_2: $u_i(t)=1$ or -1,

the third set Ω_3: $u_i(t)$=binary random signals.

To satisfy the condition $\overline{x_i(t)}=0$, the transmission lines from the retina to the element are assumed to drop dc components of $u_i(t)$, i.e.,

$$x_i(t)=u_i(t)-\overline{u_i(t)}.$$

Hence,

$x_i(t)=p(t)$ or $-p(t)$ for $i \in \Omega_1$,

$x_i(t)=0$ for $i \in \Omega_2$,

$x_i(t)$=zero-mean random signals for $i \in \Omega_3$.

The inputs belonging to the second set play no role, but those belonging to the third set give disturbances. However, if the deformations of the sample

patterns presented are relatively small, then the total power of p(t) and -p(t) in the inputs would be much larger than those of other components, and the element would give the output of p(t) or -p(t). This means a pattern dichotomy.

C. Signal Filtering

When all the input terminals of the element are connected to a tapped delay line as shown in Fig.9(b), the element works as a filter. An essential property of the filter will be shown most clearly by giving a special form of input

$$x_i(t)=x_0(t-i\Delta), \qquad x_0(t)=\sum_{K=1}^{M}\sqrt{2}c_k\cos(k\omega_0 t+\theta_k), \tag{43}$$

where

$$2\pi/\omega_0=2M\Delta, \qquad M=N/2.$$

Taking $h=2\pi/\omega_0$, we obtain

$$r_{ij}=\sum_{K=1}^{M} c_k^2\cos k\omega_0(i-j) . \tag{44}$$

In this case, two eigenvectors correspond to one eigenvalue, i.e.,

$$\underline{w}_{ck}^*=\begin{bmatrix}\cos k\omega_0\Delta\\ \vdots\\ \cos ik\omega_0\Delta\\ \vdots\\ \cos 2Mk\omega_0\Delta\end{bmatrix}, \qquad \underline{w}_{sk}^*=\begin{bmatrix}\sin k\omega_0\Delta\\ \vdots\\ \sin ik\omega_0\Delta\\ \vdots\\ \sin 2Mk\omega_0\Delta\end{bmatrix}, \qquad \lambda_k=Mc_k^2, \qquad k=1,2,\ldots,M. \tag{45}$$

If λ_k is the largest, then the stable equilibriums are given by

$$\underline{w}_k^*=\sqrt{2}f\underline{w}_{ck}^*+\sqrt{2}g\underline{w}_{sk}^*, \tag{46}$$

where

$$f^2\cos^2\theta_k+g^2\sin^2\theta_k=c_k^2/4.$$

Therefore, the steady-state output is given by

$$y_k(t)^*=2Mc_k(A\cos k\omega_0 t+B\sin k\omega_0 t), \tag{47}$$

where

$$A=f\cos\theta_k+g\sin\theta_k, \qquad B=f\cos\theta_k-g\sin\theta_k.$$

Thus, the element picks out a pure sin wave, and it is the component of largest power. More generally, the input may be of the form

$$x_0(t)=\sum_{K=1}^{n}\sqrt{2}c_k\cos(\omega_k t+\theta_k), \qquad \omega_1<\omega_2<\cdots<\omega_n. \tag{48}$$

In this case, too, it can be shown that the element gives a nearly pure sinusoidal output, if

$$n\ll N, \qquad 2\pi/\omega_n\gg\Delta\gg 2\pi/N\omega_1.$$

When the input $x_0(t)$ is a sin wave corrupted by a random noise, it picks out

the sin wave as the output[10]. When input terminals of the element are connected, not to a tapped delay line but to an antena array, the element works as an automatic focussing device.

Conclusion

A new structure of linear threshold element with self-adjusting weights has been presented and its dynamic behavior has been investigated in detail by an analysis and some simulations. It has been shown that the element has a tendency to separate its inputs into a family of orthogonal components and to pick out the component of largest power. This property can be applied to a variety of types of information processing such as majority decision logic, data storage, pattern dichotomy and signal filtering.

Acknowledgment

The author wishes to acknowledge Prof. T.Isobe for his guidance and encouragement.

References

[1] F.Rosenblatt,"Perceptual generalization over transformation groups", Self-Organizing Systems, New York:Pergmon Press, pp.63-100 (1960).

[2] H.D.Block et al.,"Analysis of four-layer series-coupled perceptron", Rev. Mod. Phys., vol.34, no.1, pp.135-142 (1962).

[3] E.R.Caianiello,"Outline of a theory of thought-processes and thinking machines", J. Theoret. Biol., vol.2, no.2, pp.204-235 (1961).

[4] C.J.Jakowatz et al.,"Adaptive waveform recognition", Proc. of the 4-th London Symp. on Information Theory, Washington, D.C.:Butterworths, pp.317-326 (1961).

[5] E.M.Glaser,"Signal detection by adaptive filters", IRE Trans. on Information Theory, vol.IT-7, no.2, pp.87-98 (1961).

[6] D.B.Cooper and P.W.Cooper,"Adaptive pattern recognition and signal detection without supervision", IEEE International Conv. Rec., pp.246-257 (1964).

[7] H.J.Scudder,"Adaptive communication recievers", IEEE Trans. on Information Theory, vol.IT-11, no.2, pp.167-174 (1965).

[8] E.M.Braverman,"The method of potential functions in the problem of training machines to recognize patterns without a trainer", Automation and Remote Control, vol.27, no.10, pp.1728-1736 (1967).

[9] B.Widrow,"Bootstrap learning in threshold logic systems", Proc. of the 3rd congress of IFAC, pp.14D.1-10 (1966).

[10] I.Morishita,"A multiparameter self-adjusting system for adaptive extraction of unknown signals", Proc. of the 3rd congress of IFAC, pp.41D.1-7 (1966).

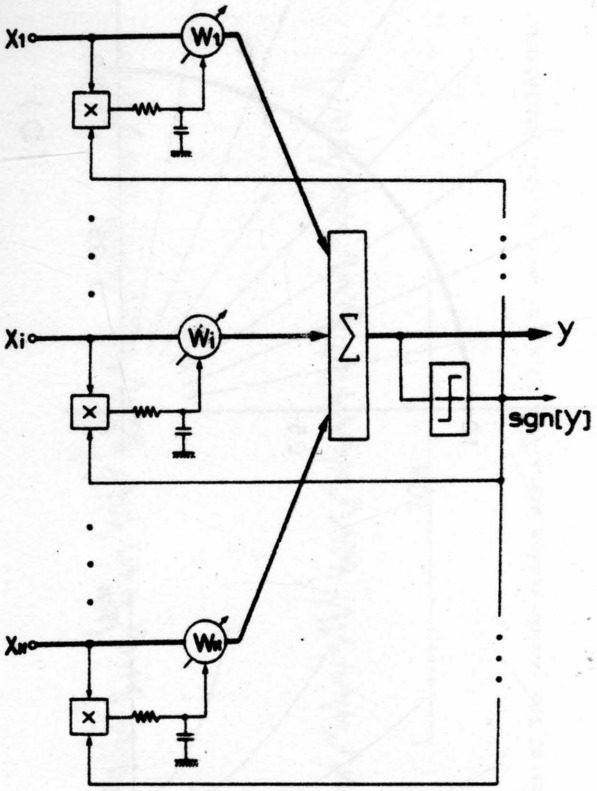

Fig.1. Block diagram of the element.

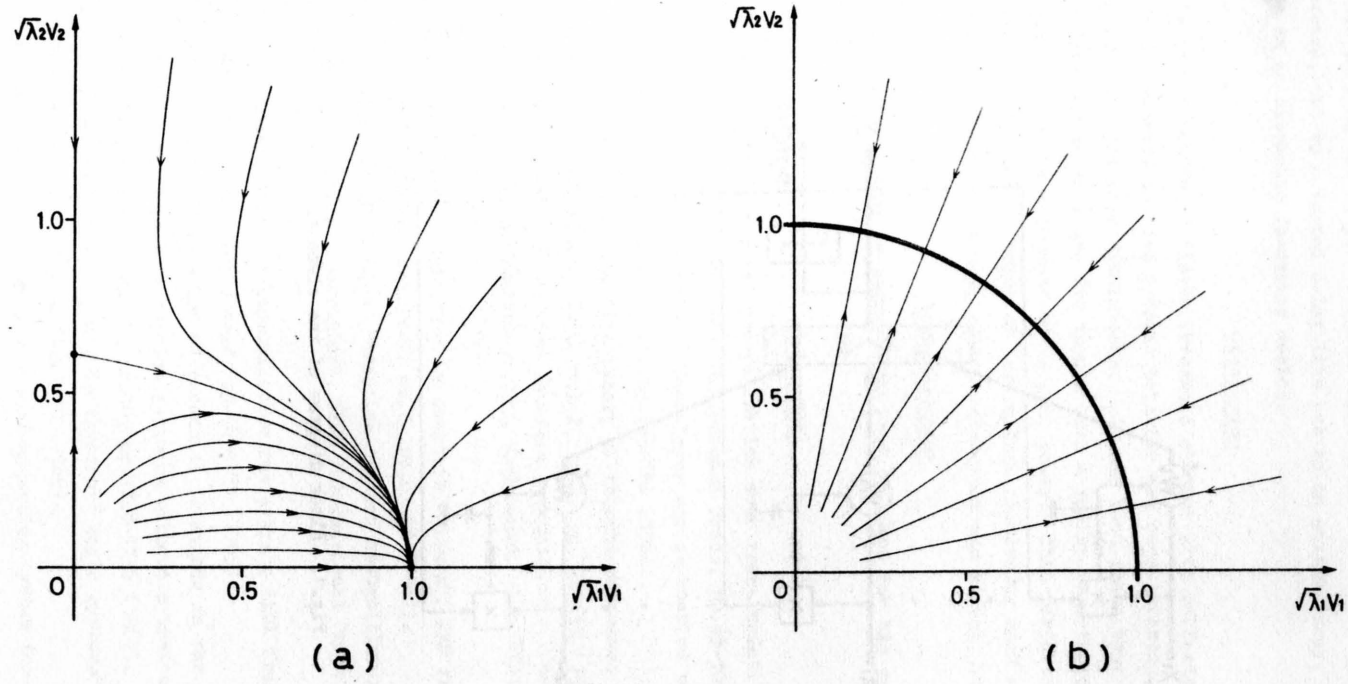

Fig.2. Theoretical phase-plane trajectories for gaussian signal inputs.
(a) $\lambda_1=1$, $\lambda_2=0.6$. (b) $\lambda_1=\lambda_2=1$.

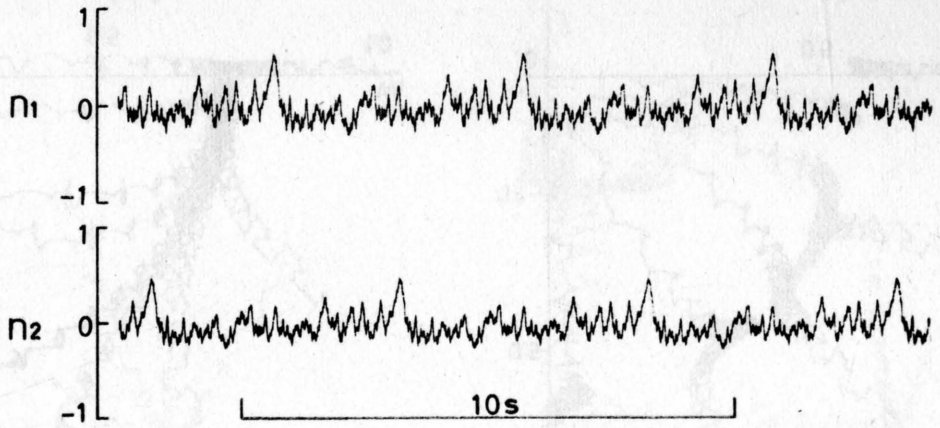

Fig.3. Waveforms of the pseudo-random signals $n_1(t), n_2(t)$ used in the simulation.

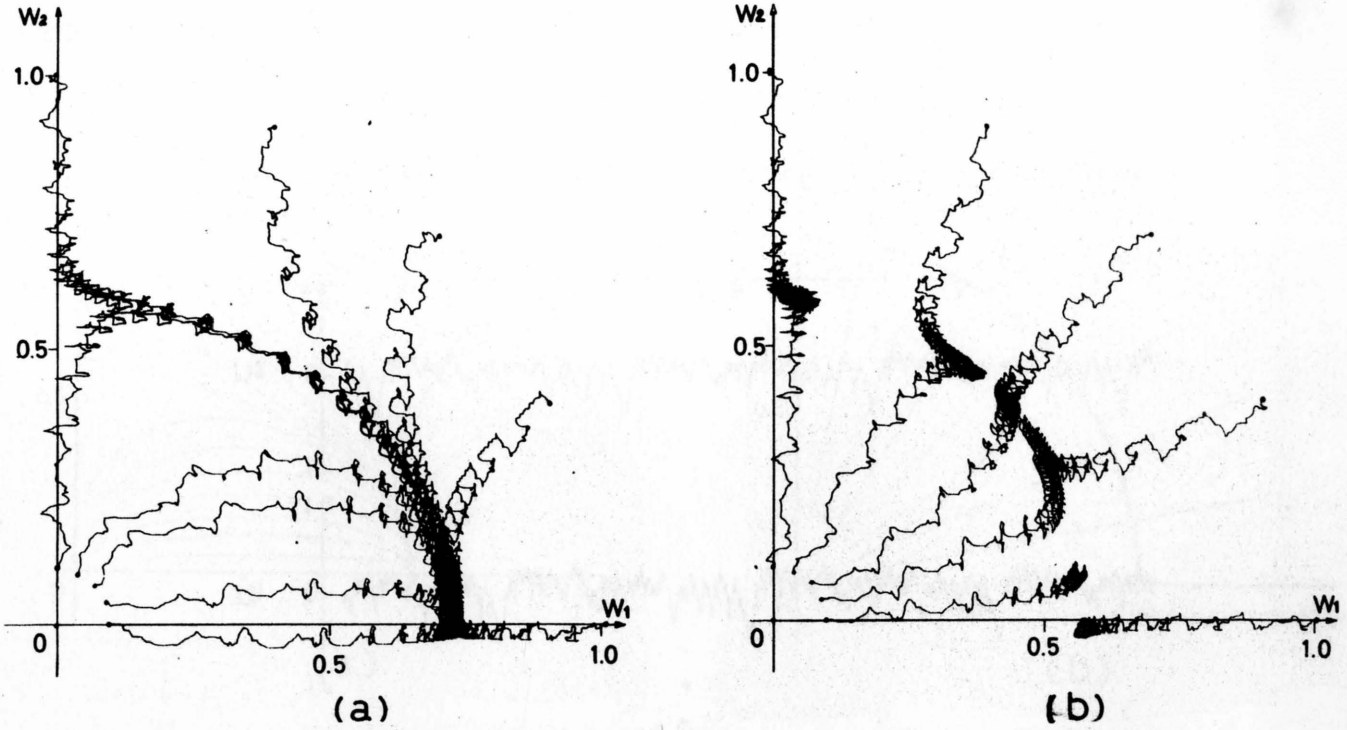

Fig.4. Experimental phase-plane trajectories for the pseudo-random signal inputs, $x_1(t)=c_1n_1(t)$, $x_2(t)=c_2n_2(t)$. (a) $\lambda_1:\lambda_2=c_1^2:c_2^2=1:0.64$. (b) $\lambda_1:\lambda_2=c_1^2:c_2^2=1:1$.

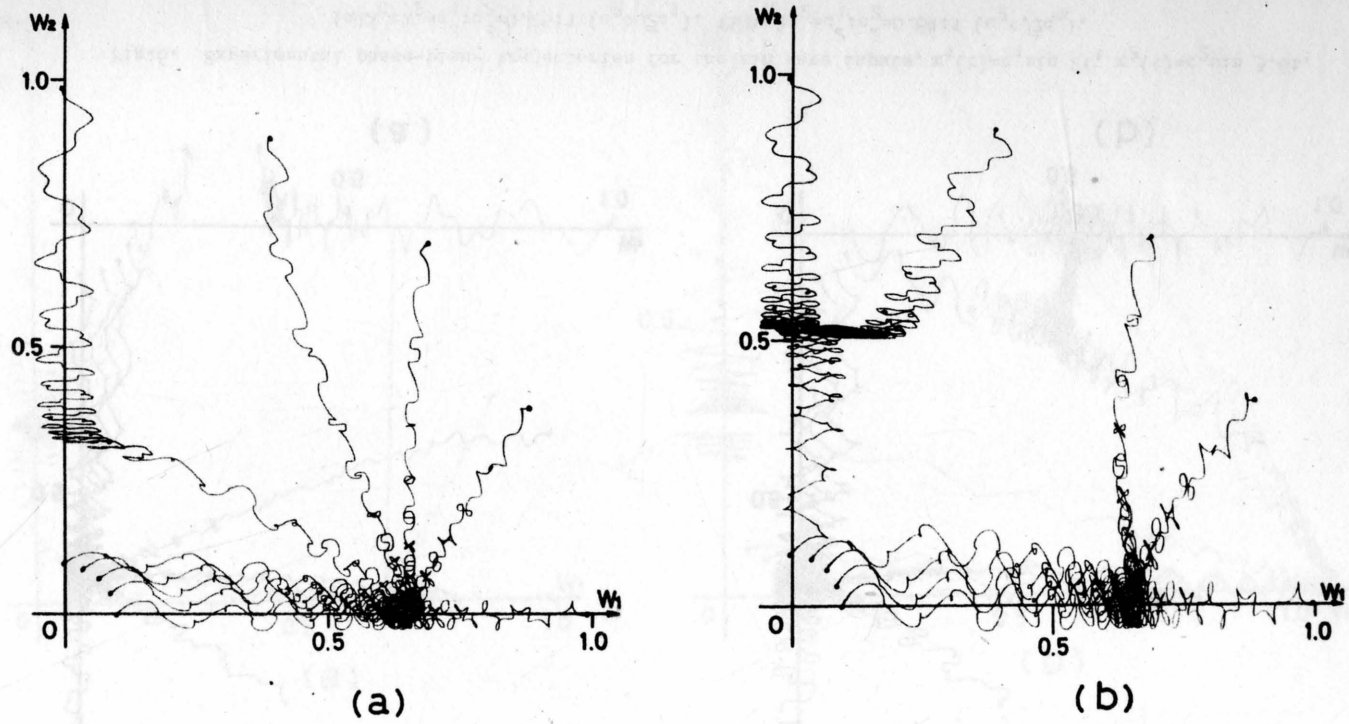

Fig.5. Experimental phase-plane trajectories for the sin wave inputs, $x_1(t)=c_1 \sin 2t$, $x_2(t)=c_2 \sin 3.6t$. (a)$\lambda_1:\lambda_2=c_1^2:c_2^2=1:0.25$ $(c_1>\sqrt{2}c_2)$. (b)$\lambda_1:\lambda_2=c_1^2:c_2^2=1:0.64$ $(c_1<\sqrt{2}c_2)$.

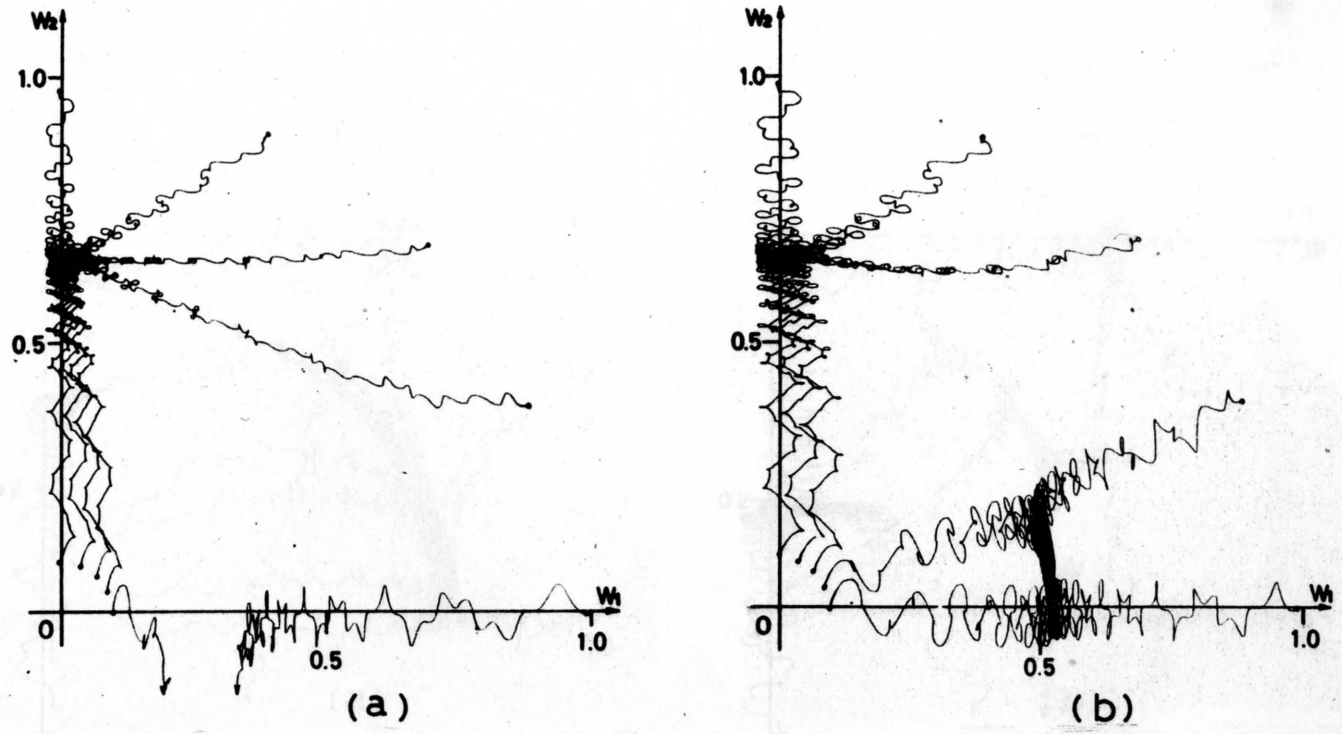

Fig.6. Experimental phase-plane trajectories for the sin wave inputs, $x_1(t)=c_1 \sin 2t$, $x_2(t)=c_2 \sin 3.6t$. (a) $\lambda_1:\lambda_2=c_1^2:c_2^2=0.25:1$ ($c_2>\sqrt{2}c_1$). (b) $\lambda_1:\lambda_2=c_1^2:c_2^2=0.64:1$ ($c_2<\sqrt{2}c_1$).

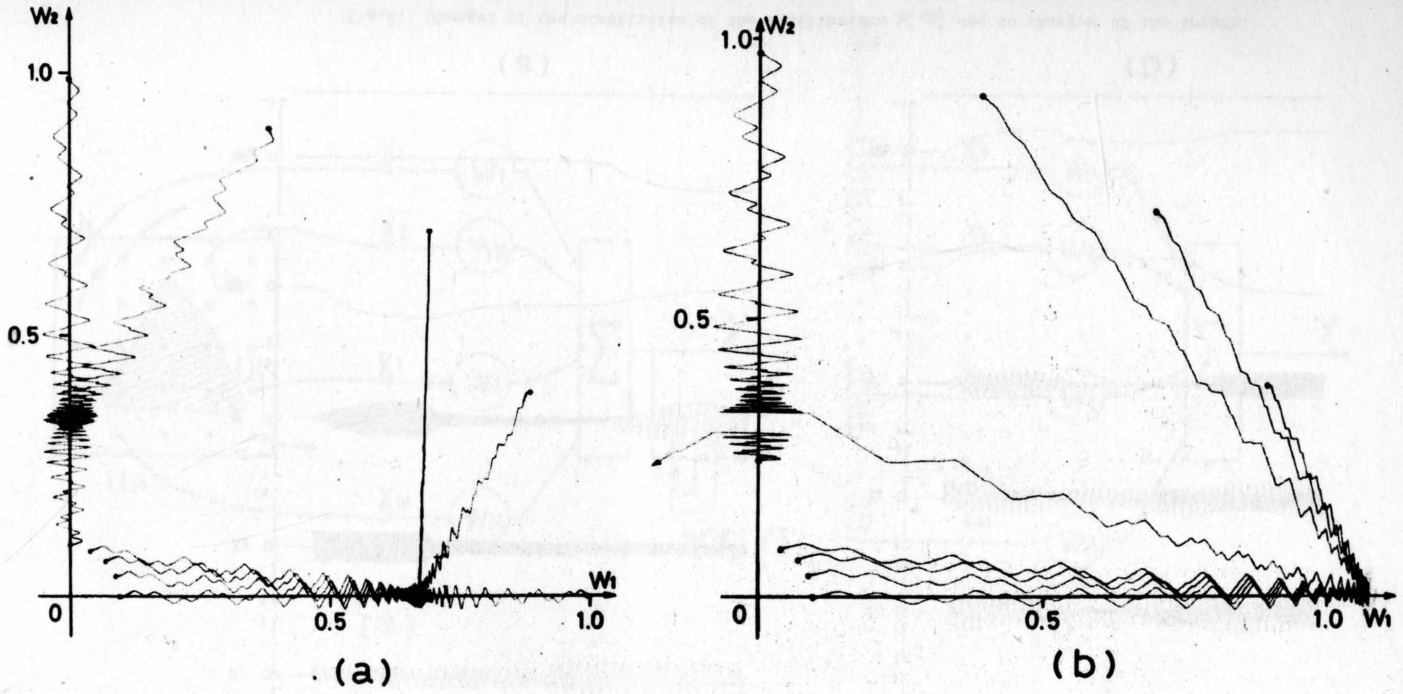

Fig.7. Experimental phase-plane trajectories for the binary signal inputs, $x_1(t)=c_1 \text{sgn sin } 2t$, $x_2(t)=c_2 \text{sgn sin } 3.6t$. (a)$\lambda_1:\lambda_2=c_1^2:c_2^2=1:0.25$. (b)$\lambda_1:\lambda_2=c_1^2:c_2^2=4:0.25$.

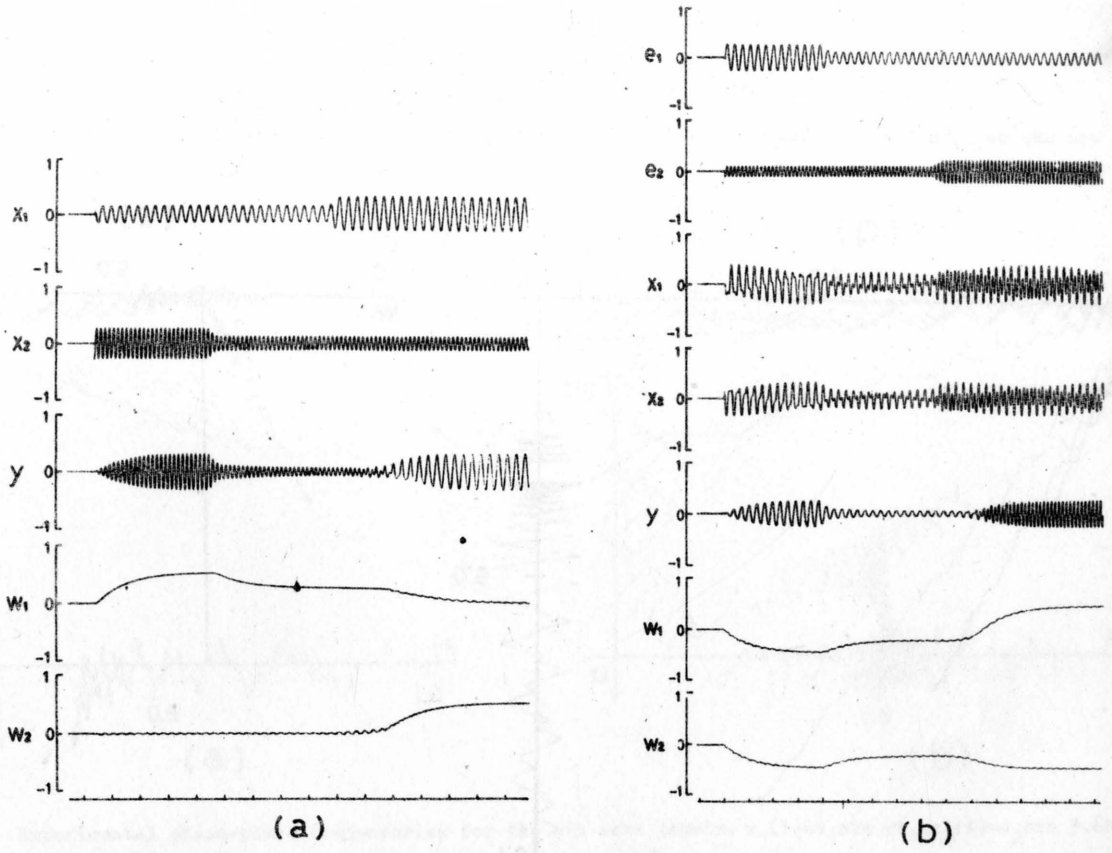

Fig.8. Changes of the stabilities of the equilibriums $\underline{w}_1^*, \underline{w}_2^*$ due to changes of the inputs.
(a)$x_1(t)=c_1(t)\sin 2t$, $x_2(t)=c_2(t)\sin 3.6t$. (b)$x_1(t)=c_1(t)\sin 2t+c_2(t)\sin 3.6t$, $x_2(t)=c_1(t)\sin 2t-c_2(t)\sin 3.6t$.

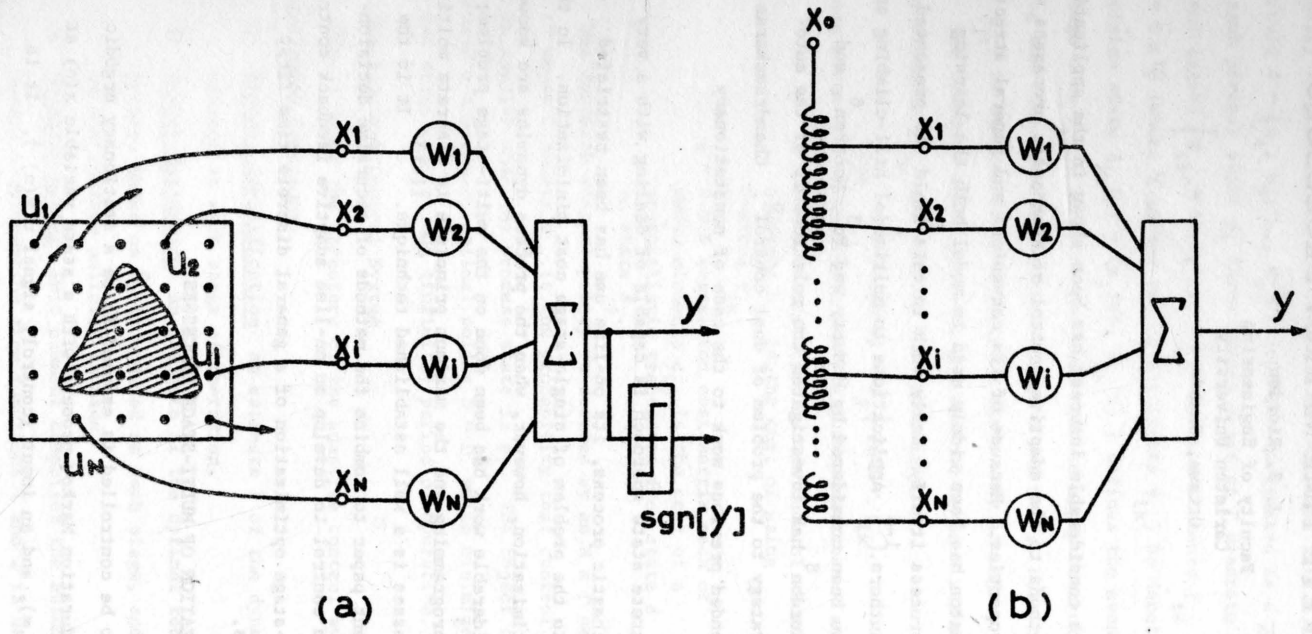

Fig.9. Two applications of the element. (a)The element connected to a retina works as a pattern dichotomizer. (b) The element connected to a tapped delay line works as a filter.

AN ADAPTIVE AUTOMATON CONTROLLER FOR DISCRETE TIME MARKOV PROCESSES

J. S. Riordon
Faculty of Engineering
Carleton University
Ottawa, Canada

1. INTRODUCTION

In recent years considerable interest has been shown in the application of discrete state methods to the adaptive control of stochastic processes with uncertain dynamic properties. Because of its convenient and general structure, the stochastic automaton has been widely used to model both the learning controller and the process itself. Early work in this field was presented by a number of Soviet authors.[1-4] Applications to multimodal hill-climbing and adaptive control have been considered by McMurty and Fu[5], McLaren[6], and Nikolic and Fu[7]. Riordon[8] has investigated the relationship of the automaton controller strategy to the problem of dual control[9]. Chandrasekaran and Shen[10] have extended previous work to the case of nonstationary processes.

While the discrete state approach is capable of dealing with a very general type of stochastic process, its on-line use has been restricted almost exclusively to the problem of single-stage cost minimization. In the case of off-line optimization, however, when the process dynamics are known statistically, considerable work has been done on the multi-stage problem; the use of dynamic programming and the maximum principle in discrete multi-stage decision processes is a well established technique.[11-13] It is the purpose of the present paper to combine the methods of recursive decision-making and automaton control to develop an on-line adaptive feedback control algorithm for multi-stage optimization of a general discrete time first order Markov process.

2. ADAPTIVE OPTIMIZATION OF MULTI-STAGE PROCESSES

2.1 Process Model

The process to be controlled is assumed to be a stationary ergodic discrete time long duration Markov process with a state variable $x(n)$ at stage $n(n=0,1,2, \ldots\infty)$, and an input (control) signal $u(x(n))$. It is assumed that the state is completely observable, so that the output is also

x(n). Variables x and u will be considered as scalars, although this is not necessary in principle. The output x is quantized into a set of N discrete intervals $\Phi = \{\phi_1, \phi_2, \ldots \phi_N\}$, each one designated as a process state. For each process state ϕ_i there exists a set of Γ discrete alternative control inputs $\{\psi_{ik}, k=1,2, \ldots \Gamma\}$. Let the elements ξ_{ik} of the space $\Xi = \Phi \times \Psi$ (where Ψ is the set of all inputs ψ_{ik}) be denoted decision states. A decision state $\xi_{ik}(n) = (\phi_i(n), \psi_{ik}(n))$ defines the event, "process state at stage n is ϕ_i; a decision has been made to apply control alternative k during the time interval between stages n and n+1". Note that the pair (ϕ_i, ψ_{jk}) is admissible as a decision state only if i=j.

The discrete state dynamics are defined by an N x N x Γ 3-matrix P whose elements p_{ijk} are unknown but stationary.

$$p_{ijk} = pr\,[\,\phi(n+1) = \phi_j \mid \xi(n) = \xi_{ik}] \qquad (1)$$

Process costs are defined by known stationary matrices B and C, where

B = N x Γ control cost matrix each of whose elements b_{ik} is the cost of using control ψ_{ik}.

C = N x N transition cost matrix each of whose elements c_{ij} is the cost of a probabilistic transition from state ϕ_i to state ϕ_j.

The feedback control policy is defined by an N x Γ decision matrix D each of whose elements d_{ik} is the probability that control alternative ψ_{ik} will be applied when the process state is ϕ_i. The object of control is to determine a stationary optimal policy $D = D^*$ which minimizes the expected cost per stage over a long (infinite) period of operation.

2.2 The Adaptive Control System

Fig. 1 shows the structure of the adaptive control system, comprising the following functions:

1. Process Identification An estimate $\hat{P}$ of the dynamics P is updated at each stage of operation.
2. Policy Estimation An estimate of the optimal feedback control policy, based on $\hat{P}$, is updated at each stage, and an evaluation of alternative policies is made.
3. Decision Making This element comprises the automaton controller proper. Information from functions 1 and 2 is used to select

one of the Γ alternative control actions for a given process state $\phi_i(n)$ at each stage n.

4. Model Structure Adjustment If x and u are continuous, then the quantization levels are themselves parameters of the overall system which must be optimized. This function is performed by a slow-acting outer loop operating at a higher level of adaptation than 1,2, and 3.

Each of these functions will now be examined in more detail.

2.3 Process Identification

The results of observed process transitions $\xi_{ik}(n) \rightarrow \phi_j(n+1)$ are stored in an N x N x Γ integer 3-matrix M each of whose elements m_{ijk} is the number of observed transitions from state ϕ_i to state ϕ_j when the control action is ψ_{ik}. Maximum likelihood estimates of the elements of P are given by

$$\hat{p}_{ijk} = \frac{m_{ijk}}{n_{ik}} \tag{2}$$

where $$n_{ik} = \sum_{j=1}^{N} m_{ijk} \tag{3}$$

The expected cost of one stage of operation starting from decision state ξ_{ik} is denoted μ_{ik}. For large values of n_{ik} (obtained in a long duration process), its estimator is normally distributed[14] with maximum likelihood value

$$\hat{\mu}_{ik} = b_{ik} + \sum_{j=1}^{N} \hat{p}_{ijk}\, c_{ij} \tag{4}$$

and estimated variance

$$\hat{\sigma}_{ik}^2 = \frac{1}{n_{ik}} \sum_{j=1}^{N} \hat{p}_{ijk}\,(1-\hat{p}_{ijk})\, c_{ij}^2 - 2 \sum_{j=1}^{N-1} \sum_{q=j+1}^{N} \hat{p}_{ijk}\, \hat{p}_{iqk}\, c_{ij}\, c_{iq} \tag{5}$$

2.4 Policy Estimation

Two problems are involved in policy estimation. The first is that of computing the estimated optimal policy $\hat{D}^*(n) = \left[D^* \mid P = \hat{P}(n)\right]$. The second is that of updating $\hat{D}^*(n)$ to obtain $\hat{D}^*(n+1)$ when a new observation changes $\hat{P}(n)$ to $\hat{P}(n+1)$. The first of these may be solved by the use of a variant of a well

known algorithm[11], necessary details of which will be stated here without derivation. Let the matrix $\hat{R}$ be defined by

$$\hat{r}_{ij} = \sum_{k=1}^{\Gamma} d_{ik}\, \hat{P}_{ijk} \qquad (6)$$

$$= pr\,[\phi(n+1) = \phi_j \mid \phi(n) = \phi_i;\ \hat{P},\ D\,]$$

and $$\hat{\ell}_i = \sum_{k=1}^{\Gamma} d_{ik}\, \hat{\mu}_{ik} \qquad (7)$$

A set of N adjoint variables $\hat{v}_i$, i=1,2, ...N may be defined, in which $\hat{v}_N = 0$ without loss of generality. If $\hat{g}$ is the conditional estimate of the expected cost per stage, then steady state operation is described by N simultaneous equations

$$\hat{v}_i = \hat{\ell}_i + \sum_{j=1}^{N} \hat{r}_{ij}\, \hat{v}_j \quad -\hat{g} \qquad (8)$$

Let $\hat{T} =$

$$\begin{bmatrix} \hat{r}_{11} & \hat{r}_{12} & \cdots & \hat{r}_{1(N-1)} & -1 \\ \hat{r}_{21} & \hat{r}_{22} & \cdots & \hat{r}_{2(N-1)} & -1 \\ \vdots & \vdots & & \vdots & \vdots \\ \hat{r}_{(N-1)1} & \hat{r}_{(N-1)2} & \cdots & \hat{r}_{(N-1)(N-1)} & -1 \\ \hat{r}_{N1} & \hat{r}_{N2} & \cdots & \hat{r}_{N(N-1)} & 0 \end{bmatrix} \qquad (9)$$

$$\underline{\hat{\ell}} = (\hat{\ell}_1, \hat{\ell}_2, \ldots \hat{\ell}_N)^T \qquad (10)$$

and define a column vector $\underline{\hat{z}}$ such that

$$\begin{aligned} \hat{z}_i &= \hat{v}_i \qquad i = 1,2, \ldots N-1 \\ \hat{z}_N &= \hat{g} \end{aligned} \qquad (11)$$

Then (8) becomes

$$\underline{\hat{z}} = \hat{T}\, \underline{z} + \underline{\hat{\ell}}$$

i.e. $$\underline{\hat{z}} = \hat{Q}^{-1}\, \underline{\hat{\ell}} \qquad (12)$$

where $\hat{Q} = (I - \hat{T})$

I = identity matrix

For any policy D, solution of (12) allows the computation of a set of variables

$$\hat{\eta}_{ik} = \hat{\mu}_{ik} + \sum_{j=1}^{N} \hat{P}_{ijk}\, \hat{v}_j \tag{13}$$

Policy improvement is obtained by adjustment of each of the N rows of D to achieve the minimum

$$\underset{D}{\text{Min}} \left\{ \sum_{k=1}^{\Gamma} d_{ik}\ \hat{\eta}_{ik} \right\}, \quad i=1,2, \ldots N \tag{14}$$

Iteration of (12), (13) and (14) results in a stationary optimal policy $D = \hat{D}^*$. Kashyap[12] has shown that if P is known, then the elements of D^* are either zero or unity; that is, a deterministic feedback policy is optimal. While $\hat{D}^*$ is similarly deterministic at any stage, it is subject to change as new process information becomes available. For a given set $\left\{B,C,\hat{P},\hat{D}^*\right\}$ every element $\hat{d}^*_{ik}$ of row i of $\hat{D}^*$ is zero except element $\hat{d}^*_{i\hat{s}}$, where the control alternative $\hat{s}=\hat{s}(i)$ is defined by

$$\hat{\eta}_{i\hat{s}} = \underset{k}{\text{Min}} \left\{ \hat{\eta}_{ik} \right\} \tag{15}$$

At stage n of the process a transition $\xi_{ik}(n) \rightarrow \phi_j(n+1)$ causes element m_{ijk} to be incremented by one unit. Equation (2) shows that only one row of $\hat{P}(n)$ need be altered to obtain $\hat{P}(n+1)$. While the updated policy estimate $\hat{D}^*(n+1)$ could be completely recomputed using the new data, such a procedure would be computationally prodigal. Instead, a simple method of updating $\hat{Q}^{-1}$ recursively will be introduced to eliminate the requirement for a matrix inversion on-line at each stage of the process.

Equations (6) and (15) show that

$$\hat{r}_{ij}(n) = \hat{p}_{ijk}(n) \Big|_{k=\hat{s}(i,n)} \quad i,j = 1,2, \ldots N \tag{16}$$

Suppose that a transition from decision state $\xi_{i\hat{s}}$ is observed at stage n. Matrix $\hat{P}(n+1)$ is easily obtained from (2). The problem is to determine whether the estimated optimal control policy remains unchanged; i.e., whether $\hat{s}(i,n+1) = \hat{s}(i,n)$ for each state ϕ_i. Initially, let

$$\hat{r}_{ij}(n+1) = \hat{p}_{ijk}(n+1) \Big|_{k=\hat{s}(i,n)} \quad i,j=1,2, \ldots N \tag{17}$$

so that no change is assumed in $\hat{D}^*$. Also, let

$\underline{e}_i >$ = N element column vector of zeros, except element i which is unity.

$\underline{w} >$ = N element column vector of units

and let the symbols $\cdot>$, $<\cdot$, $<\cdot\cdot>$, and $\cdot><\cdot$ represent respectively

a column vector, a row vector, an inner product, and an outer product (dyad).

As a result of the observed transition $\xi_{is}\hat{}(n) \rightarrow \phi_j(n+1)$ only one row of $\hat{R}(n)$ is modified; i.e.,

$$\hat{R}(n+1) = \hat{R}(n) + \underline{e}_i > < \underline{e}_i \ (\hat{R}(n+1) - \hat{R}(n)) \tag{18}$$

From (9), $\hat{T}(n)$ is given by

$$\hat{T}(n) = \hat{R}(n) \ (I - \underline{e}_N > < \underline{e}_N) - \underline{w} > < \underline{e}_N + \underline{e}_N > < \underline{e}_N \tag{19}$$

so that

$$\hat{Q}(n) = (I + \underline{w} > < \underline{e}_N - \underline{e}_N > < \underline{e}_N) + \hat{R}(n) \ (\underline{e}_N > < \underline{e}_N - I) \tag{20}$$

From (18) and (20)

$$\hat{Q}(n+1) = \hat{Q}(n) + \underline{e}_i > < \underline{\alpha} \tag{21}$$

where $< \underline{\alpha} = < \underline{e}_i \ (\hat{R}(n+1) - \hat{R}(n)) \ (\underline{e}_N > < \underline{e}_N - I)$ (22)

Application of the matrix inversion lemma to (21) yields

$$\hat{Q}^{-1}(n+1) = \hat{Q}^{-1}(n) - \hat{Q}^{-1}(n) \ \underline{e}_i > (< \underline{\alpha} \ \hat{Q}^{-1}(n) \ \underline{e}_i > + 1)^{-1} < \underline{\alpha} \ \hat{Q}^{-1}(n) \tag{23}$$

Since the inverted term is a scalar, (23) becomes

$$\hat{Q}^{-1}(n+1) = \hat{Q}^{-1}(n) - \frac{\hat{Q}^{-1}(n) \ \underline{e}_i > < \underline{\alpha} \ \hat{Q}^{-1}(n)}{< \underline{\alpha} \ \hat{Q}^{-1}(n) \ \underline{e}_i > + 1} \tag{24}$$

Inversion of $\hat{Q}$, the most time-consuming step in the policy estimation procedure, is therefore reduced to a simple recursive equation. Once $\hat{Q}^{-1}(n+1)$ is obtained, equations (12) - (14) are applied to determine whether or not $\hat{D}^*(n+1)$ differs from $\hat{D}^*(n)$. If it does not (this is the usual case), then updating is complete. Otherwise a modified version of $\hat{Q}(n+1)$ must be derived from $\hat{D}^*(n+1)$ by means of (6) and (20), and inverted. Iterative policy improvement then takes place, as previously discussed. Note that the procedure is simplified when an exploratory control action ψ_{ik}, $k \neq \hat{s}(i,n)$, is chosen at stage n; in such a case $\hat{R}(n+1) = \hat{R}(n)$ from (17), and it is unnecessary to update $\hat{Q}^{-1}(n)$ before testing the estimated control policy. A flow diagram of the on-line updating procedure is shown in fig. 2.

It can be shown[15] that the elements of row N of $\hat{Q}^{-1}(n)$ are $\hat{\pi}_1(n)$, $\hat{\pi}_2(n)$ ... $\hat{\pi}_N(n)$, where $\hat{\pi}_i(n)$ is the estimate, conditional on $\hat{P}(n)$, of the steady state probability of occupancy of process state ϕ_i. These parameters may be used for the adaptive quantization of the continuous state variable

x (see section 2.6).

2.5 Decision Making: The Dual Control Problem

When P is known, the optimal control policy D* may be computed off-line. A strategy is defined here as an on-line learning algorithm which attempts simultaneously to control the process and to discover the optimal policy when P is uncertain. In a long duration stationary process a strategy is said to be convergent if its use reduces the error probability to zero asymptotically (all $n_{ik} \to \infty$), and if the strategy itself asymptotically assumes the form of the true optimal policy.

In this section known results for the adaptive control of repetitive single-stage processes are extended to the multi-stage case by consideration of the latter as a series of single-stage decisions which are modified by, and interact through, the adjoint cost variables $\hat{v}_j$. At each stage of the process the strategy used to seek $\eta_{is} = \text{Min}\left\{\eta_{i1} \ldots \eta_{i\Gamma}\right\}$ is that which incurs minimum expected cost for a given reduction of the single-stage error probability Ω_i, where

$$\Omega_i = \text{pr}\left[\ \hat{s}(i) \neq s(i) \ \middle|\ M, B, C\ \right] \tag{25}$$

It is assumed that the estimates of $\left\{\eta_{ik}\right\}$ are normally distributed with conditional means $\left\{\hat{\eta}_{ik}\right\}$ given by (13) and variances $\left\{\hat{\sigma}^2_{ik}\right\}$ given by (5). The latter approximation, introduced for the sake of computational feasibility, ignores the variance of the last term of (13), but does not preclude the convergence of the strategy. Following the results of Riordon[8] (in which a derivation and proof of convergence of the single-stage strategy is given), a mixed strategy is used. The control decision is decomposed into two parts:

1. For a given ϕ_i, the probability θ_i of choice of the estimated optimal control action $\psi_{i\hat{s}}$ is given by

$$\begin{aligned} \theta_i &= 1 - \gamma\,\Omega_i \quad , \quad \gamma\,\Omega_i < 0.5 \\ &= 0.5 \quad , \quad \gamma\,\Omega_i \geq 0.5 \end{aligned} \tag{26}$$

   where γ is a constant fixed by the designer.

2. If $\psi_{i\hat{s}}$ is not chosen, then ψ_{ik}, $k \neq \hat{s}(i)$, is chosen so that

$$\frac{\exp(-\hat{\rho}_{ik}^2/2)}{n_{ik}\,\hat{\sigma}_{ik}} = \max_{\substack{q=1,2,\ldots\Gamma \\ q\neq\hat{s}(i)}} \left[\frac{\exp(-\hat{\rho}_{iq}^2/2)}{n_{iq}\,\hat{\sigma}_{iq}} \right] \tag{27}$$

where $$\hat{\rho}_{iq} = \frac{\hat{\eta}_{iq} - \hat{\eta}_{is}}{\hat{\sigma}_{iq}} \tag{28}$$

The value of Ω_i is given by[8]

$$\Omega_i = \sum_{\substack{k=1 \\ k\neq\hat{s}}}^{\Gamma} F_{ik}\ (\hat{\eta}_{i\hat{s}}) \tag{29}$$

where F_{ik} is a gaussian cumulative distribution function

$$F_{ik}(x) = \frac{1}{(2\pi)^{\frac{1}{2}}\,\hat{\sigma}_{ik}} \int_{-\infty}^{x} \exp\left[-\frac{1}{2}\left(\frac{y - \hat{\eta}_{ik}}{\hat{\sigma}_{ik}} \right)^2 \right] dy \tag{30}$$

The value of Ω_i is easily determined on-line by interpolation from a look-up table of normalized values of $F_{ik}(x)$. For γ constant, all values Ω_i, $i\neq s$, tend to zero with this strategy, so that the asymptotic probability of a correct control choice for every state ϕ_i tends to unity.

The parameter γ is known as the convergence factor. A high value of γ causes Ω_i to decrease rapidly by increasing the tendency of the automaton controller to experiment for estimation purposes; concomitantly a high operating cost is incurred early in the life of the process. A lower value of γ yields slower convergence, but spreads the estimation cost over a longer period of time.

2.6 Model Structure Adjustment

It is assumed that for any state ϕ_i the alternatives $\psi_{i1}, \ldots \psi_{i\Gamma}$ are samples of a continuous control variable $u_i(\phi_i)$ and that parameters $\eta_{ik}(\psi_{ik})$ are samples of a continuous variable $\eta_i(u_i)$. Then for minimum cost operation of the automaton model, one of the discrete control alternatives must be made equal to u_i^*, the value of u_i which minimizes η_i.[16] Suppose the control alternatives constitute an ordered set in which $\psi_{i1} < \psi_{i2} < \ldots < \psi_{i\Gamma}$. When P is uncertain, a first approximation to optimal control quantization is obtained (under the assumption that g is at least a locally unimodal function of u_i) if $\psi_{i\hat{s}}$ is an interior member of the set $\psi_i = \left\{ \psi_{i1} \ldots \psi_{i\Gamma} \right\}$, or is at a control constraint boundary.

To attain this goal, the structure adjustment loop in fig. 1 adjusts the quantization of u adaptively. If $\hat{s}(i) = 1$ and Ω_i is less than some threshold value, say 0.5, the range of u_i spanned by the set ψ_i is shifted by adjoining a new quantum level $\psi_{i0} < \psi_{i1}$ and deleting the maximum control level $\psi_{i\,\Gamma}$. Matrices M, $\hat{P}$, and B are modified, the rows of M and $\hat{P}$ corresponding to the new decision state being set by some a priori estimate. Similarly if $\hat{s}(i) = \Gamma$ with probability greater than 0.5, the whole range is shifted in a positive direction. In this way the control range for each state ϕ_i "creeps" either upward or downward until $1 < \hat{s}(i) < \Gamma$ or a control constraint is reached. When this adjustment procedure is complete, more sophisticated methods of stochastic hill climbing[17] may be used to determine an interpolated value of u_i^*, so that asymptotically a control input $\psi_{i\hat{s}} = \psi_{is} = u_i^*$ is selected.

A further structure adjustment loop may be added to modify the quantization of x. One way of achieving efficient state quantization is to vary the intervals covered by states ϕ_i until the steady state probabilities of occupancy, π_i, are all equal.[18] Estimates $\hat{\pi}_i(n)$ may be obtained on-line directly from the N^{th} row of matrix $\hat{Q}^{-1}(n)$, and the intervals adjusted accordingly. Because $\hat{\pi}_1, \ldots \hat{\pi}_N$ are functions of the control policy, this adaptive loop should be placed outside the control quantizing loop.

3. SIMULATION RESULTS

3.1 The Process[16]

Consider a heat treatment process involving an endothermic reaction for temperatures below 800°A, and an exothermic reaction for higher temperatures. The process dynamics are

$$x(n+1) = x(n)\left\{1.005 + 0.015 \tanh\left[0.1(x(n) - 803.446\right]\right\} + 0.00333\, u(n) + \zeta_1(n) + \zeta_2(n) + \zeta_3(n) + \zeta_4(n) \qquad (31)$$

where $x(n)$ = temperature (°A) at stage n.

$u(n)$ = heat input (kilocalories) at stage n.

$\zeta_1 \ldots \zeta_4$ are independent samples drawn from normal zero-mean distributions with the following respective standard deviations σ_i:

$$\sigma_1 = 0.0002\, x(n)\, y\, |x(n) - 800|$$
$$\sigma_2 = 0.005\, x(n)\, [1 + |x(n) - 800|^{\frac{1}{2}}]^{-1}$$
$$\sigma_3 = 0.0005\, |u| \qquad (32)$$
$$\sigma_4 = 1$$
$$y = 1, \quad x(n) > 800; \quad y = 0, \quad x(n) \leq 800$$

The object of control is to maintain the temperature at or near 800°A, which is a point of unstable equilibrium. Note that the dynamics are non-linear and that the disturbance is a function of both state and control. The state-dependent cost L_1 defines the cost in cents of deviations from the desired temperature:

$$L_1(x(n), x(n+1)) = 0.015\, [(x(n) - 800)^2 + (x(n+1) - 800)^2], \quad x < 850 \qquad (33)$$

If $x(n+1) \geq 850°$, then a shutdown occurs at a cost of \$28.80 and the process is re-started at x = 775°.

Heating and cooling effort costs two cents per 1000 kilocalories. If extremes of heating and cooling are used, a penalty cost is incurred owing to a reduction in the expected lifetime of the control equipment. In any case $|u(n)|$ cannot exceed 10^4 kilocalories. Control cost in cents is given by

$$L_2(u(n)) = 0.002\, |u(n)| + 60 \left(\frac{u(n)}{10^4}\right)^6 \qquad (34)$$

where
$$|u(n)| \leq 10^4 \qquad (35)$$

3.2 A Priori Estimates

For control purposes, the a priori estimate of system dynamics was

$$x(n+1) = x(n) + 0.003\, u(n) + \zeta(n) \qquad (36)$$

where $\zeta(n)$ is normally distributed with mean zero and variance 100. The temperature range of interest, 750°-850°A, was divided into nine quantized intervals; two more process states were added to represent temperatures outside these limits (so that N = 11).

Matrices B and C were calculated from known costs (34) and (33) respectively; $\hat{P}$ was obtained from (36). From $\hat{P}$, B, and C the a priori estimate of the optimal feedback characteristic was calculated by the method of reference 16. This characteristic, obtained by interpolation between values $u_i^*(\phi_i)$, is shown as curve A in fig. 3. Five control alternatives, spaced at 500 kilocalorie intervals and centred on $u_i^*(\phi_i)$,

were chosen for each process state ($\Gamma = 5$).

3.3 Simulated Adaptive Control

Fifteen hundred stages of operation were simulated on an IBM 7090 digital computer. A convergence factor of 10 was used with the automaton control strategy of section 2.5. Coarse adjustment of the control range, as discussed in section 2.6, was included, but no adjustment of state quantization. The results, averaged over blocks of 100 stages, are summarized in Table I. Program running time was 6.3 minutes.

TABLE I
ADAPTIVE CONTROL OF NONLINEAR HEAT TREATMENT PROCESS

Stage No.	Average of Previous 100 Stages: Mean Temp(°A)	Std. Dev'n(°A)	Cost/Stage Cents	Remarks
100	787.50	3.60	9.32	Temperature below 800°
200	796.62	13.10	10.63	Exceeds 800° at n=181
300	822.44	6.71	26.51	
400	818.94	7.72	22.04	Temperature in the
500	820.55	6.82	24.93	vicinity of 820°
600	822.49	6.67	28.32	
700	802.83	16.00	14.15	Forced below 800° at n=647.
800	789.54	2.80	7.24	
900	789.40	2.84	7.69	
1000	789.70	2.78	7.24	Temperature in the
1100	788.81	3.09	8.04	vicinity of 789°.
1200	789.55	2.92	7.33	
1300	789.32	2.81	7.43	
1400	790.11	2.87	6.97	
1500	794.31	3.57	4.37	Stable operation near 800°.

Control of this process is somewhat analogous to the problem of maintaining an inverted pendulum in an upright position, since the desired operating temperature is a point of unstable equilibrium. However, this fact was not recognized in the calculation of the a priori feedback characteristic. Consequently the temperature remained below 800° for the first 181 stages of operation since insufficient heat was applied. During this time the feedback characteristic altered adaptively so that the mean temperature increased. As soon as 800° was exceeded the unexpected exothermic reaction caused the operating point to move up to about 820°. A maximum of 844.3° was experienced at stage 523, but no plant shutdown

occurred. Again the feedback characteristic altered to accommodate the peculiar dynamics; the temperature was forced below 800° at interval 647, and remained in the range 780°-800°, gradually rising again until it exceeded 800° at stage 1424. Thereafter, stable operation in the vicinity of 800° was observed; the mean temperature during the last 35 stages was 795.6°. Mean cost per transition decreased (but not monotonically) by more than 50% between the first and last hundred stages. Curve B of fig. 4 shows that the 1500 interval estimate of the optimal feedback characteristic has altered significantly from the a priori one in the vicinity of x = 800: Also shown (curve C) is the optimal characteristic calculated from the true system dynamics.[16] The latter calculation shows that the minimum expected cost per stage is 2.023 cents. To approach this cost more closely, the controller must quantize u, and perhaps x, more finely near 800°. However the principal goal, that of obtaining stable operation at what was originally an unstable point, has been achieved.

4. CONCLUSION

A dual control algorithm has been presented for on-line multi-stage optimization of stationary discrete time long duration Markov processes. Simulation results show that the automaton controller is capable of adaptive minimization of a fairly general cost function in the presence of initially unknown dynamics, state and control constraints, system nonlinearities, and multiplicative disturbances with unknown distributions.

REFERENCES

1. M. L. Tsetlin, "On the Behaviour of Finite Automata in Random Media", Automat. Remote Control, (English translation) 22, no. 10, 1210-1219; 1961.

2. V. I. Varshavskii, I. P. Vorontsova, "On the Behaviour of Stochastic Automata with a Variable Structure", Automat. Remote Control, 24, no. 3, 327-333; 1963.

3. S. Pashkovskii, "Adaptive Control for a System with a Finite Number of States", Proc. 2nd IFAC Congress (1963), Butterworths, 241-245.

4. V. Y. Krylov, "On one Automaton that is Asymptotically Optimal in a Random Medium", Automat. Remote Control, 24, no. 9, 1114-1116; 1963.

5. G. J. McMurty, K. S. Fu, "A Variable Structure Automaton Used as a Multimodal Searching Technique", IEEE Trans. Automatic Control, 11, no. 3, 379-387; 1966.

6. R. W. McLaren, "A Stochastic Automaton Model for the Synthesis of Learning Systems", IEEE Trans. Systems Science and Cybernetics, 2, no. 2, 109-114; 1966.

7. Z. J. Nicolić, K. S. Fu, "An Algorithm for Learning without External Supervision and Its Application to Learning Control Systems", IEEE Trans. Automatic Control, 11, no. 3, 414-422; 1966.

8. J. S. Riordon, "Dual Control Strategies for Discrete State Markov Processes", Int. J. Control, 6, no. 3, 249-261; 6, no. 4, 317-330; 1967.

9. A. A. Feldbaum, "Dual Control Theory", Automat. Remote Control, 21, 874-880, 1033-1039; 1960. 22, 1-12, 109-121; 1961.

10. B. Chandrasekaran, D. W. C. Shen, "Adaptation of Stochastic Automata in Nonstationary Environments", Proc. Nat. Electron, Conf., 23, 39-44; 1967.

11. R. A. Howard, "Dynamic Programming and Markov Processes", Wiley, 1962.

12. R. L. Kashyap, "Optimization of Stochastic Finite State Systems", IEEE Trans. Automatic Control, 11, no. 4, 685-692; 1966.

13. K. J. Åström, "Optimal Control of Markov Processes with Incomplete State Information", J. Math. Anal. Appl. 10, 174-205; 1965.

14. A. M. Mood, F. A. Graybill, "Introduction to the Theory of Statistics" 2nd ed., McGraw-Hill, 1963.

15. J. S. Riordon, "Adaptive Control of Discrete State Markov Processes", Ph.D. Thesis, University of London; 1967.

16. J. S. Riordon, "Optimal Feedback Characteristics from Stochastic Automaton Models", paper 26b, Proc. JACC, 1968.

17. D. J. Wilde, "Optimum Seeking Methods", Prentice-Hall, 1964.

18. M. D. Waltz, K. S. Fu, "A Heuristic Approach to Learning Control Systems", IEEE Trans. Automatic Control, 10, 390-398; 1965.

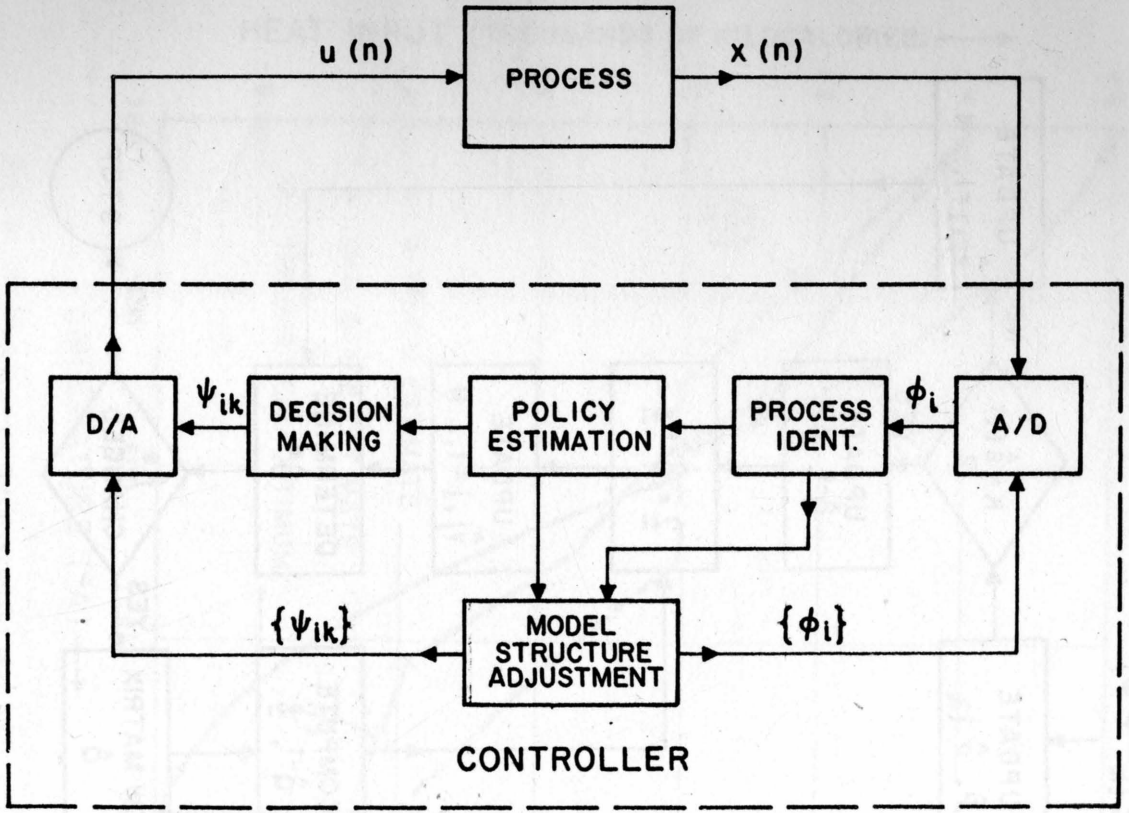

Fig. 1. Structure of the Adaptive Automaton Controller

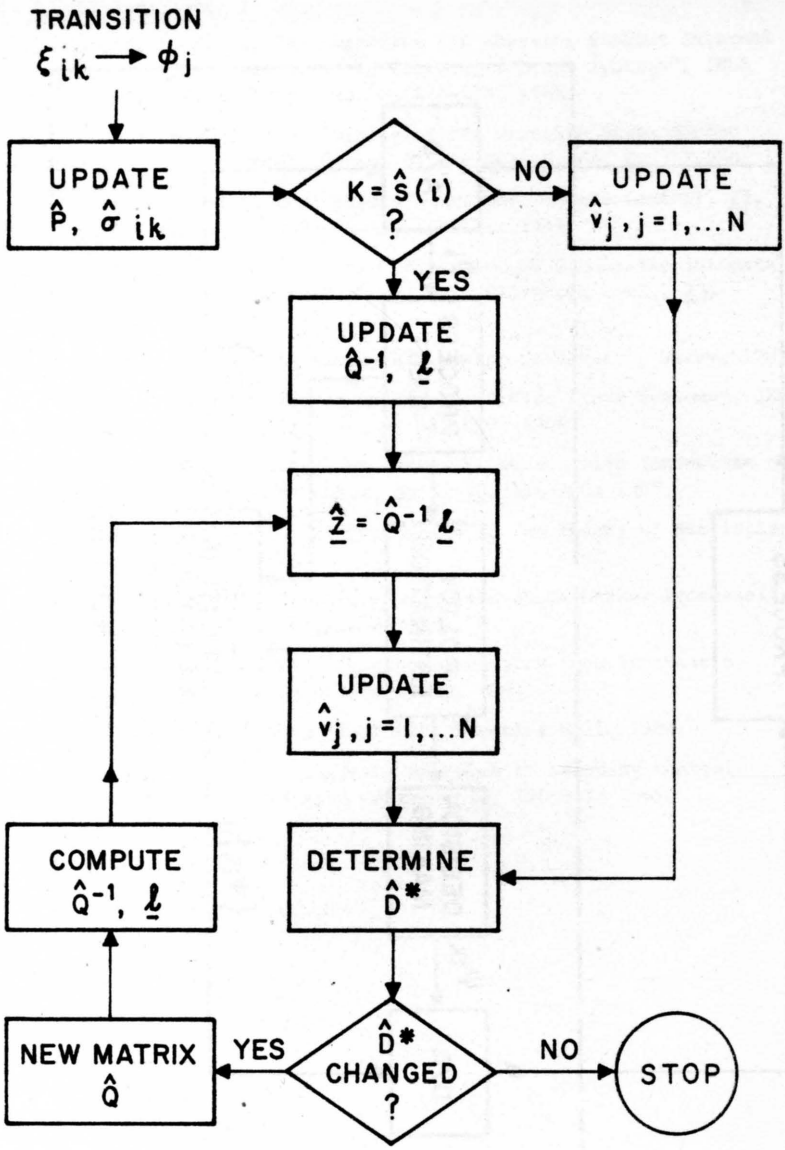

Fig. 2. Updating Routine for Control Policy Estimate

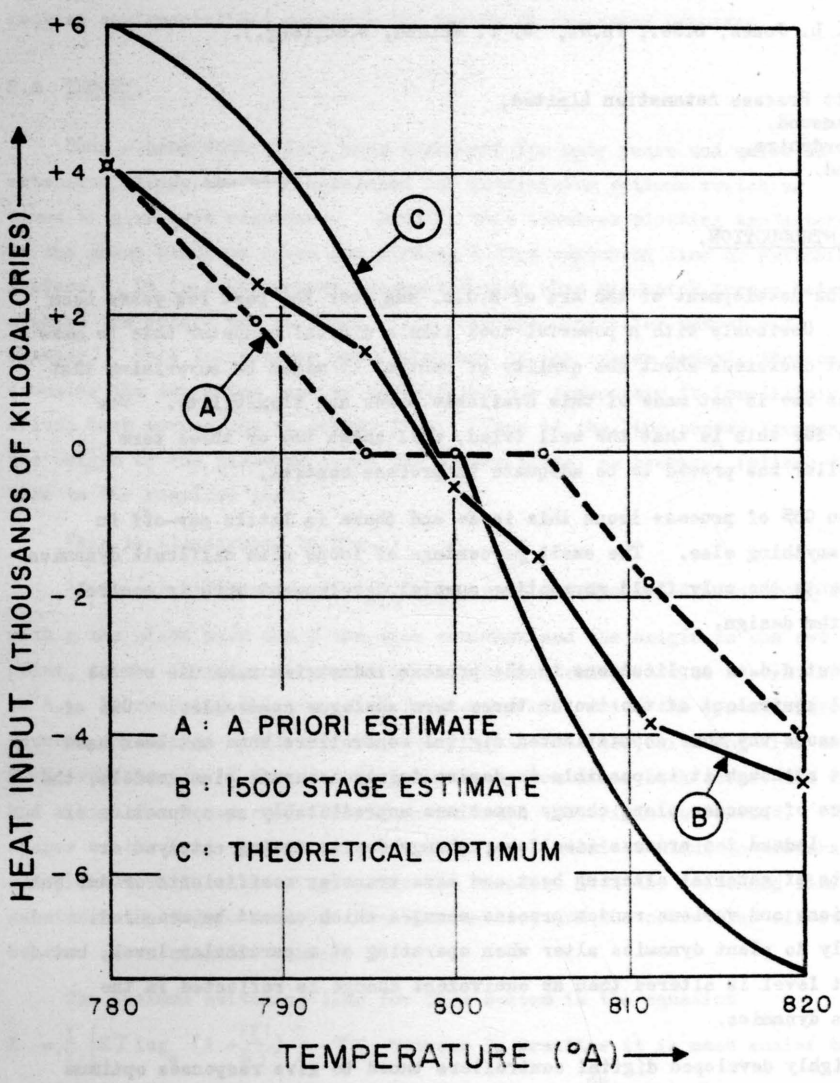

Fig. 3. Feedback Control Characteristics near 800°

A DIGITAL CONTROLLER FOR PROCESS INDUSTRIES WITH ADAPTIVE-TYPE BEHAVIOUR

By A. L. Jones, B.Sc., Ph.D., D. P. McLeod, B.Sc.(Eng.).

Elliott Process Automation Limited,
Borehamwood,
Hertfordshire,
England.

1.0 INTRODUCTION.

The development of the art of d.d.c. has over the past few years been slow. Obviously with a powerful tool like a digital computer able to make logical decisions about the quality of control it might be surprising that greater use is not made of this available power and flexibility. One reason for this is that the well tried, well known two or three term controller has proved to be adequate in process control.

On 95% of process loops this is so and there is little pay-off in using anything else. The small percentage of loops with difficult dynamics represents the only field warranting special development work in control algorithm design.

Most d.d.c. applications in the process industries make use of the digital equivalent of the two or three term analogue controller. One of the reasons why more sophisticated digital controllers have not been used is that although it is possible to derive fairly accurate plant models, the dynamics of process plant change sometimes unpredictably as a function of time. Indeed the process itself may change due to ageing catalyst or deposits of material altering heat and mass transfer coefficients or ambient conditions and various random process changes which cannot be measured. Not only do plant dynamics alter when operating at a particular level, but if that level is altered then an equivalent change is reflected in the process dynamics.

Highly developed digital controllers tuned to give responses optimum in some sense rapidly become unstable as the plant takes on some new mode of behaviour.

It is virtually impossible to predict the dynamics of process plant accurately over the operating range of the process for any reasonable length of time.

It would therefore seem that there is a definite need for a digital controller not unduly affected by varying dynamics, which ensures stability throughout the whole operating range of the process and which does not require any specialised manpower for tuning or operating purposes.

2.0 THEORY.

Bang - bang controllers have been used for many years and quite an extensive theory has been developed for determining optimum switching times to give best responses. Usually this involves plotting trajectories in the phase plane or space and finding a best switching line or switching surface. It is a well-known phenomenon that when mis-match occurs between a phase trajectory and switching line then the controller output will chatter. This takes place when behaviour of the system demands that on crossing the switching line or surface the new trajectory is immediately driven back across the switching line. Thus if the line passes through the origin of the plane or space the system state, on average, follows the line to the required goal.

This is illustrated in Fig. 1.

If the plant dynamics is $\frac{g}{S(\gamma S+1)}$ say, and the two drives are $\pm$ E, with g the plant gain and γ the time constant and the origin is the set point, then a +E trajectory will strike the switching line at a point such as A. On crossing the line a -E trajectory will drive the system state towards the origin until the trajectory again cuts the switching line at B. A +E trajectory will immediately push the system state back across the line and a high frequency chatter will occur until the origin is reached. The shapes of the trajectories are, of course, dependent on plant parameters g and γ, but while chattering occurs the response down the switching line is substantially independent of these parameters, and the controller effectively behaves in an adaptive manner.

The optimum switching line for this system is the equation $X = \frac{Y}{|Y|}\left[E\gamma \log_e \left(1 + \frac{|Y|}{E\gamma}\right)\right] - \gamma Y$, however in practice it is much easier to construct a linear controller of the form, $\left(e + a\frac{de}{dt}\right)$ where 'a' is a predictor time constant and defines the inverse slope of the switching line. In the process industries it is extremely difficult to obtain derivitive signals and while it is possible to calculate first order derivitives, it

is a prohibitive task to try to obtain higher orders.

As illustrated in the example chattering can always be induced to occur when a trajectory hits the switching line by choosing the slope to be greater than a minimum value i.e. the slope of a trajectory at the largest absolute system velocity reached.

Another important point involves the choice of sampling frequency. If the sampling period is close to the dominant time constant of the plant then difficulties can occur because amplitudes of limit cycles may be greater than some acceptable value.

2.1 Examination of Basic System Plant Dynamics.

For the most part the dynamics of process plants involve either a series of time constants or possibly a series of time constants with an integration term. If these plants are driven from constant controller outputs then the phase plane trajectories either move inwards ending at a node or a focus singularity or in case of there being an integration the plant state will eventually be driven at a constant velocity to infinity. These conditions are shown in Fig. 3.1, 3.2 and 3.3.

For any positive set point change then the initial trajectories will be those as shown. In the top half plane the trajectories always move towards the positive X values, i.e. towards the set point. If and when they hit a switching line they will immediately be placed on negative drive trajectories. However these, as long as they remain in the top half-plane also move to the right, i.e. in the direction of the set point. As long as the switching line passes through the set point then the output will be forced along it and therefore towards the set point.

This example illustrates a positive set point change and the same reasoning can be applied to a negative set point change.

Changes in time constants, plant gains and even order may take place without altering this basic concept. If, of course, part of the plant becomes non-minimum phase then this no longer holds.

3.0 CHOICE OF CONTROLLER CONSTANT.

3.1 Slope of Switching Line.

3.1.1 Plant equation is $\frac{g}{S(\tau S+1)}$

The trajectory shape is shown in Fig. 2.

A positive drive trajectory reaches a maximum velocity value of Eg. At this value the slope of negative trajectories is given by $\frac{dY}{dX} = \frac{Eg + Y}{Y\gamma}$

$$= -\frac{2}{\gamma}$$

Since the slope of the trajectory is always greater than this, then with this slope of switching line on, off chatter is guaranteed.

3.1.2 Plant equation is $\frac{g}{(\gamma_1 S+1)(\gamma_2 S+1)}$

Since this transfer function has no integration term then the trajectory shape alters with X. In the case where the plant is more than critically damped the shape of the trajectory is as shown in Fig. 2.1. This can be split into two parts corresponding to the effect of the eigen-values.

The first is for large values of velocity where the lines are almost straight and parallel and the second is the common run-in line, down to the abscissa value into which all trajectories merge.

It is suggested that the maximum value of linear velocity feedback that need be considered is that given by the inverse slope of the switching line parallel to the trajectories at large positive values of velocity.

This can be derived as $\frac{\gamma_1 . \gamma_2}{\gamma 1 + \gamma 2}$ which is equal to $\frac{1}{2}$ for a critically damped system.

It is interesting to note the difference between a first order system - either γ_1 or γ_2 is zero - and a second order system with one of the time constants very small.

If $\gamma_1 = 0$, $\gamma_2 = 40$ say then the switching line is vertical in the phase plane, but if $\gamma_1 = 1$ and $\gamma_2 = 40$ then the switching line slope is approximately unity. Hence, a change of just one second has the effect of rotating the switching time through 45°. In practice so called first order systems are nearly all of this type.

3.2 Value of Drive Force.

For best response to set point changes and process disturbance the drive force used should be as large as possible. The limiting factor in the choice of the drive is the acceptable amplitude of the limit cycle experienced around the set point. The amplitude $\bar{X}$ of this limit cycle

can be defined theoretically in the following way.

a) First order plant with no deadtime.

Plant equation is $X = \frac{E.g}{\tau S+1}$

If $\pm X_i$ is the initial position of X the equation becomes

$$\tau(S\mathcal{L}X-X_i) + \mathcal{L}X = \frac{E}{S}$$

$$\text{or} \quad \mathcal{L}X = \frac{E + \tau SX_i}{S(\tau S+1)}$$

Taking the inverse transform and bearing in mind the symmetry of the limit cycle, it can be shown that the peak limit cycle amplitude is

$$\bar{X} = +E \tanh T/2\tau$$

b) Second order plant with no deadtime.

Plant equation is $X = \frac{E.g}{S(\tau S+1)}$

In a manner similar to that used for the first order system, expression for the amplitude of the limit cycle can be shown to be

$$\bar{X} = E\tau \log_e \left[\cosh \frac{nT}{2\tau}\right]$$

where n is a positive integer. This means that 2 nT samples occur per limit cycle period.

c) Second order plant.

Plant equation is $X = \frac{E.g}{(\tau_1 S+1)(\tau_2 S+1)}$

For this plant equation the limit cycle magnitude is given by

$$\frac{\bar{X}}{E} = \frac{(\tanh \frac{nT}{2\tau_1} + 1)\frac{\tau_1}{\tau_1+\tau_2}}{(\tanh \frac{nT}{2\tau_2} + 1)\frac{\tau_2}{\tau_1+\tau_2}} - 1$$

4.0 TUNING.

Two methods of tuning the controller must be used depending on whether the system has inherent integration or not. Systems with integration are easily recognised, and are to be found in some chemical reactors. If the system has integration in it then the drive forces must be opposite in sign.

The size of these drive forces depends on the nature of the process; if the process "runs away" in 2 minutes or 5 minutes then the drive must be chosen for the worst case.

In the case of plants with no integration a band round the set point should be chosen say ± 10% for the drive forces. If the set point is changed, this band could be moved automatically with respect to the new set point value.

The slope of the switching line has been found to be generally applicable to most situations when the predictor time constant takes a value between 5 and 10.

However an estimate can be made for the maximum slope of the line using the theoretical approach described in Section 3.1.

By using Figs. 4.1 and 2, and knowing the maximum allowable limit cycle amplitude, a value of drive can be calculated.

If the sampling rate of the controller is such that the control element, e.g. a valve, moves slowly with respect to one sample period, then no problem exists in calculating the value of drive.

5.0 RESULTS.

Step responses have been obtained considering three types of plant. These were a predominantly first order plant, a plant with two time constants and a second order plant with an integration term. Figs. 5.1 and 5.2 show an array of step responses obtained for plants with dynamics $\frac{g.e^{-DS}}{(\gamma_1 S+1)(\gamma_2 S+1)}$

Since many plants in the process industries have approximately first order dynamics then for this first case γ_1 was made equal to one second and a range of γ_2 was considered from 10 to 60 seconds. Deadtime of 4 seconds was included in some of the runs and for the most part did not degrade the responses. Only with γ_2 = 10 did the deadtime cause the limit cycle amplitude to become noticeable. The responses are all well-damped with no overshoot. Changes of plant gain were tried but these had no great effect. All the responses in Fig. 5.1 were obtained with the identical controller with a time constant of 5 seconds.

Fig. 5.2 shows the curves obtained for a system with two time constants where γ_1 = 10 seconds. γ_2 was varied from 20 to 60 seconds. Again, it can be seen that all the responses are well controlled despite the range

of variation of γ_2. Deadtime of 4 seconds was included in some of the runs but again had little effect. The controller was again fixed for all the changes in dynamics, also with a predictor time constant of 5 seconds. Gain changes have little effect and the system stability is ensured with well-damped control.

Plots for the results from the third system are shown in Fig. 5.3 where the controller is again of fixed form with a time constant of 15 seconds. Plant dynamics of this sort sometimes occur for exothermic reactions. Deadtime of 10% of the plant time constant was included and the plant gain changed by a factor of 4. Only with both of these factors involved did the limit cycle amplitude reach a value which might not be acceptable.

6.0 CONCLUSION.

A different approach has been proposed for d.d.c., in the process industry. The major advantage of it is that control is to a large degree very much insensitive to large variations in plant dynamics. Also the rate of approach to a set point is a function of the controller and not of the plant. Tuning of the controller mainly involves the choice of the switch drive forces. The range of choice of the predictor constant is narrow and should be very easily selected. The higher the sampling frequency, the better, since the plant state then has little opportunity to move far away from the switching line, before the next sample can take the necessary corrective action. In this paper it has been assumed that a sampling period of a second has been used and dominant plant time constants of as low as 10 seconds have been shown to work satisfactorily. Generally speaking though, the higher the ratio of plant time constant to sampling time, the better the quality of control. Now that solid-state multiplexers are becoming more common place in process control computers, with sampling rates of say 3000 channels per second, then fast sampling should provide little difficulty.

Lastly, with this type of control, a simplification of computer output peripheral equipment could arise. In the simplest case the controller drives would only need to be output to a change-over switch. Consequently no problems would occur with manual to auto-transfer since if the wrong drive had been selected it would only require a period of one sample time to select the correct drive.

NOMENCLATURE.

g	is steady-state plant gain.
s	is operator d/dt, where t is time.
γ's	are plant time constants.
Y	is $\frac{dX}{dt}$
a	is predictor time constant.
e	is set point - X.
$\mathcal{L}$ X	is the Laplace transform of X.
$\bar{X}$	is the peak amplitude of X.
T	is the computer sample time.
D	is plant deadtime in seconds.
δ	is $e^{-T/\gamma}$

Subscript p refers to sampling instant
and m is the number of samples of deadtime.

Appendix.

The results from this work were obtained using a simulation program on an Elliott 903 computer. The equations used in the computer were obtained by taking z transforms of the analogue plant equations. These are listed below:

$$X = \frac{g.E\ e^{-DS}}{(\tau S+1)} \qquad \text{giving}$$

$$X_{p+1} = \delta X_p + (1-\delta) g.E_{p-m} \tag{1}$$

$$X = \frac{g.E\ e^{-DS}}{(\tau_1 S+1)(\tau_2 S+1)} \qquad \text{giving}$$

$$X_{p+1} = (\delta_1 + \delta_2) X_p - \delta_1 \delta_2 X_{p-1} + \left[\frac{\delta_1 \tau_1 - \delta_2 \tau_2 - \tau_1 + \tau_2}{\tau_2 - \tau_1} \right] E_{p-m} + \left[\frac{\delta_1 \delta_2 (\tau_2 - \tau_1) + \delta_2 \tau_1 - \delta_1 \tau_2}{\tau_2 - \tau_1} \right] E_{p-1-m} \tag{2}$$

$$X = \frac{g.E\ e^{-DS}}{S(\tau S+1)} \qquad \text{giving}$$

$$X_{p+1} = (1+\delta) X_p - \delta X_{p-1} + \left[T - \tau_1 (1-\delta) \right] E_{p-m} - \left[\delta T - \tau (1-\delta) \right] E_{p-1-m} \tag{3}$$

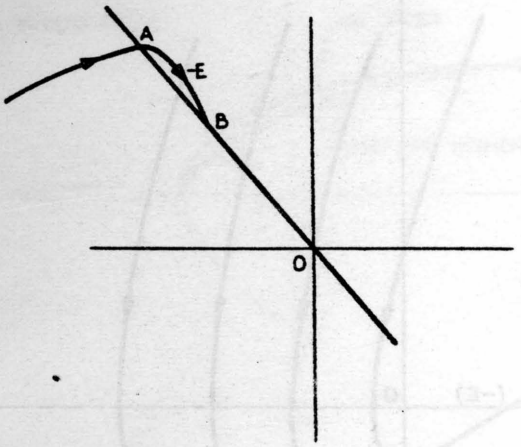

FIG 1

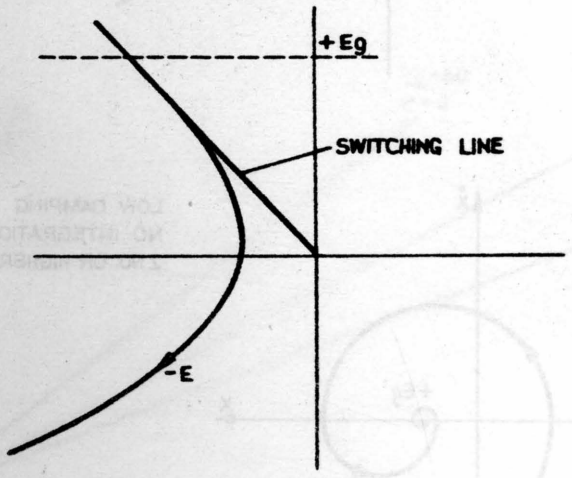

FIG 2

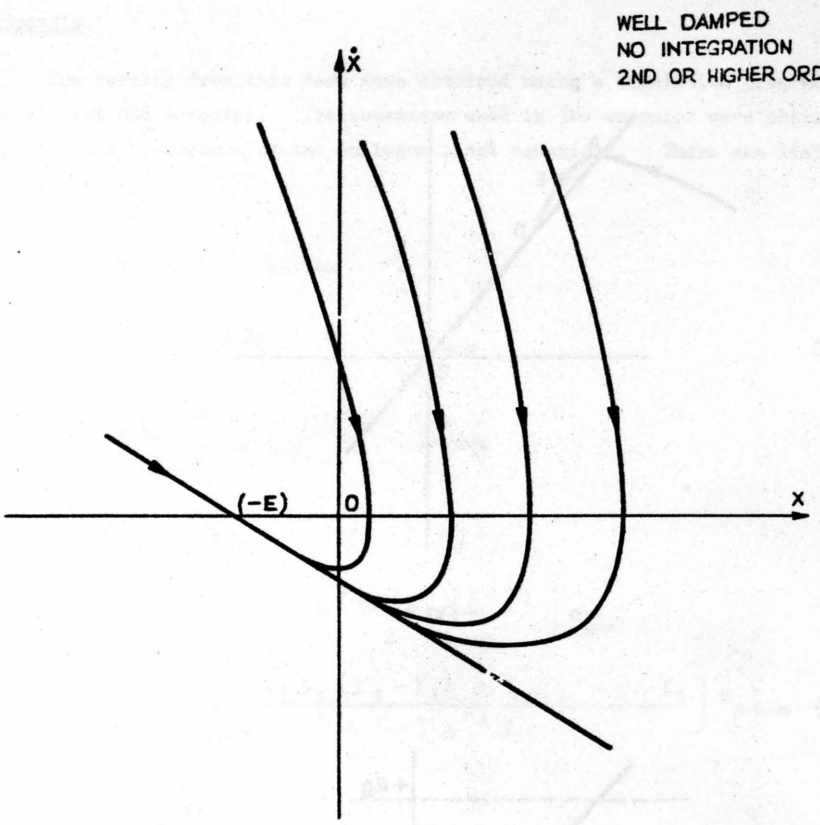
WELL DAMPED
NO INTEGRATION
2ND OR HIGHER ORDER
$\dot{X}$
(-E)
0
X

FIG. 3·1

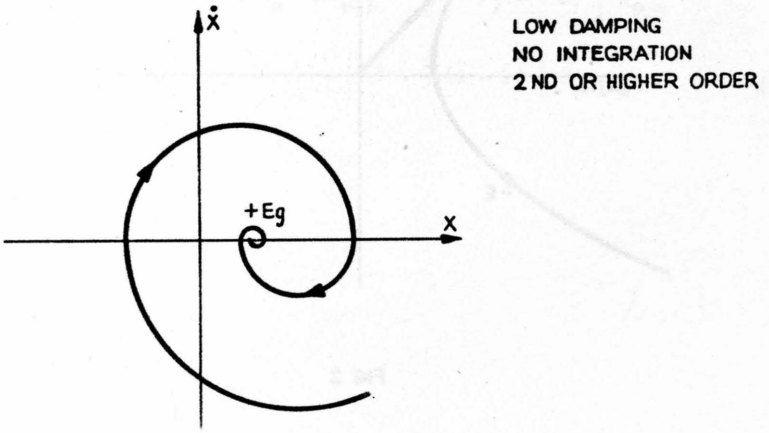
LOW DAMPING
NO INTEGRATION
2 ND OR HIGHER ORDER
$\dot{X}$
+Eg
X

FIG. 3·2

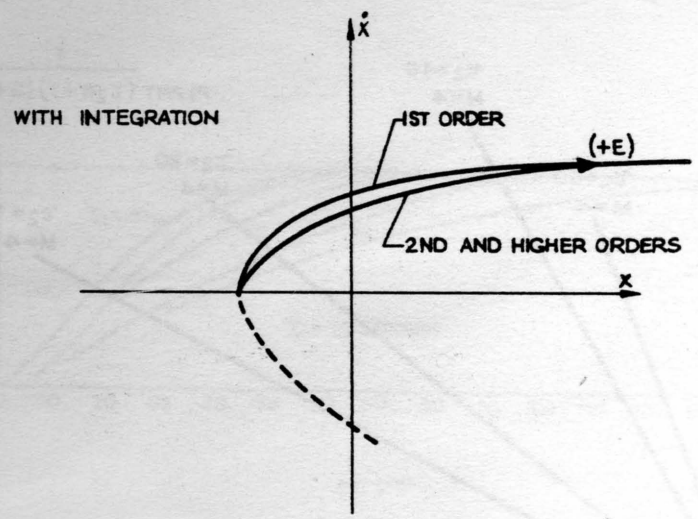
WITH INTEGRATION
1ST ORDER
(+E)
2ND AND HIGHER ORDERS
ẋ
x

FIG. 3·3

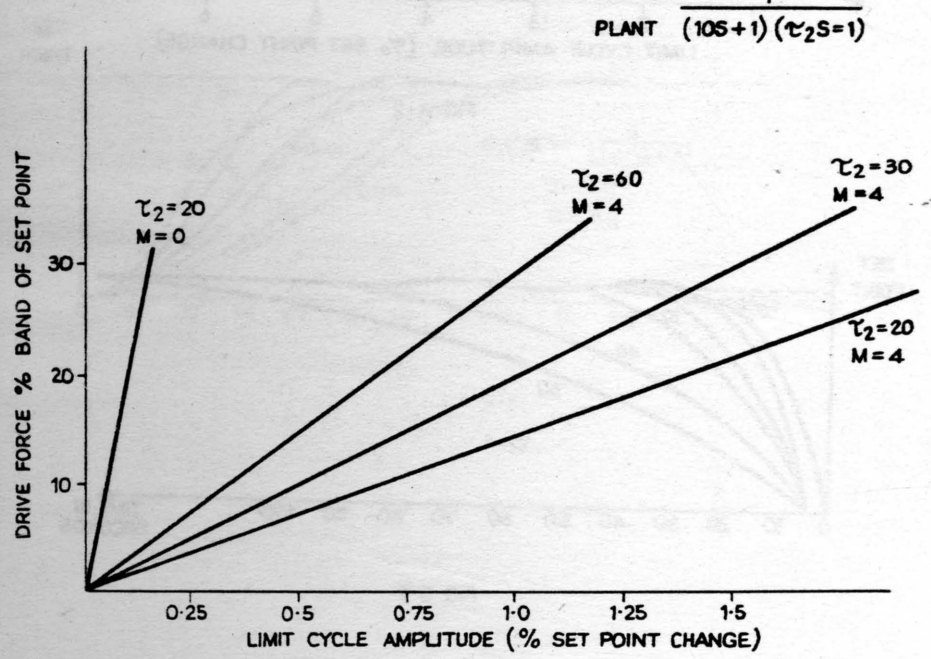
PLANT 1 / (10S+1)(τ2S+1)
τ2=20 M=0
τ2=60 M=4
τ2=30 M=4
τ2=20 M=4
DRIVE FORCE % BAND OF SET POINT
30
20
10
0·25
0·5
0·75
1·0
1·25
1·5
LIMIT CYCLE AMPLITUDE (% SET POINT CHANGE)

FIG. 4·1

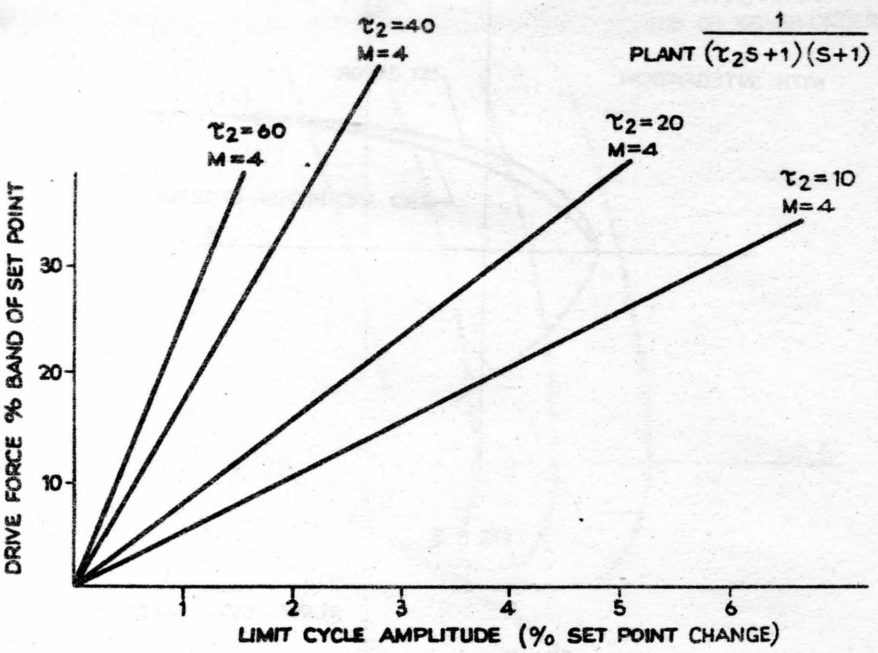
$\tau_2=40$
M=4
PLANT $\frac{1}{(\tau_2 S+1)(S+1)}$
$\tau_2=60$
M=4
$\tau_2=20$
M=4
$\tau_2=10$
M=4
DRIVE FORCE % BAND OF SET POINT
30
20
10
1
2
3
4
5
6
LIMIT CYCLE AMPLITUDE (% SET POINT CHANGE)

FIG 4·2

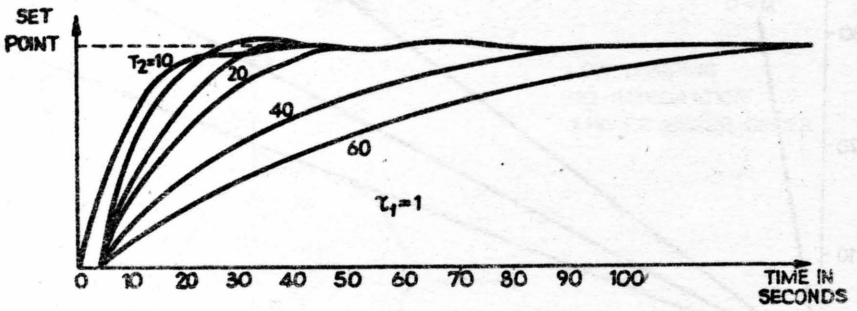
SET POINT
τ_2=10
20
40
60
τ_1=1
0
10
20
30
40
50
60
70
80
90
100
TIME IN SECONDS

FIG. 5·1

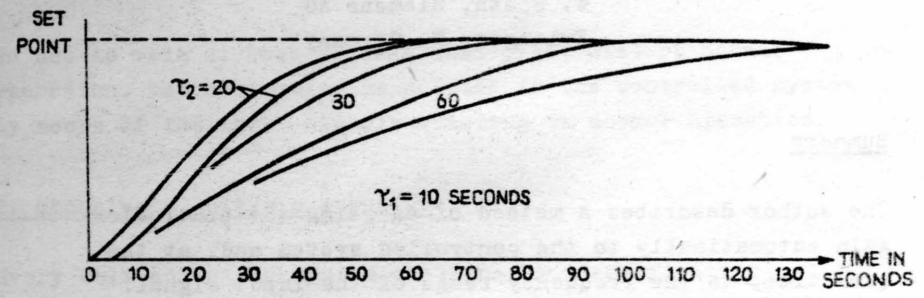
SET
POINT
$\tau_2 = 20$
30
60
$\tau_1 = 10$ SECONDS
0 10 20 30 40 50 60 70 80 90 100 110 120 130
TIME IN
SECONDS

FIG 5·2

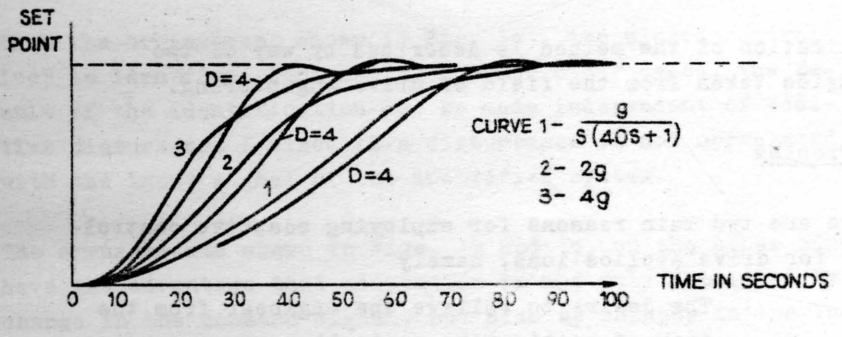
SET
POINT
D=4
3
2
D=4
1
D=4
CURVE 1- $\frac{g}{s(40s+1)}$
2- 2g
3- 4g
0 10 20 30 40 50 60 70 80 90 100
TIME IN SECONDS

FIG 5·3

SIMPLE METHOD FOR THE RAPID SELF-ADAPTATION OF AUTOMATIC CONTROLLERS IN DRIVE APPLICATIONS

W. Speth, Siemens AG
Erlangen, W. Germany

Summary

The author describes a method of adapting the controller gain automatically to the controlled system and, at the same time, to the frequency range of the input signal. The oscillograms of Fig. 4 are characteristic for the application of the method.

A particularly simple case of the method in question is logarithmic control which, however, can be used for certain types of controlled system only.

Application of the method is described by way of two examples taken from the field of drive engineering.

1. Problem

There are two main reasons for employing adaptive controllers for drive applications, namely

1. The desire to relieve the engineer from the task of setting the controller parameters, and
2. The necessity of controlling controlled systems whose parameters vary with time.

The aim is to construe a standard controller which will adapt itself to the controlled system in such a way that the closed control loop assumes a pre-determined transfer function. The investigation showed that the controller can also be adapted to the input signal by simple means.

The author limits himself to the case where, in addition to the gain of the controlled system and additive disturbances, all the parameters of the controlled system are known. This case is characteristic of most automatic drive controls.

No use is made of test signals that might disturb normal operation. The controller is adapted to the controlled system by means of the input signals existing in normal operation.

2. Choosing a suitable structure

Every self-adjusting system contains an identification system, though sometimes in rudimentary form, which supplies the information necessary for setting the controller.

Depending on which part of the system is identified, one of the structures shown in Fig. 1 abc) is obtained. The decision rests between these structures.

With the arrangement shown in Fig. 1a), the closed control loop is identified. Contrary to the two other cases, the result of the identification can be made independent of additive disturbance L since this disturbance is not correlated with the input signal of the identified system.

The arrangements shown in Figs. 1b and 1c, on the other hand, have the advantage that adaptation is not only initiated by a change in the command signal, but also by changes in the load or controlled system parameters, for all these changes result in changes in the deviation and correcting condition. This permits renewed identification and, consequently, controller adaptation. This is such a great advantage that the arrangement as shown in Fig. 1a can be eliminated.

With arrangements as shown in Figs. 1a and 1b, controller adaptation is a closed loop process, whereas an open-loop process is involved in Fig. 1c. In the case of closed loop adaptation it is not necessary to determine the system para-

meters completely; it is sufficient to ascertain whether they deviate from the reference values. This can be done with a simpler identification arrangement than required for open-loop adaptation.

In the case of arrangements with closed-loop adaptation, the controller parameters may be adjusted slowly only (except in the case of highly sophisticated arrangements), otherwise identification would be disturbed. With open-loop adaptation, on the other hand, identification is unaffected by the rate at which the controller is adjusted. Since particular importance is attached to quick-response adaptation, therefore, the arrangement shown in Fig. 1c is chosen.

3. Identification

Identification should take place as quickly as possible to permit the controller to adjust itself at a rate that will prevent an initial unstable setting from having any effect.

Considerations are limited to linear controlled systems with the general structure shown in Fig. 2a), or a simpler structure developed from 2a) by omitting individual system elements. An example of this is shown in Fig. 2b.

The only signals capable of being measured are those representing the correcting condition $Y(t)$ and the controlled condition $X_M(t)$, the latter consisting of the system output $X(t)$ and additional noise $n(t)$. Let quantity L be an additive random disturbance signal whose influence on the controlled condition is to be reduced by the controller. The second disturbance signal forms the unknown controlled system gain K_p which has to be identified for adjusting the controller. The remaining parameters of the controlled system and its structure are known.

The following can be read off from Fig. 2a):

$$z_p(t) + L = \frac{\dot{x}(t)}{K_p} \qquad (1)$$

Let it be assumed first of all that disturbances K_p and L change only slowly; by differentiation of (1) the following then applies:

$$\dot{z}_p(t) K_p = \ddot{x}(t) \qquad (2)$$

This formula is suitable for determining K_p, provided suitable equivalent quantities can be found for variables $Z_p(t)$ and $\ddot{x}(t)$ which cannot be measured. Fig. 3 shows how identification can be realised together with the entire control loop.

An equivalent substitute quantity is obtained for $Z_p(t)$ by filtering the correcting condition via a simplified model F_M of the part of the controlled system F_p (cf. Fig. 2). The output variable X(t) is replaced by the noisy controlled condition $X_M(t)$.

The measured values $Z_M(t)$ and $X_M(t)$ now have to be differentiated. Since differentiating elements cannot be realised, the frequency response of the differentiating filters is given a denominator other than one, but is the same for both filters.

The signals thus processed are referred to as $Z_D(t)$ and $X_D(t)$ and replace the non-measurable variables $\dot{Z}_p(t)$ and $\ddot{X}(t)$. Equation (2) could therefore be written

$$z_D K_M = x_D \qquad (3)$$

However, it would not be practical to calculate K_M from this equation by means of a fast dividing network since Z_D often disappears. A divider with memory is therefore used which retains the result of the preceding calculation at its output when small signals are applied to its input. Division is performed by a closed control loop which slowly adjusts the product $K_M Z_D$ to the value X_D (see Fig. 3b). In order to ensure that this loop always has a negative

feedback, the sign of the deviation must be changed over as a function of sign Z_D. The following equation then applies:

$$x_D = K_M z_D + \dot{K}_M \frac{T}{\operatorname{sign} z_D}$$

or (4)

$$\frac{x_D}{z_D} = K_M + \dot{K}_M \frac{T}{|z_D|}$$

The factor $\frac{T}{|z_D|}$ indicates the rate at which K_M adjusts itself. At $|z_D| \to 0$ this factor approaches ∞ and K_M undergoes no further change.

When the amplitudes of Z_D are greater, the fact that the rate at which K_M adjusts itself is dependent on $|z_D|$ can be a source of annoyance. This can be avoided by employing the control loop shown in Fig. 3b for forming the quotient $\frac{x_D}{z_D}$. In this case the loop is not only adapted to the sign, but also to the amplitude, of Z_D. The adjusting time of the loop thus becomes constant: For Fig. 3b equations (4) are therefore replaced by

$$x_D = K_M z_D + \dot{K}_M z_D$$

and (5)

$$\frac{x_D}{z_D} = K_M + \dot{K}_M T$$

For very small values of Z_D, however, equations (4) still apply, as can be seen from Fig. 3b. This is necessary in order to guarantee the memory effect in the case of disappearing input signals.

For practical purposes the additional hardware otherwise required to obtain an adjustment rate independent of the amplitude is generally not necessary. Fig. 3a will therefore be taken as a basis for the following considerations.

The error resulting when the equivalent variables X_D and Z_D required for calculating K_M do not coincide with $\overset{\vee}{X}$ and Z_p will now be considered.

The following applies $x_D = \ddot{x}_M * g = \ddot{x} * g + \ddot{n} * g$ (6)

$$z_D = \dot{z}_M * g = \dot{z}_p * g + \dot{\Delta z} * g$$

where $z_M = z_p + \Delta z$

The convolution with $g(t) = \mathcal{L}^{-1}\left\{\frac{1}{1 + pA + p^2 A^2}\right\}$ describes the unwanted signal deformation caused by the denominator in the frequency response of the non-ideal differentiators.

By substituting (6) in (4) we obtain

$$(\ddot{x} + \ddot{n}) * g = K_M (\dot{z}_p + \dot{\Delta z}) * g + \dot{K}_M \frac{T}{\operatorname{sign} z_D}$$

Dividing by $\dot{z}_p * g$ and combining with (2) this yields

$$K_p + \underbrace{\frac{\ddot{n} * g}{\dot{z}_p * g}}_{1} = K_M \Big(1 + \underbrace{\frac{\dot{\Delta z} * g}{\dot{z}_p * g}}_{2}\Big) + \underbrace{\dot{K} \frac{T}{M \dot{z}_p * g \operatorname{sign} z_D}}_{3} \qquad (7)$$

Since n is not correlated with Z_p summand 1 due to noise has little effect, for its mean value is then zero, and K_M cannot follow the rapid changes of this component if the time constant T is large enough.

Component 2 is determined by the input signal and the degree of approximation of filter F_M to the frequency response F_P. Measurements carried out with the analogue computer have shown that the mean value of this expression is negligibly small in the case of a suitable approximation (see the example described in the following section).

Component 3 influences the adjustment rate only, but not the final value.

The method of identification described is similar to that proposed by Marŝik[1] and also investigated by Parks[2]. However, the gradient system is not employed and the quality criterion applied results in a lesser dependence on amplitude.

Fig. 3a shows how the controller gain is adjusted as a result of the identification. A divider, which divides the controller output by the identified controlled system gain K_M, is arranged on the output side of controller section C with fixed parameters.

4. Example: Automatic speed control

The following contains a treatment of the results obtained by measurement in an automatic speed control system for a d.c. motor.

The controlled system is as shown in Fig. 2a. The system element F_P represents a sub-loop for torque which, in the example, has the frequency response

$$F_P = \frac{1}{1 + pA + p^2\frac{A^2}{2} + p^3\frac{A^3}{8}} \qquad A = 30\,ms$$

$Z_p(t)$ is the driving motor torque and $L(t)$ the braking load torque. The unknown gain K_p is inversely proportional to the inertia mass of the motor together with the driven machine to which it is coupled.

The controller with identification and compensation is arranged according to Fig. 3a.

The controller is set in accordance with the symmetrical optimum specified by Kessler[3] and has the frequency response

$$C = \frac{1 + pA}{pA}\,\frac{1s}{A}$$

The model F_M of the sub-loop for torque F_P required for the identification only simulates the equivalent time constant of the sub-loop and has a frequency response of

$$F_M = \frac{1}{1 + pA}$$

The complete control system is analogue. The multipliers

are very simple and operate on the principle proposed by Widlar and Giles[5].

Fig. 4a shows the oscillogram of the speed v(t) and the identified value $K_M(t)$ after the drive has been switched on. The controller was set to a fixed value beforehand and the load is constant. The speed that would have resulted had K_M had the correct value K_P from the outset is shown by a dotted line.

Fig. 4b shows v(t) and $K_M(t)$ in the event of a pronounced step change in the load. It can be seen that identification is falsified at first if the load changes. However, subsequent corrective action of the controller in response to the load change once more permits correct identification.

If neither the command variable nor the load change over a prolonged period of time, the value of K_M changes due to the drift of the analogue memory. By applying a constant bias to the input of the memory for K_M, the latter can be made to change slowly towards zero if no control action takes place. The controller gain thus increases steadily until the control loop becomes unstable. The resultant oscillation of increasing amplitude initiates a new identification, with the result that K_M increases again.

Fig. 4c illustrates this process. As can be seen, the speed amplitude occurring is sufficiently low.

Fig. 4d shows how the system reacts to a step change in the load when K_M is too small. A comparison with the dotted curve shows that the adaptive system is superior to the fixed-parameter system here.

Slight changes in the load are corrected with higher gain than sudden large load changes or step changes in the set value. In this way the controller gain also adjusts itself to the input signals. The maximum possible gain is determined by the stability limit and is reached when the input signals remain unchanged over a prolonged period of time. In the case

of a fixed-parameter controller such a high gain would not be permissible because of the tolerances. With the self-adjusting controller, on the other hand, stability is not jeopardised since, as shown in Fig. 4c, the slightest control action in the control loop once more reduces the gain.

5. Logarithmic control

In the special case of the controlled system shown in Fig. 2b the method described becomes a logarithmic control system.

Instead of equation 2, the following equation is obtained for the controlled system in Fig. 2b:

$$z_p(t)K_p = x(t) \tag{7}$$

or, substituting Z_D, which is formed with the aid of the simplified model F_M of the known part of the controlled system F_P,

$$K_M = \frac{x(t)}{z_D(t)} \tag{8}$$

Fig. 5a shows the identification, including compensation, realised according to this formula. Division can be effected direct in this case (as opposed to Fig. 3), provided the operating point $Y(t) = Z(t) = X(t) = 0$ is excluded.

The two loops obtained in Fig. 5a can be separated even further from each other if the dividers are represented by logarithmic and exponential characteristics with subtraction points (cf. Fig. 5b). The inner of the two loops shown can be approximately replaced by a two-term controller (proportional plus integral action) with a frequency response of F_C and followed by a function generator with exponential characteristic. The approximation applies for small values of e. The single-loop arrangement shown in Fig. 5c is now obtained. In the case of the example of the automatic speed

control with the arrangement shown in Fig. 3a, a corresponding modification in the structure was not possible.

The arrangement according to Fig. 5c can also be found more quickly directly by trying to compensate the two characteristics in the controlled system. In this way, the exponential function f_1 is compensated by its inverse function g_1 and the logarithmic function f_2 by its inverse function g_2. (In this case compensation is disturbed by the interposing part of the system F_p, and applies strictly for low amplitudes only).

Such a logarithmic control can also be derived from the algebraic methods according to Oppenheim[4] if these are applied to control problems. Realisation of the controller shown in Fig. 5 is particularly simple since exponential and logarithmic functions are available in the form of the transistor characteristics between the base-emitter voltage and the collector current. The proposals of Widlar and Giles are also based on this principle.

The automatic control of the strip tension on a coiler is a typical example for the application of logarithmic control.

The set-up of such a control system is shown in Fig. 6. The coiler is driven by a d.c. motor whose current is controlled by a sub-loop, the system F_p in Fig. 5. The primary loop controls the logarithm of the strip tension which is measured by means of load cells on the bearings of a deflector roll.

The signal flow diagram of the controlled system is as shown in Fig. 2b. Here the reciprocal of the changing coil radius corresponds to the unknown gain, for $xr = Z_p$, neglecting the elastic oscillations.

References

1 Marsik, J.
Quick-response adaptive identification

Preprints of the IFAC Symposium
Prague Czechoslovakia 12-17 June 1967

2 Parks, P.C.
Stability problems of model-reference and identification systems
Preprints of the IFAC Symposium
Prague Czechoslovakia 12-17 June 1967

3 Kessler, C.
Das Symmetrische Optimum
Regelungstechnik 6 (1958) 11 and 12 pp. 395-400 and 432-436

4 Oppenheim, A.V.
Superposition in a class of nonlinear systems
International Convention Record 1964 pp. 171 to 177

5 Widlar, R.J. - Giles, J.N.
Optimale Verwendung von analogen integrierten Schaltungen
Internationale Elektronische Rundschau 1967 No.10, pp.249-253

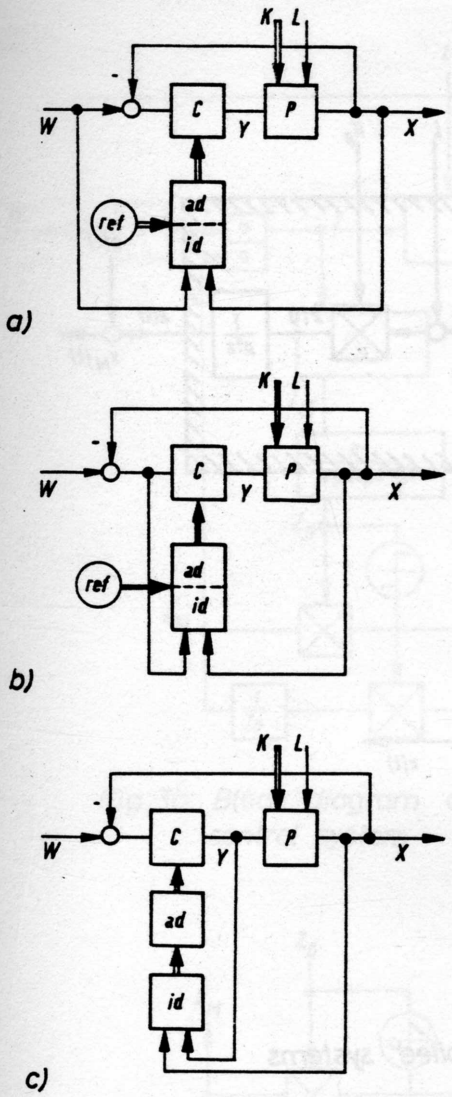

X = Controlled condition

Y = Correcting condition

W = Command signal

C = Automatic controller

P = Controlled system

K = Parameters of controlled system

L = Disturbances to be corrected

id = Gain identification

ad = Gain adjustment

ref = Reference parameters of the identified system

Fig.1: Various adaptation structures

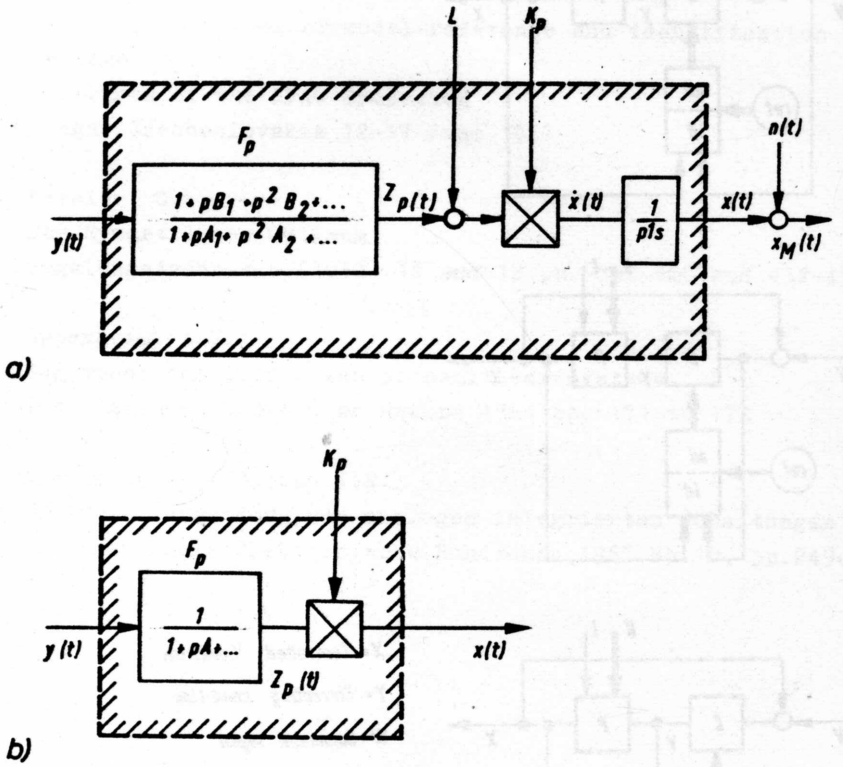

Fig. 2

Structure of the controlled systems to be identified

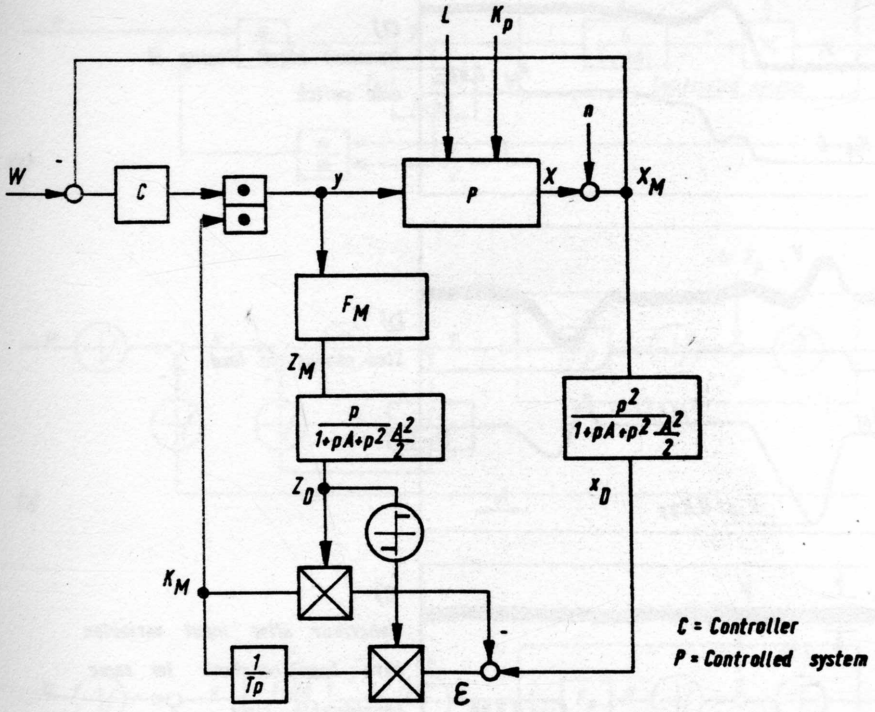

Fig. 3a: Block diagram of self-adjusting control system

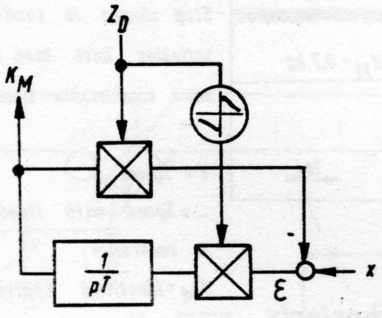

Fig. 3b: Improvement of identification

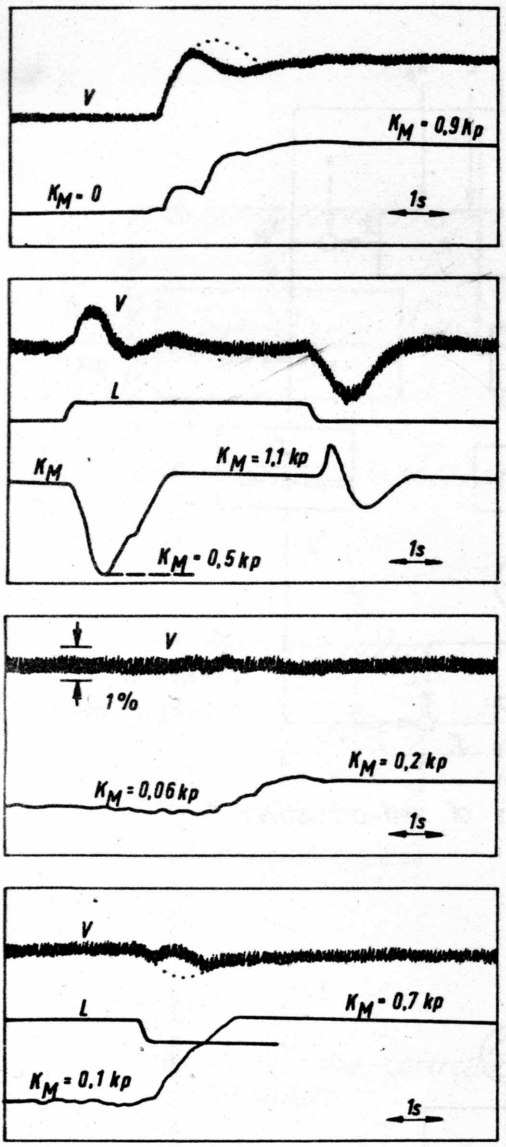

a) Transient after closing of main switch

b) Step change in load

c) Behaviour after input variables have been constant for some considerable time

d) Step change in load after input variables have been constant for some considerable time

V = Speed

... = Speed with fixed - parameter controller

K_M = Identified controlled system gain

L = Load

Fig.4

Speed control loop transients

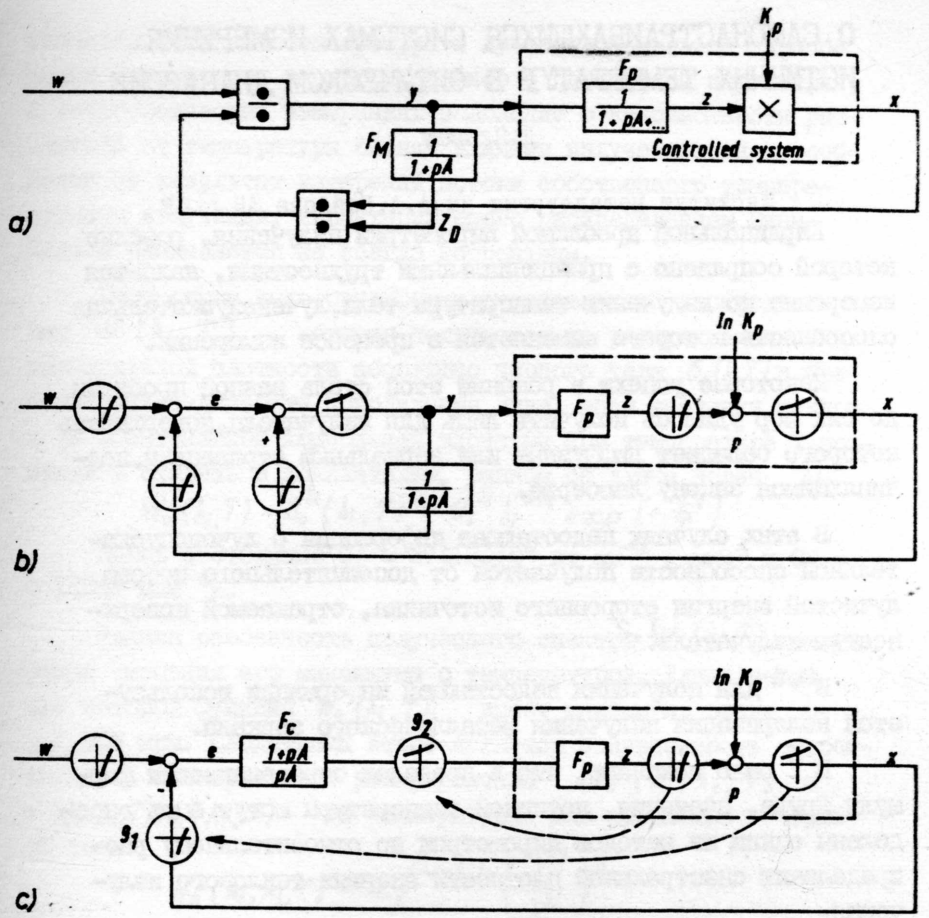
a)
w
y
F_M
$\frac{1}{1+pA}$
Z_D
K_p
F_p
$\frac{1}{1+pA+...}$
z
x
Controlled system
b)
w
e
y
$\frac{1}{1+pA}$
F_p
z
$\ln K_p$
p
x
c)
w
e
F_c
$\frac{1+pA}{pA}$
g_2
g_1
F_p
z
$\ln K_p$
p
x

Fig.5

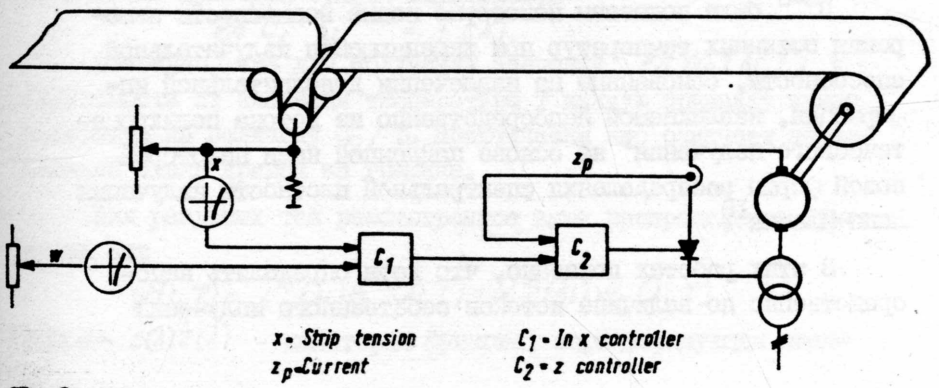
x
w
C_1
z_p
C_2
x - Strip tension
z_p - Current
C_1 - ln x controller
C_2 - z controller

Fig.6

О САМОНАСТРАИВАЮЩИХСЯ СИСТЕМАХ ИЗМЕРЕНИЯ ИСТИННЫХ ТЕМПЕРАТУР В ОПТИЧЕСКОМ ДИАПАЗОНЕ

Д.Я.Свет

Институт металлургии им.А.А.Байкова АН СССР

Кардинальной проблемой пирометрии излучения, решение которой сопряжено с принципиальными трудностями, является измерение по излучению температуры тела, лучеиспускательная способность которого изменяется в процессе измерения.

Некоторые успехи в решении этой столь важной проблемы до сих пор удалось получить лишь для излучателя, поверхность которого обладает диффузным или зеркальным отражением, подчиняющимся закону Ламберта.

В этих случаях недостающая информация о лучеиспускательной способности получается от дополнительного потока лучистой энергии стороннего источника, отражаемой поверхностью излучателя.[1,2]

В[3,4] для получения недостающей информации используется поляризация излучения металлического зеркала.

В [5] было показано, что в пределах справедливости формулы Друде, значения истинной температуры могут быть определены одним из методов пирометрии по относительному распределению спектральной плотности энергии теплового излучения.

Однако этот метод применим лишь в области достаточно низких температур.

В[6-8] были показаны некоторые новые возможности измерения истинных температур при изменяющейся излучательной способности, основанные на извлечении дополнительной информации, извлекаемой непосредственно из потока полихроматического излучения[9] на основе найденной нами некоторой новой формы распределения спектральной плотности излучения Вина-Планка[10].

В этих работах показано, что хотя определить непосредственно по величине потоков собственного излучения

значения истинной температуры и лучеиспускательной способности невозможно, распространенное в оптической пирометрии и астрофизических измерениях положение о невозможности раздельной от температуры оценки влияния излучательной способности на результат измерений потока собственного температурного излучения, характеризуемого распределением Вина-Планка оказывается не всегда корректным.

Рассмотрим некоторую форму спектрального распределения $W_i(\lambda_i, T)$, которая получается из распределения спектральной плотности абсолютно черного тела $B_0(\lambda_i,T)$ в пределах справедливости приближения Вина, если значения каждой i-й спектральной компоненты изотермы при температуре T возвести в степень с показателем, равным ее длине волны λ_i

$$W_0(\lambda_i,T) = B_0^{\lambda_i}(\lambda_i,T) = C_1^{\lambda_i}\lambda_i^{-5\lambda_i} exp\left(-\frac{C_2}{T}\right)$$

Здесь постоянные $C_I = 37413.10^4$ вт см$^{-2}$. мкм^4 и $C_2 =$ = I4388 мкм ^oK.

Важная особенность полученного спектра $W_0(\lambda_i,T)$ – отсутствие смещения его максимума с температурой. Длина волны, при которой функция $W_0(\lambda_i,T)$ имеет максимум, равна $\lambda_m =$ = I.905 мкм. Следствием этого является независимость относительного спектрального распределения $R_0(\lambda_i,\lambda_j,T) =$ $= W_0(\lambda_i,T)W_0(\lambda_j,T)$ от температуры. Для абсолютно черного тела

$$R_0(\lambda_i,\lambda_j,T) = C_1^{(\lambda_i-\lambda_j)}\left(\frac{\lambda_j^{\lambda_j}}{\lambda_i^{\lambda_i}}\right)^5$$

При любых значениях i и j

$$\partial R_0(\lambda_i,\lambda_j,T)/\partial T = 0$$

На рисунке приведен график зависимости

$$\ell n\, C_1^{\lambda_i}\lambda_i^{-5\lambda_i} = f(\lambda)$$

Очевидно, что для получения значений $\ell n\, W_0(\lambda_i,T)$ в зависимости от значений температуры T каждую ординату нужно уменьшить на величину C_2/T. Практически это означает параллельный сдвиг кривой на графике.

Для реальных тел рассмотренное выше распределение будет иметь вид

$$W(\lambda_i,T) = \alpha^{\lambda_i}(\lambda_i)B_0^{\lambda_i}(\lambda_i,T) = \alpha^{\lambda_i}(\lambda_i)W_0(\lambda_i,T)$$

где $\alpha = \varepsilon(\lambda)\tau(\lambda)$ – некоторая функция, характеризующая спек-

тральное распределение коэффициента лучеиспускательной способности $\varepsilon(\lambda)$ излучателя и коэффициента пропускания промежуточной среды (включая элементы оптической системы); Очевидно, что отношение любой пары компонентов (i-й и j-й) распределения $R(\lambda_i, \lambda_j, T)$ также не будет зависеть от температуры[x]

$$R(\lambda_i, \lambda_j) = \frac{\alpha^{\lambda_i}(\lambda_i)}{\alpha^{\lambda_j}(\lambda_j)}$$

Выполнение равенства $R(\lambda_i, \lambda_j) = R_o(\lambda_i, \lambda_j)$ при $\tau(\lambda_i) = \tau(\lambda_j) = 1$ является своеобразным критерием "абсолютной черноты" излучения $[\alpha(\lambda_i) = \alpha(\lambda_j) = 1]$, за исключением случаев, когда

$$\alpha^{\lambda_i}(\lambda_i) = \alpha^{\lambda_j}(\lambda_j) \quad , \text{ но} \quad \alpha(\lambda_i) \neq \alpha(\lambda_j)$$

Для трех и более компонентов спектра ($i, j, \kappa \ldots$), частоты которых $\nu = C_0/\lambda$ удовлетворяют условию $\sum_i^n \nu_i = \sum_j^m \nu_j$ (причем всегда $i \neq j$), так же можно получить относительное распределение $L(\lambda_i, \lambda_j)$, величина которого в пределах справедливости приближения Вина определяется только параметром $\alpha(\lambda)$ и от температуры не зависит.

Распределения эти в общем случае будут описываться выражениями вида[xx]

$$L(\lambda_i, \lambda_j) = \frac{\prod_i^n B(\lambda_i, T)}{\prod_j^m B(\lambda_j, T)} = \frac{C_1^p \prod_i^n \lambda_i^{-5} \alpha(\lambda_i)}{C_1^q \prod_j^m \lambda_j^{-5} \alpha(\lambda_j)}$$

где n и q – соответственно количества спектральных компонентов в числителе и знаменателе.

Для сего излучения:

$$L_o(\lambda_i, \lambda_j) = \frac{\prod_i^n \lambda_i^{-5}}{\prod_j^m \lambda_j^{-5}} \; C_1^{(p-q)}$$

В частном случае трех компонент, частоты которых удовлетворяют соотношению $\nu_1 = \nu_2 + \nu_3$, для абсолютно черного тела можно написать:

---

x. при $\partial\alpha(\lambda)/\partial\lambda = 0$

xx. Очевидно, что можно создавать и третий вид относительных распределений (удовлетворяющих условию независимости от температуры (основанных на комбинированных отношениях типа R и L.

$$L_o(\lambda_1,\lambda_2,\lambda_3) = \frac{\alpha(\lambda_2)\alpha(\lambda_3)}{\alpha(\lambda_1)} L_o(\lambda_1,\lambda_2,\lambda_3)$$

Это же относительное распределение для реального тела примет вид:

$$L(\lambda_1,\lambda_2,\lambda_3) = \frac{\alpha(\lambda_2)\alpha(\lambda_3)}{\alpha(\lambda_1)} L_o(\lambda_1,\lambda_2,\lambda_3)$$

Аналогично для четырех компонентов, частоты которых удовлетворяют соотношению $\nu_1 + \nu_2 = \nu_3 + \nu_4$

$$L_o(\lambda_1,\dots\lambda_4) = \left(\frac{\lambda_3\lambda_4}{\lambda_1\lambda_2}\right)^5;\ L(\lambda_1,\dots\lambda_4) = \frac{\alpha(\lambda_1)\alpha(\lambda_2)}{\alpha(\lambda_3)\alpha(\lambda_4)} L_o(\lambda_1,\dots\lambda_4)$$

Выполнение условия $L(\lambda_i,\lambda_j,\dots) = L_o(\lambda_i,\lambda_j,\dots)$ при одинаковом числе составляющих спектра в числителе и знаменателе относительных распределений типа L является критерием серого характера излучения $\partial\alpha(\lambda)/\partial\lambda = 0$. Исключением являются частные случаи, для которых при $\partial\alpha(\lambda)/\partial\lambda \neq 0$ имеет место равенство произведений вида:

$$\alpha(\lambda_1)\alpha(\lambda_2) = \alpha(\lambda_3)\alpha(\lambda_4)$$

Рассмотренный метод извлечения информации о характере $\alpha(\lambda)$ из потока собственного излучения эффективно используется (в ряде радиационных систем), в частности, в пирометре для измерения истинной температуры излучателя, лучеиспускательная способность поверхности которого изменяется в процессе измерения.

Созданная в ИМЕТ АН СССР система для измерения по излучению истинной температуры является самокорректирующейся.

Технически система реализована в виде пирометра, снабженного устройством, вырабатывающим сигнал, определяемый величиной отношения типа R_i или L_i. В зависимости от величины этого сигнала, получаемого одновременно с сигналом температуры, определяемой по относительному распределению спектральной плотности энергии излучения, в показания пирометра автоматически вводится величина поправки ΔT_i.

Соответствие этой последней сигналам, определяемым значениями функций $R(\lambda_i,\lambda_j)$ или $L(\lambda_i,\dots\lambda_j)$ достигается с помощью предварительного обучения системы.

Практически, процесс обучения сводится к некоторым несложным операциям предварительной градуировки. Обычно,

последнюю достаточно осуществить лишь для нескольких экстремальных значений функции $\varepsilon(\lambda)$.

Так, например, для автоматического контроля истинной температуры жидкой стали с изменяющейся в процессе измерения лучеиспускательной способностью вследствие появления или исчезновения пленки окислов и обеспечением суммарной погрешности[X] измерений не хуже ± I% достаточно осуществить процесс обучения – градуировки по 3-м значениям. Интересным и весьма удобным для практики оказалось, что один и тот же цикл обучения удовлетворяет самым разнообразным по химическому составу окисным пленкам.

Это явление хорошо объясняется результатами исследования излучательной способности окислов в видимой и близкой инфракрасной областях спектра, приведенными, например, в[II].

Для пояснения сказанного рассмотрим связь между температурной поправкой в значениях обратной температуры ΔT^{-1} и функцией распределения $R(\lambda_i, \lambda_j)$. Обозначим через $\varepsilon_м(\lambda_i)$, $\varepsilon_м(\lambda_j)$ – спектральные излучательные способности чистой металлической поверхности, для значений эффективных длин волн λ_i и λ_j ; через $\varepsilon_п(\lambda_i)$ и $\varepsilon_п(\lambda_j)$ обозначим соответствующие значения спектральной излучательной способности окисной пленки.

За счет явления дисперсии, для металлов $\varepsilon_м(\lambda_i) > \varepsilon_м(\lambda_j)$, если $\lambda_i < \lambda_j$.

Известно также, что вследствие дисперсии, в том числе и аномальной $\varepsilon_м(\lambda_i) < \varepsilon_п(\lambda_j)$.

Обозначим через M – часть поверхности металла свободного от пленки, а через N – часть, покрытую пленкой окисла. Для "нормированной" поверхности $M+N = I$.

При измерении температуры по отношению двух лучистостей со значениями эффективных длин волн λ_i и λ_j , величину поправки на неполноту излучения в обратных значениях температуры можно записать как:

X. Под суммарной погрешностью здесь понимается сумма погрешностей инструментальной и методической (за счет неполноты излучения).

$$\Delta T^{-1} = \frac{\Lambda}{C_2} \ln \frac{\varepsilon_м(\lambda_i) + N[\varepsilon_п(\lambda_i) - \varepsilon_м(\lambda_i)]}{\varepsilon_м(\lambda_j) + N[\varepsilon_п(\lambda_j) - \varepsilon_м(\lambda_j)]}$$

где $\Lambda = \frac{\lambda_1 \cdot \lambda_2}{\lambda_2 - \lambda_1}$ значение эквивалентной длины волны. Для чистой металлической поверхности:

$$\Delta T_1^{-1} = \frac{\Lambda}{C_2} \ln \frac{\varepsilon_м(\lambda_i)}{\varepsilon_м(\lambda_j)}$$

Соответственно для поверхности полностью окисленной $\Delta T_2^{-1} = 0$, ибо излучение пленки серое. Для случая, когда часть, например, половина поверхности зеркала металла закрыта окисной пленкой ($M = N = 0{,}5$).

$$\Delta T_3^{-1} = \frac{\Lambda}{C_2} \ln \frac{\varepsilon_м(\lambda_i) + \varepsilon_п(\lambda_i)}{\varepsilon_м(\lambda_j) + \varepsilon_п(\lambda_j)}$$

Значения функции $R(\lambda_i, \lambda_j)$, соответствующие этим значениям поправки будут:

$$\delta_{T_1} = K \frac{\varepsilon_м^{\lambda_i}(\lambda_i)}{\varepsilon_м^{\lambda_j}(\lambda_j)}, \qquad \delta_{T_2} = K \varepsilon_п^{\lambda_i - \lambda_j}$$

и

$$\delta_{T_3} = K \frac{[\varepsilon_м(\lambda_i) + \varepsilon_п(\lambda_i)]^{\lambda_i}}{[\varepsilon_м(\lambda_j) + \varepsilon_п(\lambda_j)]^{\lambda_j}}, \text{ где } K = const$$

Вероятность появления многозначности, за счет нелинейного характера зависимости функции $R(\lambda_i, \lambda_j)$ от излучательных способностей, в данном случае исключается автоматически благодаря упомянутому выше явлению дисперсии, характеризуемому убывающим характером функции $\varepsilon(\lambda)$ в видимой и близкой инфракрасной области спектра для всех металлов.

С несколько иным алгоритмом обучения данная система позволяет измерять значения истинной температуры поверхности с неизменной излучательной способностью, но и с переменным коэффициентом пропускаемости промежуточной среды. Примерами такой задачи в металлургии является запыление парами металла, при плавке в вакууме смотрового окна, а при астрофизических измерениях, например, температуры солнца – появления дымки от облаков и др.

Не менее интересные результаты получаются при осуществлении самокорректирующейся системы на основе распределения спектральной плотности типа $L(\lambda_i, \ldots \lambda_j)$.

Введение избыточности за счет использования более двух спектральных составляющих позволяет существенно повысить устойчивость и точность измерений при наличии различных нерегулярных воздействий.

Создание самообучающихся пирометрических систем на основе распределений R и L позволяет успешно решить некоторые вопросы с диагностикой плазмы, дефектоскопией поверхности и др.

Принципиальная схема автоматического пирометра с самокорректировкой изображена на рис. I.

Здесь S – поверхность излучателя с изменяющейся лучеиспускательной способностью.

О – концентрирующая и визирная оптическая система пирометра
М – монохроматизирующее устройство
Ф – приемники излучения
У – усилительное устройство
П – предварительный преобразователь
Б.К. – блок корреляции
Л – логометрирующее устройство
Р – измерительно-регистрирующий выходной прибор.

Работает система следующим образом: из потока излучения от S с помощью – О на монохроматизирующем устройстве М концентрируется поток последуемого излучения. Приемник или приемники "Ф" преобразуют спектральные лучистости на выходе монохроматизирующего устройства М в электрические сигналы, усиливаемые У и преобразуемые в требуемую форму с помощью преобразователя П.

С выхода последнего преобразованные сигналы поступают на логометрирующее устройство Л и на блок коррекции Б.К., который в зависимости от предварительного обучения градуировки – "выдает" требуемое значение сигнала коррекции. Последний может подаваться либо непосредственно на измерительно-регистрирующий прибор Р, либо предварительно на один из каскадов логометрирующей системы. На основе этой схемы были созданы различные варианты самонастраивающихся пирометрических систем.

Для иллюстрации, на рис. 2 приведены сравнительные данные показаний различных пирометрических систем на плавках стали в индукционной печи, снабженной специальным устройством, позволяющим создавать на поверхности металла пленку необходимого химического состава или иметь чистое металлическое зеркало в атмосфере аргона.

В процессе плавки пленка могла "рваться" частично или полностью исчезать. Это хорошо иллюстрируется показаниями пирометров яркостного, суммарного излучения и цветового. Пирометрическая система истинной температуры ПИТ-I, созданная в ИМЕТ АН СССР во всех случаях, по сравнению с термопарой, не выходила за класс I, т.е. $\delta_{T_{ист}} = \pm 15$

При тех же условиях показания цветового пирометра изменялись на δ Тцв = 50 – 60°, яркостного на δ Тярк = = I00 – I30° и пирометра суммарного излучения на I80–300°.

Следует отметить, что условия плавки в экспериментальной установке с точки зрения эксплуатации системы ПИТ-I были более сложными, чем на полупромышленной сталеплавильной печи. Здесь при длительной эксплуатации на различных марках стали погрешность $\delta_{T_{ист}}$ составляет ± I0°, т.е. в условиях открытых плавок, результаты применения, эксплуатации системы ПИТ-I достаточно высокие.

ЛИТЕРАТУРА

I. W.G. Fastie - J.Opt.Soc. I95I, 4, 872.

2. А.А. Свет, Авт. свид. № I5855I от 20 ноября I952 г.

3. C.Tungwaldt, U. Shley - Z.Instrum ,I96I,69,N.7,205

4. W.Pepperhoff Arch. Eisenhuttenwes ,I959,30,I3I.

5. А.А. Свет, "Металлургия СССР за 40 лет", изд-во Металлургиздат. I958 г.

6. А.А. Свет "Объективные методы высокотемпературной пирометрии при непрерывном спектре излучения", I963 г.

7. Д.Н. Свет, авт. свид-во № 207736, Бюллетень № 13, 1 декабря 1967 г.

8. Д.Н. Свет, Авт. свид-во № 208967, Бюллетень № 1, 9 февраля 1968 г.

9. Д.Н. Свет. Д.А.Н. т. 170, № 4, стр. 825. 1966 г.

10. Д.Н. Свет. Теплофизика № 6, 1967 г.

11. Д.Н. Свет. "Температурное получение металлов и некоторых веществ". 1964 г. "Металлургиздат".

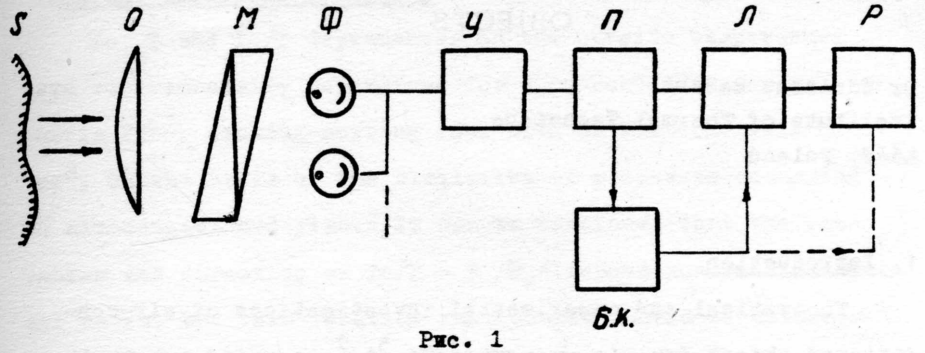
S
О
М
Ф
У
П
Л
Р
Б.К.

Рис. 1

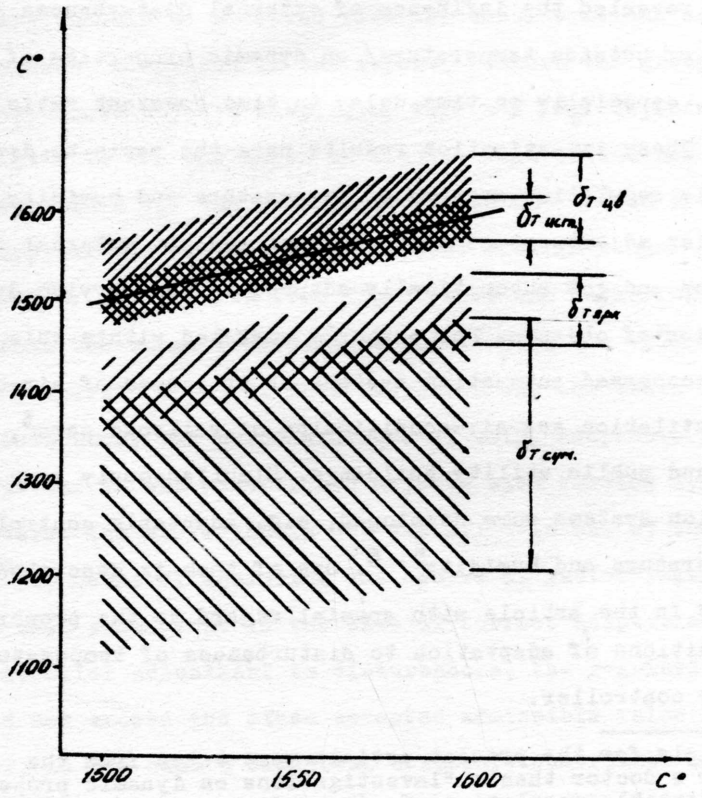
С°
1600
1500
1400
1300
1200
1100
1500
1550
1600
С°
δТ цв
δТ ист.
δТ арм.
δТ сум.

Рис. 2

ADAPTABLE REGULATION SYSTEM OF TEMPERATURE AND HUMIDITY IN AIR-CONDITIONED OBJECTS

Dr Zdzisław Barski
Institute of Thermal Technique
Łódź, Poland

1. Introduction

Theoretical and experimental investigations of air-conditioned object dynamic properties[2, 3, 7], carried out by the author, revealed the influence of external disturbances /e.g. changes of outside temperature/ on dynamic properties of these objects, especially on time delay to time constant ratio /To/T/. These investigation results were the basis to develop adaptable regulation systems of temperature and humidity, the controller adjustment of which changed against external disturbances and got automatically adapted to the varying dynamic properties of objects. The author's work led within this scope mainly concerned automation systems of processes of air-heating, ventilation and air-conditioning of railroad cars[3], sea ships[4] and public utility buildings. Simultaneously some new automation systems were developed, e.g. adaptable controllers of temperature and humidity[5, 6]. One of them is described and analyzed in the article with special regard to the properties and conditions of adaptation to disturbances of temperature or humidity controller.

---

* Materials for the present article were taken from the author's doctor thesis "Investigations on dynamic properties and adaptable regulation of air-conditioned objects" carried out under the guidance of professor M. Klimek.

2. The influence of outside temperature on dynamic properties of air-conditioned objects

To, T and To/T dependences on the outside temperature were experimentally determined for a connected in series synthetic fibre packing-sorting room with an air-condition chamber[2]. On the basis of the similarity of processes occurring in air-conditioned plants it can be concluded that the character and direction of $To/T = F(\vartheta_z)$ dependence is similar in all cases, but this function real course should be determined for every group of objects by separate investigations. It, therefore, should be accepted that the considerations on adaptable systems, comprised in the report, concern the group of air-conditioned objects displaying $To/T = F(\vartheta_z)$ dependence approximate to the one shown in fig. 1. This dependence has been determined for the temperature range $\Delta\vartheta = -1.6 \div 17.5^{\circ}C$, being approximate to most frequent year average range $/+2 \div +18^{\circ}C/$. It results from fig. 1 that the ratio To/T changes within the range from 0.24 at the temperature $+2^{\circ}C$ to 0.11 at the temperature $+18^{\circ}C$. This statement was the basis to pose the thesis about the purposefulness of using adaptable regulation systems to air-conditioned objects with varying dynamic parameters. The above thesis was justified in one of the papers[7] by means of analysing the course of factor regulation. It has been shown that in the case of correct adaptation of the controller adjustment to disturbances, the regulation factor did not exceed the often accepted admissible value 1.4. However, in the case a classical structure controller and unchangeable adjustment are applied, the regulation factor reaches the maximal value ≥ 2. Then, if there is a change of the given

value of the required controller, fluctuations would occur which may cause a reverse switch on and off of heating and cooling installations, being an undesirable phenomenon. While considering the purposefulness of adaptable system application, economical and technical premises had been taken into account. It was also considered that the regulation equipment for air-conditioned plant automation should be not too complex and expensive, i.e. controllers - destined for such object automation ought to be cheap and satisfy the conditions of adaptability.

3. Adaptable temperature or humiduty regulation system

3.1. Regulation system block-diagram

An exemplary block-diagram of a temperature regulation system in a multicompartment railroad car is given in fig. 2. An on-off temperature controller /R/ is installed in each compartment. Most frequently it consists of contact thermometers switched to temperatures 19, 21, 23°C, and equipped with an output relay with switch contacts. Contact thermometers /R/ carry out the on-off control of air-intake throttle with a rotary electromagnetic drive /Z/, and regulate the supply of warm air to the compartments. They simultaneously act upon the adaptable controller /S/ summing system which controls the effectiveness of the central heating chamber /K/ by means of the executive element /W/. The latter may be either a steam-heater electromagnetic valve or a contactor for high voltage electric heater. The controller /S/ considers the changes of heat demand signalized by contact thermometers /R/, as well as external condition changes, e.g. outside temperature and wind velocity.

3.2. Regulation system circuit-diagram

The regulation system circuit-diagram is shown in fig. 3. The system comprises contact thermometers or hygrometers /11/ and an adaptable controller. The controller consists of two basic parts: a bimetallic summing relay and a manometric thermometer sensor connected by a mounting plate. The relay contains a working bimetal /13/ with a heating resistor /14/ isolated from bimetal by micanite plates. An anvil is fastened on the end of the working bimetal, pressing the microswitch /6/ at bimetal swings. The microswitch /6/ is fixed on the end of the compensation bimetal /5/, which makes the controller operation independent of the ambient temperature. The bimetal /5/ can fluctuate in a bearing and it is fixed to a lever with a tension spring on its end. This spring tension can be changed by means of changing the position of the tension spring hand wheel /4/.

The tension spring with the hand wheel are set in the controller support construction. Besides the tension spring, a point pushrod of changeable length acts upon the bimetal lever. The other end of the pushrod is set in a socket of the segment fixed on the resilient spiral end /3/, which is the end of manometric thermometer sensor capillary /1/. The capillary is placed within a cube fastened to the housing.

The manometric thermometer sensor /1/ is partly placed inside the mixed air flow channel /external and circulating air/, and partly outside the channel within the housing /2/ equipped with adjustable gaps and variable diaghraghms. The latter enable the change of external condition influence /wind velocity and outside temperature/ upon the controller operation.

The controller electric circuit can be supplied from a direct current or variable current source /17-26 V/. Two in parallel connected barretters /7/ are placed within the supply circuit. These barretters make the value of the circuit current independent of the supply voltage fluctuation and circuit resistance changes.

The electric circuit has two parallel branches. One of them contains a switched on heating resistor /14/ and an auxiliary resistor /9/. The latter can be opened or closed by contacts of the controller /S/ relay. The other - a regulated resistor /10/ and in parallel to it is a range of resistors /12/ switched on by contacts of compartment thermometer contact relays /11/. The summarized value of the circuit current is approximately constant, but this current propagation is variable and depends on the adjustment of controller /10/ and on the number of resistors /12/ switched on by compartment thermometer contacts. The more resistors are on the lesser is the current passing through the heating resistor.

The resistance decrease of resistor /10/ bridged over by resistor /12/ results in a decrease of resistor /14/ current value. With a determined current value of the controller heater, after a determined time period, the microswitch contacts /6/ are changed over and the controller relay contacts /8/ are opened. This causes a rush change of the value of the current passing through resistor /14/, the value of which depends on the resistance value of resistor /9/.

After a certain time, depending on the value of resistor /9/, there occurs a repeated switch over of microswitch contacts /6/. This circuit is an inertial feedback which corrects the controller dynamic properties.

4. Analysis of an adaptable regulation system of temperature or humidity

4.1. The structure of the system treated as a system of adaptable compensation of ambient temperature influence, compensation circuit amplification factor being simultaneously adapted

The regulation system discussed in p. 3.2 can be analyzed as a system of temperature or humidity stabilization with a compensation of external disturbance influence /e.g. temperature and wind velocity/, compensation circuit amplification factor being the function of object temperature and humidity. Figure 4 presents this system block-diagram. As seen, external disturbances Z act on both: regulation object /1/ and, by means of the compensation element /5/, on the initial compensation signal level /W/. The object output signals y_1, $y_2 \cdots y_n$ act by means of contact thermometers or hygrometers /2/ and the summing node /3/ on the amplification factor K_w of the feedback inertial element /4/. The relay /6/ is the disturbance compensation element embraced by the inertial feedback /4/. Its approximate transmittance for mean values can be expressed by the following

$$\frac{\overline{U}/s/}{\overline{W}/s/} = \frac{Ts + 1}{Kw} \qquad /1/$$

The amplification factor K_w being nonlinearily dependent on error signals for separate inputs of the object /y_1, $y_2 \cdots y_n$/ can be written as follows

$$K_w = K_o + K_i \sum_{i=1}^{n} \operatorname{sign} /y_{io} - y_i/ \qquad /2/$$

Beside the above discussed viewpoint the system may be considered from a different one. The adaptation circuit of the amplification factor K_w of disturbance compensation circuit can be treated as a particular nonlinear feedback. This permits to consider the system in question as an output signal regulation system, the properties of its controller getting adapted to external disturbances and varying dynamic object properties.

This approach will be applied to further considerations. Indeed, it is less exact but, allows a more object analysis of controller adaptable features and a formulation of its adjustment adaptation conditions against disturbances as well.

4.2. The structure of the system treated as a nonlinear output signal regulation system, the controller properties being simultaneously adapted to external disturbances

The system block-diagram is presented in fig. 5. The following elements operate in mutual conjunction: contact thermometers or hygrometers /1/, current summing resistance system /2/, element of adaptable dependence of controller adjustment on external disturbances /7/, nonlinear pulse system is denoted by a double line. The above system contains a bimetal relay with a microswitch /6/ embraced by an inertial feedback with $\frac{K_w}{Ts + 1}$ transmittance, an adjuster of preliminary microswitch position to the working bimetal /Xo/, and a resistor to adjust the initial value of the current passing through the bimetal heater /Jo/.

The period of pulse system oscillations, made up by the sum of times T_z and T_w /the time the controller microswitch is

on and off/, can be preliminary adjusted by choosing appropriate values X_o and I_o. While choosing the period of oscillation admissible temporary deviations of the parameter regulated from the mean value, and an admissible frequency of switching the switch equipment are taken into account. Comprise solution being chosen as a rule.

The mean output signal from the controller Y is the function of duty factor, which in turn depends on the time of the controller microswitch being on and off /T_z and T_w/. External disturbances /outside temperature ϑ_z/ and internal signals deriving from contact thermometers and hygrometers /1/ influence T_z and T_w time values. External disturbances, represented by the manometric sensor temperature ϑ_{cz}, influence the position of compensation bimetal with a microswitch by means of the proportional element /7/ with amplification factor K. Then, changes the duty factor of the output signal Y on which the Kp factor of the controller is dependent.

Moreover, contact thermometers and hygrometers /1/ influence the value of currents I, Iz and Iw by acting upon the current summing system /2/. In consequence thermal energy released in working bimetal heater, cause corresponding changes of amplification factor Kw of internal feedback $\frac{Kw}{Ts + 1}$.

This results in a dependence of the mean output signal from Y controller on signals originating from contact thermometers or hygrometers /1/.

4.3. The dependence of the amplification factor of controller Kp^* on its constructional parameters

Let us assume that the controller operates in conjunction with only one contact thermometer or hygrometer. This makes pos-

sible to analyze the influence of external disturbances on the controller amplification factor. A simultaneous analysis of the number of cooperating contact thermometers or hygrometers is not needed.

The main output signal from Y controller can be expressed by the following

$$\overline{Y} = \frac{T_z}{T_z + T_w} \qquad /3/$$

On the other hand, Y signal can be dependent on U error signal according to the following formula:

$$\overline{Y} = Kp\ U$$

where: Kp - controller amplification factor,

U - error signal

To generalize the considerations and make them independent of the regulated parameter choise /temperature or humidity/ it is convenient to use relative or percent values Kp, U and $\overline{Y}$. These values will be denoted by letters with asterisks /Kp^*, U^*, Y^*/.

Therefore, expressions for Kp^*, Y^* and U^* will be the following

$$Y^* = \frac{T_z}{T_z + T_w}\ 100\%, \quad U^* = \frac{\vartheta - \vartheta_o}{\vartheta}\ 100\% \text{ or } U^* = \frac{\varphi - \varphi_o}{\varphi}\ 100\%$$

In the case the controller operates in conjunction with one contact thermometer or hygrometer with the zone of intensitivity h[°C] or h[% w.w.], U can be also expressed as $U^* = \frac{h}{\vartheta}\ 100\%$ or $U^* = \frac{h}{\varphi}\ 100\%$.

Therefore, Kp will be the following:

$$Kp^{*} = \frac{\bar{Y}^{*}}{U^{*}} = \frac{Tz}{/Tz + Tw/\ U^{*}} = \frac{Tz}{/Tz + Tw/\ h_t} \text{ or } Kp = \frac{Tz}{/Tz + Tw/\ h_w}$$

where: ϑ [°C] - contact thermometer ambient temperature

ϑ_o [°C] - temperature set on contact thermometer

h [°C] - zone of insensibility of a contact thermometer

φ, φ_o, h_w [% w.w.] - denote the same values related to a contact hygrometer

In order to use the value h of the zone of insensibility to determine the relative error U^{*}, an immediate reaction of contact thermometer to the changes of ambient temperature should be assumed, which is a certain idealization of real processes. The times of Tz and Tw depend on the outside temperature represented by manometric sensor themperature ϑ_{cz}. This involves the amplification Kp^{*} to be the outside temperature too

$$Kp^{*} = \frac{Tz\ /\ \vartheta_{cz}/}{[Tz\ /\ \vartheta_{cz}/ + Tw\ /\ \vartheta_{cz}/]U^{*}} \qquad /4/$$

On the basis of the analysis of adaptable controller construction elements, the following formulae can be deduced for the times Tz and Tw of the controller microswitch

$$T_z = \frac{Qc}{q^{S}} \ln \frac{\dfrac{kI_z^2 R_g}{qS}}{\dfrac{kI_z^2 R_g}{q\ S} - \dfrac{4h/y_{mz} - y_m/}{3/\alpha_2 - \alpha_1/ t^2}} =$$

$$= \frac{Qc}{q^S} \ln \frac{kI_z^2 R_g}{3kI_z^2 R_g / \alpha_2 - \alpha_1 /^2 - 4hqs/y_{mz} - \frac{ktRR1}{k_r R_1^2 + k_s R_2^2} \Delta \vartheta_{cz}} \qquad /5/$$

$$T_w = \frac{Qc}{q^S} \ln \frac{kI_w^2 R_g}{3kI_w^2 R_g / \alpha_2 - \alpha_1 / 1^2 - 4\, hqS/y_{mz} - \Delta_y +}$$

$$+ \frac{\overline{k_t RR_1}}{k_r R_1^2 + k_s R_2^2} \Delta \vartheta_{cz} / \qquad /6/.$$

The controller amplification factor may be dependent upon its constructional parameters and outside temperature, according to formulae /5/ and /6/ derived for Tz and Tw. After formulae for Tz and Tw are substituted to the formula for Kp^* amplification factor and some transformations made, one obtains

$$Kp^* = \frac{\ln \frac{3kI_z^2 R_g}{3kI_z^2 R_g / \alpha_2 - \alpha_1 / l^2 - 4hqS/y_{mz} - \frac{k_t}{k_r + k_s} \Delta \vartheta_{cz} /}}{U^* \left[\ln \frac{3kI_z^2 R_g}{3kI_z^2 R_g / \alpha_2 - \alpha_1 / 1^2 - 4hqS/y_{mz} - \frac{k_t}{k_r + k_s} \Delta \vartheta_{cz} / +} \right.}$$

$$+ \ln \frac{kI_w^2 R_g}{3kI_w^2 R_g / \alpha_2 - \alpha_1 / l^2 - 4hqS/y_{mz} - \Delta y + \frac{k_t}{k_r + k_s} \Delta\vartheta_{cz}} \qquad /7/$$

where:

- l [mm] - bimetal length
- h [mm] - bimetal thickness
- I_z [A] - controller switch on current
- I_w [A] - controller switch off current
- k_r [G/mm] - resilient spiral flexivity
- k_s [G/mm] - tension spring stiftness
- k_t [G/°C] - manometric sensor temperature coefficient
- Rg [Ω] - working bimetal heater resistance
- q [kcal/m^{2}h°C] - bimetal-air heat conduction coefficient
- S [m^2] - heat intercept area
- y_{mz} [mm] - bimetal flexivity needed to switch on a microswitch
- y_{mw} [mm] - bimetal flexivity needed to switch off a microswitch
- Δy [mm] - microswitch mechanical hysteresis
- $\Delta\vartheta$ [°C] - rise of manometric sensor ambient temperature
- α_1, α_2 - bimetal linear expansion coefficients

4.4. Discussion on Kp^* controller dependence on outside temperature

According to fig. 1, for the range of most frequent year average temperatures /+2 ÷ 18°C/, the ratio To/T changes within the limits from 0.24 at the temperature +2°C to 0.11 at the

temperature + 18°C. The then required range of changes Kp, which corresponds to optimal adjustment of P controller with aperiodic course, with minimum tp^8 is

$$K_p = \frac{K_{o\,18} - K_{o2}}{K_{p18}} = 63\% \qquad /8/$$

Therefore, the range of admissible controller constructional parameter changes should be determined so as to ensure the gain of Kp variation resulting from adaptation conditions.

The following denotation are used in formula /7/

$$kI_z^2 R_g = A$$

$$kI_w^2 R_g = B$$

$$3kI_w^2 R_g \left(\mathcal{L}_2 - \mathcal{L}_1\right) 1^2 - 4hqS/y_{mz} - \Delta y/ = C \qquad /9/$$

$$3kI_z^2 R_g \left(\mathcal{L}_2 - \mathcal{L}_1\right) 1^2 - 4hqSy_{mz} = D$$

$$4hqS \frac{k_t}{k_r + k_s} = E$$

A, B, C, D, E denotations are parametric indicators, constant for the given controller type and the determined operating point.

After A, B, C, D, E denotation are substituted to formula /7/, the $K_p^{\ast}$ expression is the following

$$Kp^{\ast} = \frac{\ln \frac{A}{D - E\,\Delta\vartheta_{cz}}}{U \ln \frac{A}{D - E\,\Delta\vartheta_{cz}} + \ln \frac{B}{C + E\,\Delta\vartheta_{cz}}}$$

or after some transformations

$$Kp^{*} = \frac{\ln A - \ln /D - E\,\Delta\vartheta_{cz}/}{U^{*}\left[\ln A - \ln /D - E\,\Delta\vartheta_{cz}/ + \ln B - \ln /C+E\,\Delta\vartheta_{cz}/\right]} \qquad /10/$$

If denoting constant coefficients at Kp^{*} respectively

$$\ln A = c_1$$
$$\ln A + \ln B = c_2 \text{ with } c_2 > c_1 \qquad /11/$$
$$C = D = c_3$$

and introducing to formula /10/ the denotation

$$E\,\Delta\vartheta_{cz} = x$$

one obtains

$$Kp^{*} = \frac{c_1 - \ln /c_3 - x/}{U^{*}\left[c_2 - \ln /c_3 - x/ - \ln/c_3 + x/\right]} \qquad /12/$$

with $c_2 > c_1$

Assuming the controller operating in conjunction with only one contact thermometer or hygrometer, the controller is supposed to react to the constant value of U^{*} error which equals the contact thermometer or hygrometer zone of intensitivity divided by values of temperature ϑ_o or humidity φ_o set on a contact thermometer or hygrometer.

The above said being taken into account we are actually interested in the variability of the whole product $Kp^{*}\,U^{*}$, as a component uniformely determining Kp^{*} variability in the function of temperature $\Delta\vartheta_{cz}$

$$Kp^{*}U^{*} = \frac{c_1 - \ln /c_3 - x/}{c_2 - \ln /c_3 - x/ - \ln /c_3 - x/} \qquad /13/$$

The value of U^{*} should be adjusted to the needs of regulation circuits by the choice of contact thermometers and hygrometers with appropriate zones of intensitivity.

The course of the component $Kp^{*}U^{*}$ in temperature function is shown in fig. 6, c_1, c_2, c_3 parameter values being assumed.

On the basis of the above given dependences it can be shown that conditions of the discussed controller, adaptability for a group of objects with dynamic parameters To and T varying in the function of outside temperature, in the range given in figure 1, are the following

$$c_1 = \ln kI_z^2R_g = 0,9$$

$$c_2 = \ln kI_z^2R_g + \ln kI_wR_g = 2,4$$

$$c_3 = 3kI_w^2R_g \,/\mathcal{L}_2 - \mathcal{L}_1/\, l^2 - 4hqS\,/y_{mz} - \Delta y/ = 2 \qquad /14/$$

where: $E = 0.05$ $x = 0.1 \div 0.9$ correspond to the outside temperature changes within the range $\Delta\vartheta_{cz} = +2 \div 18^{\circ}C$.

The above given general dependences provide only one of the variants adaptation conditions. Therefore, they are treated as an example indicating adaptation properties of the discussed controller.

4.5. Controller operation in construction with several contact thermometers and hygrometers

Considerations given in point 4.3 are valid in the case of a controller operating in conjunction with several contact

thermometers or hygrometers. In addition it should be taken into account that currents I_z and I_w are functions of the number of contact thermometers, which transmitted signals about the excess of the temperature being set. In order to formulate these dependences an electric scheme of summing circuits was analyzed.

It has been shown that the dependences of I_z and I_w currents on the number of switched on contact thermometers are nonlinear and the proportion coefficient of Y^* controller output signal and U^* error, i.e. Kp^* controller amplification factor changes in the function of the number of switched on contact thermometers.

In this case, the change of Kp^* amplification factor occurs due to the changes of the feedback element amplification factor Kw. The above changes result from the changes of energy released in the controller heater.

In consequence there appears a progressive controller operation in the function of error, caused by Kp^* controller amplification factor being dependent on U^* error value.

Because of a lack of place and the essential aim of the paper, i.e. the analysis aim of the paper, i.e. the analysis of adaptation of external disturbance controller adjustment, the controller progressive operation in the function of U^* error value will be not analyzed more exactly.

5. Results of investigations on regulation systems with the application of an adaptable controller

The discussed regulation systems have been up till now used and investigated in air-heating of railroad cars produced

in the B. Cegielski plant in Poznań and in ventilation and air-conditioning installations of seaships built in Szczecin and Gdańsk shipyards. The investigations revealed that adaptable controllers permit temperature stabilization with the accuracy up to about $1^{o}C$ and relative humidity with the accuracy to about 5% independent of external and internal disturbances. The results obtained authorize to an extended use of adaptable controllers of temperature and humidity to automatic regulation systems of: heating, ventilation, air-conditioning of railroad cars, sea ships, public utility buildings, housing, and so on. This was reached due to the use of reliable devices, the functions of which were rather complex but the construction - simple.

6. Conclusions

On the basis of the analysis of the system with an application of adaptable temperature or humidity controller, the following conclusions can be drawn:

1. The dependence of the amplification factor Kp^{*} on the outside temperature by formula /7/ is characteristic of an adaptable temperature or humidity controller.
2. The following conditions being satisfied:

$$\ln kI_z^2 R_g = 0.9$$

$$\ln kI_z^2 R_g + \ln kI_w^2 R_g = 2.4$$

$$3kI_w^2 R \left(\alpha_2 - \alpha_1\right)/l^2 - 4hqS \left(y_{mz} - \Delta y\right) = 2$$

the adaptable temperature or humidity controller ensures the adjustment of the amplifier factor Kp^{*} to

dynamic properties To, T and To/T for the group of objects with $0.1 < To/T < 0.25$ in the function of most frequent outside temperature changes, within the limits $+2 \div +18^{\circ}C$.

3. If the adaptable controller operates in conjunction with several contact thermometers or hygrometers, there exists a nonlinear, progressive influence of contact thermometers or hygrometers switched on in turn to Tz and Tw by means of Iz and Iw current changes. This leads to the changes of Kp^{*} amplification factor in the function of U^{*} error value, and avoids overregulation in regulation systems with averaging measurement pulses.
4. According to investigations it has been found that adaptable controllers permit to stabilize the temperature with the accuracy to about $1^{\circ}C$ and relative humidity with the accuracy of about 5% independent of external and internal disturbances. This is reached due to the use of reliable devices the functions of which are rather complex but the simple construction.

Literature

1. Boundarel René i inni. Ekstremalne i adaptacyjne układy automatyki. Wydawn. P.A.N. Wrocław 1963 r.

2. Z. Barski. Analiza eksperymentalna właściwości dynamicznych przemysłowych obiektów klimatyzowanych jako obiektów regulacji. Etap II. Badanie w zakładach włókien sztucznych w okresie letnim. Praca ITC /nieopublik./ Łódź 1965 r.

3. Z. Barski. Automatyczna regulacja temperatury w instalacjach ogrzewania nawiewnego wagonów kolejowych. Prace ITC. Zeszyt 33, Łódź 1967 r.

4. Z. Barski. Automatyzacja systemu klimatyzacji w pomieszczeniach szpitalnych na statku bazie B 67. Praca ITC /nieopublik./ Łódź 1965 r.

5. Z. Barski. Dispositif de régulation de la température dans les installations de chauffage pour les véhicles, en particulier pour les véhicles sur rails. Brevet d'invention nr 1403902, République Française oraz patenty: Wielka Brytania, Austria, NRF, NRD.

6. Z. Barski. Sposób i urządzenie do regulacji temperatury lub wilgotności. Zgłoszenie patentowe w U.P. PRL nr P 113499.

7. Z. Barski. Badanie właściwości dynamicznych i regulacja adaptacyjna obiektów klimatyzowanych. Praca doktorska. Łódź 1968 r.

8. W. Findeisen. Technika regulacji automatycznej. P.W.N. Warszawa 1965 r.

9. A. Wierzbicki. Zagadnienia dynamiki regulatorów krokowych, P.A.K. nr 1/1963.

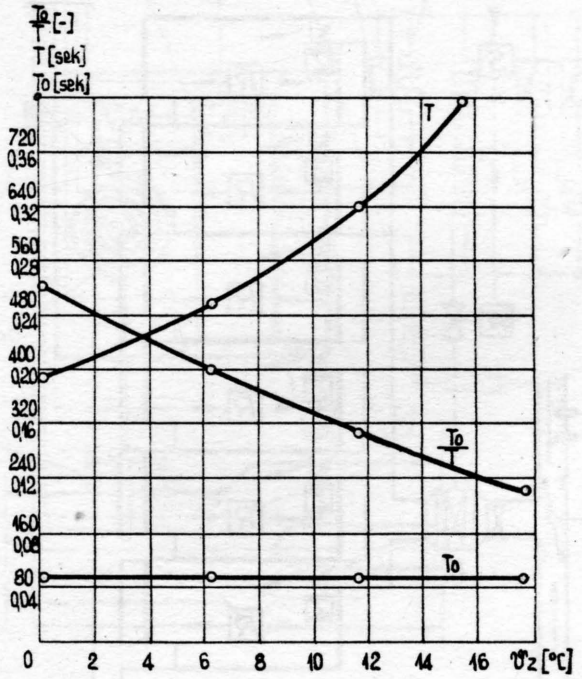

Fig. 1. Characteristics T = f /ϑ_z/, To = f /ϑ_z/, To/T = = f /ϑ_z/ in the range of temperatures +2 ÷ +18°C.

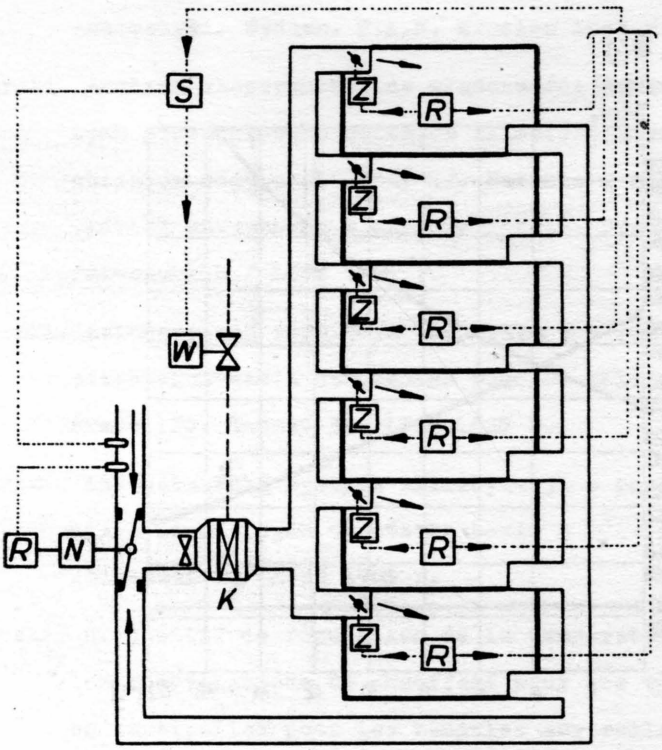

Fig. 2. Block diagram of temperature regulation system in a multicarriage railroad car: R - contact thermometer with a relay, Z - air intake throttle electromagnetic drive, S - adaptable temperature controller with a bimetallic summing relay, W - executive element of the central heater, K - heating chamber, N - circulating air cap drive.

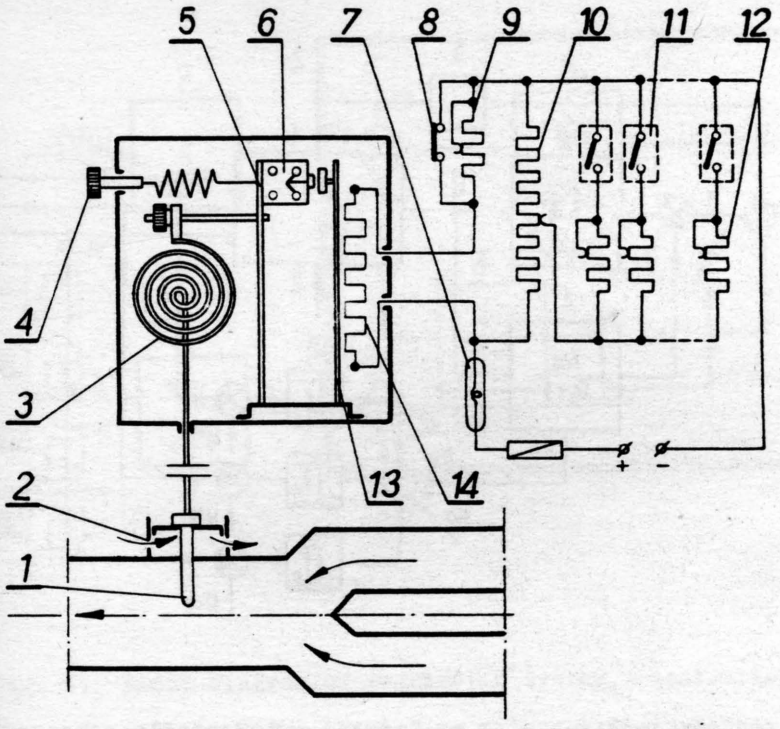

Fig. 3. Circuit diagram of adaptable temperature controller: 1 - manometric thermometer sensor, 2 - sensor coating, 3 - resilient spiral, 4 - tension spring hand wheel, 5 - compensation bimetal, 6 - microswitch, 7 - barretter, 8 - controller relay contacts, 9 - auxiliary resistor, 10 - regulation resistor, 11 - contact thermometer relay, 12 - additional resistor, 13 - working bimetal, 14 - heating resistor.

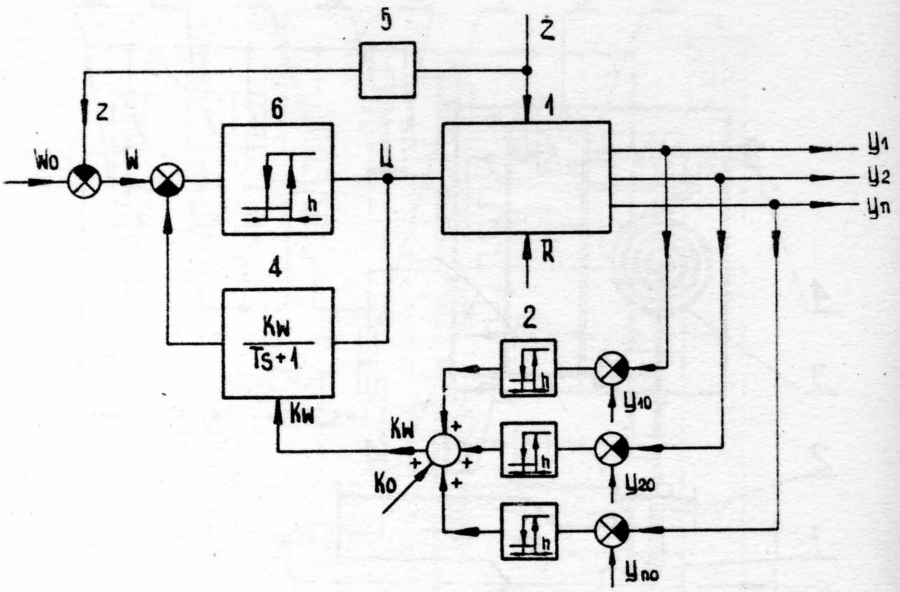

Fig. 4. Block diagram of the system of adaptable compensation with compensation amplification factor.

1 - object of regulation, 2 - contact thermometer or hygrometer, 3 - summing node, 4 - inertial feedback element, 5 - element of external disturbance compensation influence, 6 - controller microswitch.

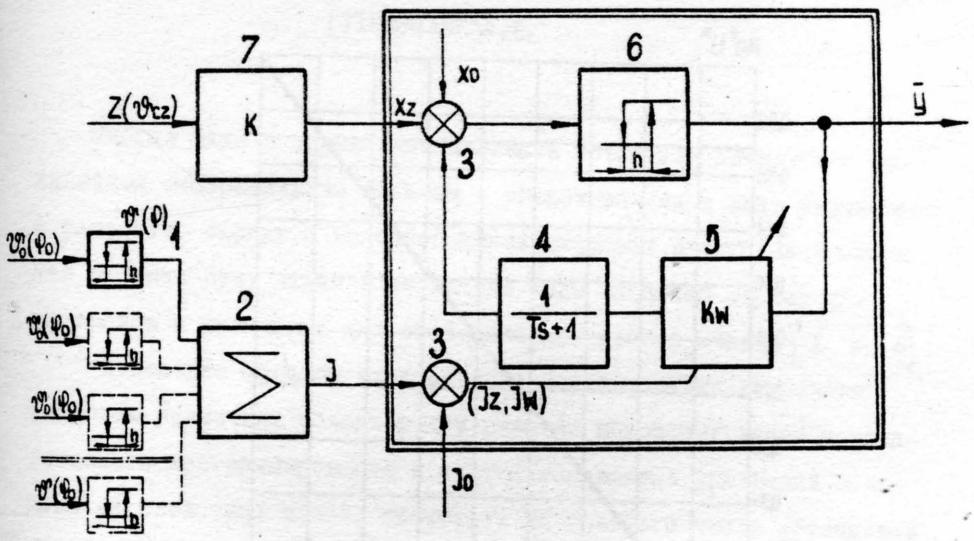

Fig. 5. Block diagram of regulation system, controller properties being adapted to external disturbances:
1 - contact thermometer or hygrometer, 2 - resistance, current summing system, 3 - summation node, 4 - inertial feedback element, 5 - feedback element varying amplification factor, 6 - controller microswitch, 7 - element of adaptable controller settings dependent on external disturbances,

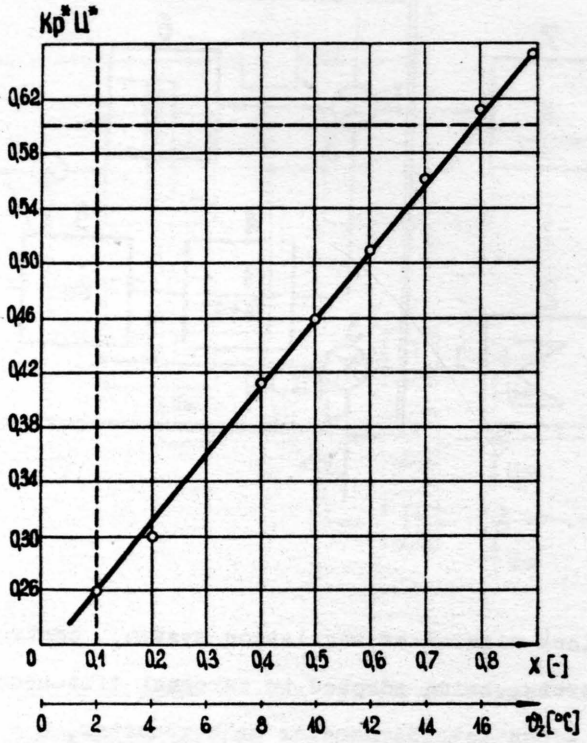

Fig. 6. Characteristics of $Kp^{*}\ U^{*} = f\ /\vartheta_z/$ two-position adaptable temperature and humidity controller for temperature range +2 ÷ 18°C.

НОВЫЕ АНАЛОГОВЫЕ МОДЕЛИ ДЛЯ ЦЕЛЕЙ УПРАВЛЕНИЯ

ГУТЕНМАХЕР Л.И.

Многие задачи управления сложными объектами сводятся к нелинейным экстремальным задачам с ограничениями в виде неравенств и равенств. Наряду с использованием цифровых электронных машин для решения этих задач в последние годы возникло стремление построить и применять для этой цели аналоговые модели [I ÷ 6].

Известные способы электронного моделирования на основе аналогии различных объектов при решении некоторых задач математического программирования и систем нелинейных уравнений основаны на свойствах цепей, состоящих из большого числа источников постоянного во времени напряжения, тока, диодов и трансформаторов постоянного тока [I ÷ 7].

Как известно можно составить из двухполюсников электрическую модель сложных сетей или сеток топологически сходственную по структуре заданным объектам [8, 9]. В рассматриваемых моделях в основном используются активные двухполюсники с отдельными внутренними источниками эдс, а неравенство эдс определяется автоматически с помощью диодных или транзисторных ключей. Использование диодов для установления неравенств известно давно и применяется для измерительных целей [8, IO, II], для построения нелинейных преобразователей [9, I2] и ключей логического типа, а в последнее время и для решения некоторых задач математического программирования [I - 6].

Основным недостатком всех этих известных статических способов моделирования объектов является необходимость в очень большом числе источников постоянного напряжения с малым

внутренним сопротивлением. Все эти источники не должны иметь общей точки соединения (общей "земли"). Напряжение этих источников должно регулироваться и устанавливаться по величине от нуля до 100% через 0,5 ÷ 1,0%. Их внутреннее сопротивление должно быть значительно меньше сопротивлений остальных элементов модели. При очень большом числе источников это приводит к необходимости построения сложных, громоздких и дорогих установок. В одних случаях используются транзисторные стабилизаторы напряжения с делителями напряжения, включенные на отдельные индуктивно изолированные обмотки трансформатора сети переменного тока [1], в других случаях применяются усилители с положительной обратной связью для компенсации сопротивлений [2]. В нелинейных моделях сетей устанавливают мощные выпрямители с изолированными делителями напряжения с малым сопротивлением [7].

Предлагаемый способ моделирования позволяет решать те же задачи на основе переходных процессов в электрических цепях, содержащих ёмкости и импульсные трансформаторы тока (помимо диодов и сопротивлений).

Модели объектов в этом случае являются не статическими, а динамическими. Решение поставленных задач получается в определенные моменты времени переходного процесса в виде мгновенных значений величин тока и напряжений в ветвях и узлах электрической цепи. Принцип экстремальности получается справедливым и для таких искусственно построенных электрических цепей, которые содержат ёмкости, играющие роль внутренних источников напряжения двухполюсников.

Сравнение динамических моделей объектов, построенных по

предлагаемому способу, с известными статическими моделями тех же объектов показывают, что в новых моделях роль источников напряжения успешно играют ёмкости. Каждая заряженная ёмкость может быть заменена, как известно, источником напряжения с ничтожно малым внутренним сопротивлением последовательно включенным с не заряженной ёмкостью.

Зарядка всех ёмкостей схемы на заданные различные напряжения решается предлагаемым способом сравнительно просто. Для этой цели с помощью пары разделительных диодов каждая ёмкость модели присоединяется к одному общему делителю источника переменного напряжения (см.рис.I). В этом случае при соответствующей полярности одной из полуволн переменного напряжения $U_{\sim 1}$, ёмкости заряжаются на заданные общим делителем части общего напряжения.

Во время действия другой полуволны напряжения $U_{\sim 2}$ (при полярности обратной направлению выпрямления пар разделительных диодов), это напряжение $U_{\sim 2}$ запирает указанные диоды. В это время все ёмкости модели практически можно считать отсоединенными от источника зарядки. Следовательно, в этот отрезок времени можно подавать на модель различные импульсы напряжения и тока, производить измерения мгновенных или средних значений величин тока и напряжений в ветвях и узлах модели.

Таким образом, по предлагаемому способу схемы моделей объектов составляют из ёмкостей, диодов и в некоторых случаях из сопротивлений, импульсных трансформаторов тока и транзисторных ключей. Требуется задать на все ёмкости, имеющиеся в схеме, определенные начальные условия, т.е. необходимо зарядить все ёмкости на заданные напряжения и подвести к некоторым узловым

точкам заданные граничные условия.

Решение каждой задачи получается в виде ряда мгновенных значений токов и напряжений в модели в переходном процессе.

С целью упрощения способа задания начальных условий и способа измерения мгновенных или средних значений токов и напряжений весь процесс, как уже сказано, искусственно повторяется во времени, путем использования переменного во времени напряжения от общего источника. При этом, при одной полуволне, производится задание начальных условий (происходит зарядка), а при другой полуволне происходит нужный переходный процесс в электрической модели.

Предлагаемый способ проверен экспериментально:

при определении критического пути в сетевом графике;

при построении моделей нелинейных сетей;

при решении задачи о нахождении кратчайшего пути в сети.

Для работы моделей по предлагаемому способу необходим общий источник переменного напряжения постоянной частоты периода T. Форма кривой (прямоугольной) этого напряжения показана на рис.I. Она имеет вид прямоугольных импульсов разной полярности, как это видно на рис.I, причем, длительность τ_1 и величина (амплитуда) положительной полуволны может отличаться от длительности τ_2 отрицательной полуволны. Величина запирающего отрицательного напряжения U_2 должна быть всегда больше положительного значения напряжения U_1. Часть положительной полуволны длительностью τ_1 используется для зарядки всех основных ёмкостей моделей. Процесс работы моделей в необходимом режиме проходит во время τ_2 каждого периода. Причем все источники напряжения и тока, играющие роль граничных условий

и правых частей уравнений при моделировании должны действовать в той части $\frac{T}{2}$ периода T, когда источник напряжения уже не заряжает основные ёмкости модели и когда отрицательная полуволна напряжения запирает все пары разделительных диодов.

На рис.I показана для примера форма импульсов i одного такого внешнего источника тока.

На рис.2 представлена схема модели обобщенной ветви, по которой "движется" поток некоторой величины при решении задач о распределении потока в сложной цепи [2, 3]. С помощью таких элементов (ветвей) могут быть построены модели объектов для решения задач о кратчайшем и о длиннейшем пути и о распределении потока в сетях сложной конфигурации. Оптимальное распределение потока определяется распределением электрических токов по этим ветвям в модели.

На рис.2 показано соединение с источником переменного напряжения I только одного элемента. Таких элементов можно, разумеется, присоединить множество.

К общему для всей модели источнику I с целью установки заданной величины напряжения на ёмкости присоединены две части делителя напряжения 2а и 2в. Одна часть делит напряжение, например, через одну сотую, а другая часть делит с помощью отводов через одну десятую от полного напряжения. Если, например, в первой 2а и во второй части 2в будет по 9 отводов, то с помощью двух переключателей можно установить на входных клеммах напряжение от нуля до 99 процентов, т.е. через один процент от полного напряжения источника I. Такая декадная система весьма удобна, так как требует небольшой коммутатор для установки через диоды 3 заданного напряжения на ёмкостях 4.

Разумеется такая система коммутации позволяет и расширить пределы величины напряжения задаваемого для зарядки ёмкости. Так, например, части делителя 2а и 2в можно изготовить не по 9, а по 20 выводов, что даёт возможность задавать напряжение через I : 400 от полного напряжения, и т.д. Кстати отметим удобство использования в этом случае шаговых искателей и подобных им коммутаторов для дистанционной установки напряжений на ёмкостях модели.

С помощью трансформатора переменного тока 5, первичный ток которого устанавливается индивидуально для каждого шунтом 6, создается определенная сила тока в ограничивающем диоде 7. (Для обеспечения нормального режима трансформатора тока необходимо вторую полуволну переменного тока пропускать через диод 8, который может быть установлен в дополнительной вторичной обмотке трансформатора 5, как показано на рис.8, или непосредственно параллельно основному диоду).

Для обеспечения прохождения тока в двух направлениях в задачах с двухсторонним потоком в ветвях используется диодный мостик 9, который даёт возможность току от внешней цепи, например, от источника IO проходить через ёмкости 4 и диод 7 при любой полярности напряжения или тока внешнего источника IO.

На рис.8 представлена та же схема, что и на рис.8, но без источника I и делителя 2, (см. вместо них пунктир и диоды 3 у ёмкости 4).

При составлении схем сложных моделей сетей можно не показывать общие для всех ёмкостей источник I и делитель 2. Заметим к тому же, что при наличии диодного мостика 9 можно не ставить диод 7, так как диоды мостика 9 заменяют этот диод.

Таким образом, любая сложная модель при решении задач о

кратчайшем пути, о распределении потока и других задач может быть составлена из ветвей рис.3 (или 4). Подавая к граничным точкам этой модели токи или напряжения в моменты периода τ_2 и измеряя при этом распределение токов по ветвям, можно, как сказано выше, решить поставленные задачи.

В случае, когда та или иная ветвь не ограничивает величину потока, можно не ставить ограничивающий диод 7 и связанный с ним трансформатор тока 5 с шунтом 6 и дополнительным диодом 8. Эта часть ветви нужна только тогда, когда величина потока ограничена в данной ветви определенным значением (например, пропускной способностью дороги).

В некоторых случаях можно заменить трансформатор тока 5 действием вспомогательной ёмкости 4 (см.рис.4), которую следует заряжать на достаточно большее напряжение с помощью дополнительного источника переменного напряжения через диоды 3. Эта ёмкость 4 будет разряжаться в части периода τ_2 на ограничивающий диод 7 через сравнительно большие сопротивления II и этим создавать заданный ток в диоде 7. (Рационально также использовать схему транзисторного преобразователя напряжения на ёмкости в силу тока ограничителя).

Наиболее простая схема ветви и модели получается при однонаправленном потоке и при неограниченной пропускной способности. При этом не требуется диодный мостик 9 и трансформатор тока 5 (или соответствующая ему ёмкость 4 на рис.5).

На рис.5 представлена принципиальная схема нелинейного элемента модели сети, предназначенной для решения задач по расчету гидравлических, газовых, теплофикационных и др.сетей.

В этом нелинейном элементе дополнительно имеются несколько ёмкостей 4 (в данном примере три), которые разряжаются через

диоды 5 и сопротивления 6.

Внешнее напряжение (источник 9) через диодный мостик 8, если оно больше какого-либо из напряжений на указанных ёмкостях, запирает с помощью диодов 5 те или иные цепи (диод 5, сопротивление 6). В схеме, показанной на рис.5, ёмкости 4 включены так, что они представляют собой вместе ёмкостной делитель напряжения при их зарядке током от источника I через делители напряжения 2а, 2в.

Схема 5 показывает, как можно использовать предлагаемый способ для построения нелинейных звеньев, позволяющих создать двухполюсник с кусочно-ломанной характеристикой. Напряжение на входе этого двухполюсника сопоставляется с некоторым рядом опорных напряжений ёмкостей 4, а диоды 5 выключают те или иные сопротивления 6 и этим изменяют величину общего сопротивления двухполюсника.

Разумеется в модели из таких нелинейных звеньев также могут быть включены ограничители тока, показанные на рис.2-4.

Предлагаемый способ моделирования позволяет построить то или иное моделирующее устройство.

Пусть, например, имеется объект, где необходимо решать задачи сетевого планирования. В этом случае известна структура сетевого графика, известна длительность каждой работы, а требуется прежде всего определить критический путь от начала до конца работы.

Динамическая модель для этих задач (рис.6 и 7) составляется из связанных диодами одинаковых ёмкостей, шунтированных одинаковыми сопротивлениями. На делителях напряжения 2а, 2в устанавливаются значения напряжения, которые прямо пропорциональны длительности работ, а к граничным точкам модели объекта,

соответствующим началу и концу всей работы, присоединяется импульсный источник тока 8, который должен быть синхронизирован с общим источником переменного напряжения I, питающим через делитель все ёмкости. Импульс тока необходимо подавать в той части периода, когда уже прекращается зарядка ёмкостей.

Решение задачи - определение критического пути - получается путем наблюдения на индикаторах 7 за прохождением импульсного тока по диодам основной схемы модели. Этот ток будет проходить по наиболее длинному пути (критическому).

Достаточно поменять в этой модели направление диодов или транзисторных ключей в основной схеме и импульсный ток пройдет по наиболее короткому пути.

Следует отметить, что когда известна та или иная статическая модель объекта (на постоянном токе), то очень легко построить эквивалентную динамическую модель с ёмкостями по предлагаемому способу.

Таким образом, предлагаемый автором способ моделирования отличается тем, что с целью построения эквивалентных известным статическим моделям ("на постоянном токе") для решения упомянутых задач, но малогабаритных, более надежных, менее трудоёмких и потребляющих меньше энергии динамических электронных моделей, во все ветви цепей, где по условиям задач необходимы источники эдс, включаются заряженные ёмкости, а во все ветви цепей, в которых по условиям несбходимы ограничители силы тока, включаются диодные ключи, присоединенные со вторичными обмотками импульсных трансформаторов тока.

Для одновременной периодической зарядки всех ёмкостей модели используется один общий источник переменного напряжения с делителем, к которому каждая ёмкость присоединяется через

пару "разделительных" диодов.

Внешние источники (граничных условий) подводятся периодически в момент действия отрицательной полуволны переменного напряжения, запирающего цепи "разделительных" диодов. В этот же момент времени переходного процесса производится измерения искомых величин в ветвях и узлах модели.

Способ моделирования с помощью динамических моделей, содержащих ёмкости, по эффективности эквивалентен способу создания нового источника постоянного напряжения с ничтожно малым внутренним сопротивлением и легко изменяющимся на выходе напряжением источника, который по габаритам и стоимости соответствует обычной ёмкости (конденсатору). Только гипотетическое создание такого способа изготовления новых источников постоянного напряжения может позволить сравнить эффективность старых (известных) и нового предлагаемого способа моделирования объектов с очень большим числом ветвей в модели.

Л И Т Е Р А Т У Р А

I. АНИСКОВ В.В., ВИТЕНБЕРГ Расчет и оптимизация сетевых графиков, Госинти, № I4-67-690/6, Москва, I967 г.

2. ВАСИЛЬЕВ В.В., КЛЕПИКОВА А.Н., ТИМОШЕНКО А.Г. Решение задач оптимального планирования на электронных моделях, Изд-во "Наукова думка", I966 г.

3. ДЕННИС Дж. Б. Математическое программирование и электрические цепи, Изд-во ИЛ, I96I г.

4. КАНТОРОВИЧ Л.В. Гидравлическая модель для решения транспортной задачи, Сборник " Проблемы повышения эффективности работы транспорта" изд-во АН СССР, I949 г.

5. ПУХОВ Г.В., ВАСИЛЬЕВ В.В. Устройство для моделирования сетевого графика, авт.свид. № I75749, бюл. изобретений № 20, I965 г.

6. ПУХОВ Г.Е., БОРКОВСКИЙ, ВАСИЛЬЕВ В.В., СТЕПАНОВ А.Е. Моделирующее устройство для решения задач линейного программирования, авт.свид. № I56703, бюл. изобр. № I5, I96I г.

7. БАГРИНОВСКИЙ А.Д. Электрическая модель для расчета сетей трубопроводов, Вестник АН СССР, I962 г. 5,

8. ГУТЕНМАХЕР Л.И. Электрические модели . Издательство АН СССР, I949 год.

9. КОГАН Б.Я. Электронные моделирующие устройства, ГИ, Физматлит, I959 г.

I0. ГУТЕНМАХЕР Л.И. Применение электронных ламп для определения угла сдвига фаз, ж. Электричество, № 2, стр. 40, I936 г.

II. ГУТЕНМАХЕР Л.И. Устройство для измерения угла сдвига фаз, авт.свид.48798, класс 2Ie, 7, от II.3. I936г. Изд-во Бюро Новизны Комитета по изобрет. при СТО.

I2. ГУТЕНМАХЕР Л.И. Нелинейный диодный преобразователь, авт.свид.№ 83668, класс 42, I4 от I4 апреля I947г. Из-во Бюро Новизны Комитета по изобрет.при СТО.

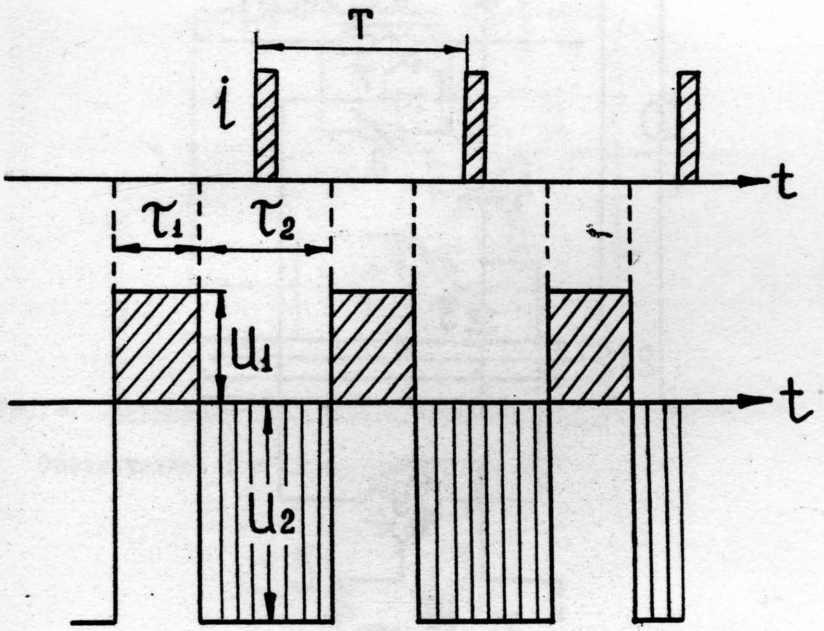

Рис.I. Диаграммы токов и напряжений.

Обозначения: t - время; T - период; τ_1 -длительность положительной полуволны ; τ_2 - длительность отрицательной полуволны переменного напряжения $\underset{\sim}{U}$ общего источника ;

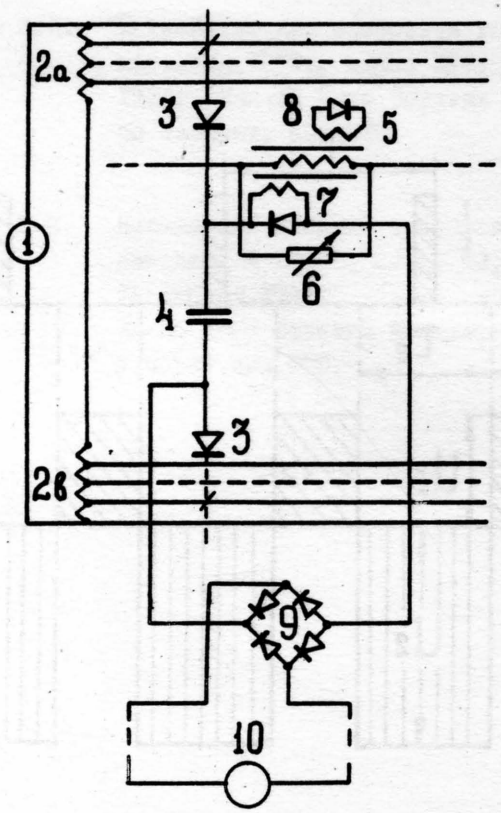

Рис.2. Схема элемента модели с внутренним источником напряжения (ёмкостью) и источником тока (трансформатором тока)

Обозначения:

I - источник переменного напряжения;
2а и 2в - делители напряжения;
3 - диоды для зарядки ёмкостей;
4 - ёмкость;
5 - трансформатор тока;
6 - шунт для регулировки силы тока;
7 - "ограничивающий" диод;
8 - вспомогательный диод;
9 - диодный мостик;
10. - внешний источник.

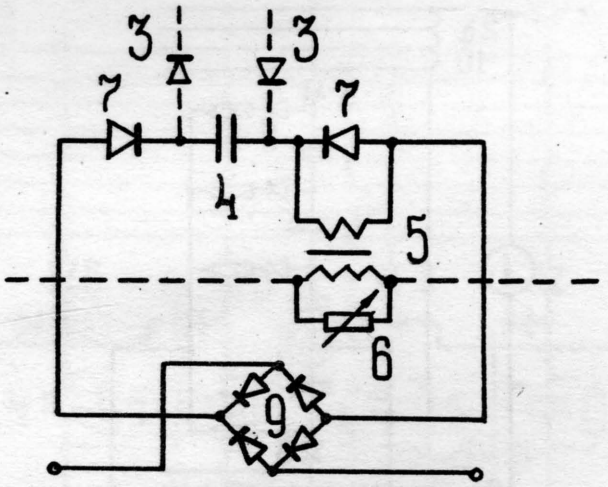

Рис.3. Принципиальная схема элемента модели (аналогично рис.3)

Обозначения т е ж е, что на рис.2.

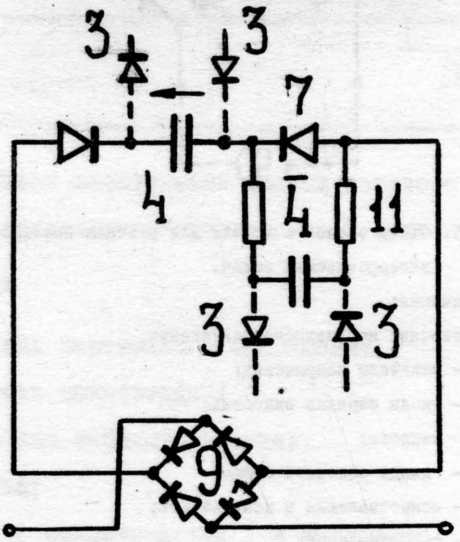

Рис.4. Схема элемента модели с дополнительной ёмкостью 4 в качестве источника тока.

Обозначения т е ж е, что на рис.2. II -добавочное сопротивление.

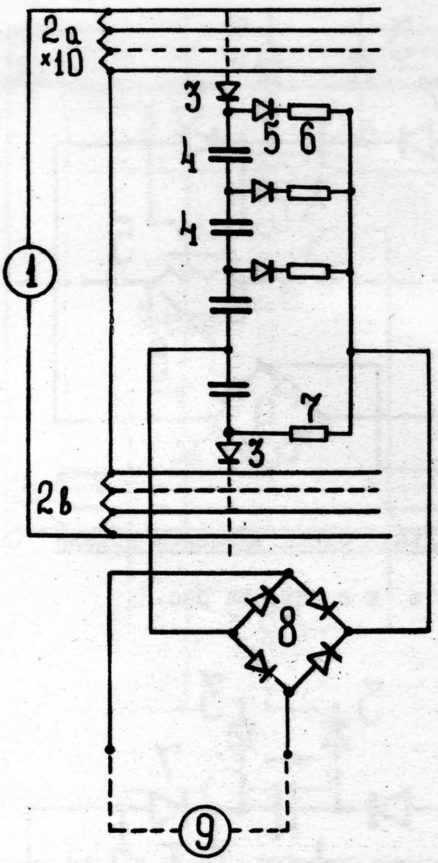

Рис. 5. Схема элемента модели для решения нелинейных алгебраических задач.

Обозначения:

I – источник переменного напряжения;

$2_а, 2_б$ – делители напряжения;

3 – диоды зарядки емкостей;

4 – емкости;

5 – диоды основной схемы;

6 – сопротивления в цепи диодов;

7 – сопротивление;

8 – диодный мостик;

9 – внешний источник.

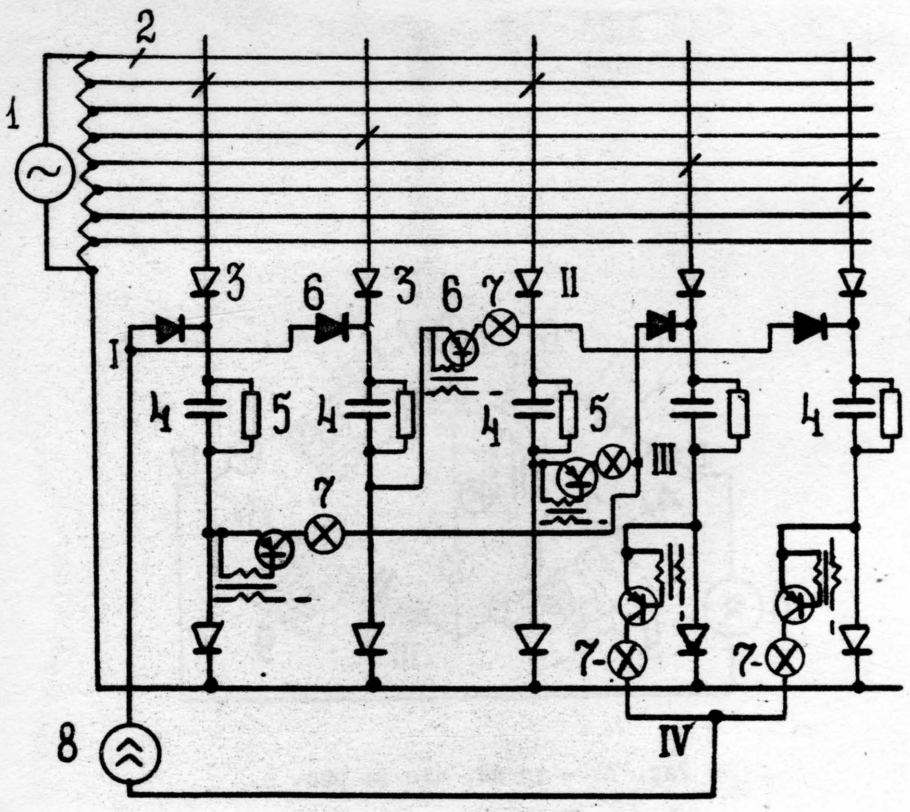

Рис. 6. Схема электронной модели сетевого графика для определения "критического" пути.

Обозначения:

I - источник переменного напряжения;

2 - делитель напряжения ;

3 - диоды для зарядки емкостей;

4 - емкости;

5 - шунты (сопротивления) к емкостям;

6 - транзисторные ключи;

7 - индикаторы тока;

8 - внешний импульсный источник силы тока;

I - IУ - узловые точки модели.

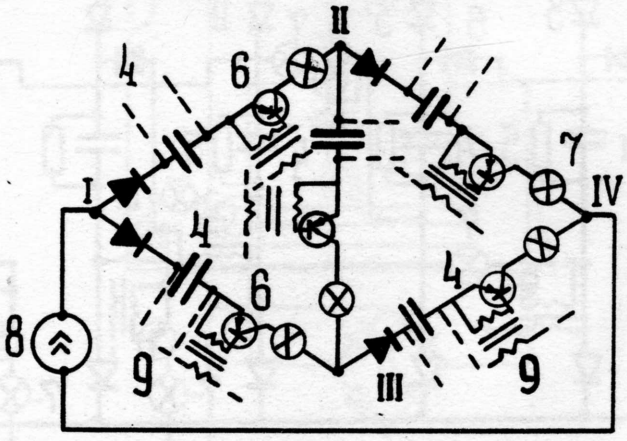

Рис. 7 - то же, что на рис. 6.